ILMATIETEEN LAITOS
METEOROLOGISKA INSTITUTET
FINNISH METEOROLOGICAL INSTITUTE

NKS/EKO-4(97)1

REPORT OF THE SECOND MEETING ON NORDIC DISPERSION / TRAJECTORY MODEL INTERCOMPARISON WITH THE ETEX-1 FULL-SCALE EXPERIMENT

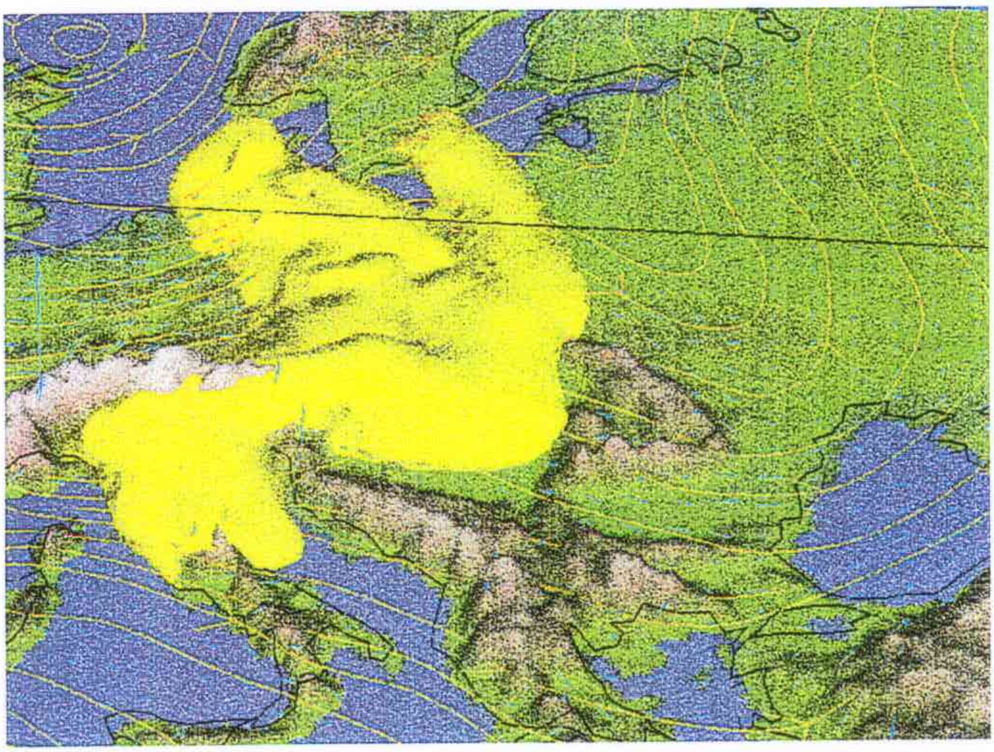

NKS/EKO-4 intercomparison / validation exercise held at FMI, Helsinki, 4th and 5th December 1996

NKS/EKO-4(97)1
REPORT OF THE SECOND MEETING ON NORDIC DISPERSION/TRAJECTORY MODEL INTERCOMPARISON WITH THE ETEX-1 FULL-SCALE EXPERIMENT

NKS/EKO-4 intercomparison/validation exercise
held at FMI, Helsinki, 4th and 5th December 1996

Ed.: Ulf Tveten, IFE, Kjeller, Norway

Published by

Finnish Meteorological Institute
P.O. Box 503
FIN - 00101 HELSINKI
Finland

Series title, number and report code of publication

Date
March 1997

Authors

Ulf Tveten, Editor

Name of project
EKO-4 (NKS)

Commissioned by

Title

Report No.: NKS/EKO-4(97)1
Report of the second meeting on Nordic dispersion/trajectory model intercomparison with the ETEX-1 full-scale experiment. NKS/EKO-4 intercomparison/validation exercise held at FMI, Helsinki, 4th and 5th December 1996.

Abstract

On the 4th and 5th December 1996 a meeting was held at the Finnish Meteorological Institute in Helsinki, where calculations of the atmospheric transportation and dispersion of the ETEX-1 release carried out by a number of institutions in the Nordic countries were presented.

In addition, recent modeling developments and current development plans were presented. Several institutions also demonstrated animated computer displays of the results.

The meeting was the second Nordic meeting of this kind, and the rate of development since the first meeting, less than one and a half year ago, is impressive. Meetings such as these are seen as an important supplement to the other, international ETEX-meetings, as the discussions in the Nordic meetings naturally are more focused on problems related to the particular models adopted for use by the institutions in the Nordic countries.

Publishing unit

Classification (UDC)

Key words
Meteorology
Dispersion, Advection
Experiment

ISSN and series title

Language
English

ISBN
951-697-483-X

Sold by
Finnish Meteorological Institute
Library
P.O.Box 503
FIN-00101 Helsinki
Finland

Pages
142

Price

Note

EXTENDED SUMMARY

On the 4th and 5th December 1996 a meeting was held in Helsinki. The Finnish Meteorological Institute acted as generous and efficient host of the meeting. Simulations of the atmospheric transportation and dispersion of the ETEX-1 release, carried out by a number of institutions in the Nordic countries were presented. Similar simulations by the United Kingdom Meteorological Office (whose representative had shown strong interest in this form of Nordic cooperation and had been specially invited to the meeting as the only "outsider") were also presented. In addition, recent modeling developments and current development plans were presented, as well as some Chernobyl-related simulations. A presentation of the future European forecasting system RODOS was also given, and two presentations described exercises, one with Nordic participation, and one with European. Several institutions also demonstrated impressive animated computer displays of the results. The present report contains edited versions of the presentations given at the meeting.

The meeting was the second Nordic meeting of its kind, and the participant expressed strong hopes that it would not be the last, as it has been found that these meetings (like the past meetings within the NKS-project BER-1) prove to be particularly fertile and inspiring. Meetings such as these are presently seen as an important supplement to the other, international ETEX-meetings, as the discussions in the Nordic meetings naturally are more focused on problems related to the particular models adopted for use by the institutions in the Nordic countries.

There were 16 presentations at the two-day meeting. It was obvious that the rate of model development since the first meeting, less than one and a half year ago, is impressive. Several new models have been developed or are in an advanced stage of development. Generally the agreement between the simulations from the different institutions are better than at the first meeting of this kind; though it may be argued that this is not unexpected, since the ETEX measurement results are now known to the participants.

From the extensive discussions throughout and at the conclusion of the meeting, emerged several recommendations, the most important of which are:

Recommendations

- The progress in modeling has greatly outstripped that in application and operational structures. Results from calculations for the same accident situation performed by different institutions may look confusingly dissimilar; even though the results actually turn out to be in excellent agreement upon closer inspection. It is **strongly recommended that the efforts on harmonization of result presentation initiated in the NKS-project BER-1 are revitalized within the next NKS program**.

- The mode of communication is a matter of grave concern. The exchange of results between Nordic institutions at present, at least in the emergency exercises that have been carried out, is mainly via fax machines, and the transfer is not at all satisfactory, as can be seen from examples included in this report. Efforts to find a standard way of communicating have been undertaken within the NKS-project EKO-4, but the meteorological institutes must also become involved in this effort in the future.

- It was also pointed out that expanded **contact with the Baltic States** in this area is highly desirable, and ought to be an **area of concern within the next NKS program.**

CONTENTS

1 A short summary about the ETEX experiment

Jens Havskov Sørensen
Danish Meteorological Institute
Copenhagen, Denmark

The European Tracer Experiment (ETEX) (Archer *et al.,* 1996; Archer *et al.,* 1997 and Klug *et al.,* 1997) was carried out in the autumn of 1994. The purpose of the experiment was to provide data for validation of long-range dispersion models. Two controlled releases of inactive non-depositing tracer gases (perfluorcarbon compounds) were performed.

ETEX was inspired by the Atmospheric Transport Model Evaluation Study (ATMES) (Klug *et al.,* 1992) performed by the World Meteorological Organisation (WMO) and the International Atomic Energy Agency (IAEA) in 1990 on the basis of radiological measurements from a two-week period following the accident at the Chernobyl nuclear power plant in 1986. This evaluation suffered, however, from lack of detailed knowledge of the amount of radioactivity released from the reactor as a function of time.

The planning of ETEX involved three dry runs in which the experiment was simulated. The main objective of the dry runs was to test communications. Before carrying out the experiments, a sampling network of 168 surface based tracer gas samplers was set up, mainly at WMO synoptic stations. The instruments sampled the gas by drawing air through sampling tubes by means of a pump. The tracer gas was retained by an adsorbing material inside the tubes. The distribution of sampling stations over Europe is shown in *Figure 1.1.*

The first release took place on the 23rd of October 1994, starting at 16 UTC, and continuing for 12 hours. The tracer gas was released at a constant rate of 7.9 grams/s. The release point was at (48° 4' N, 2° 1' W), near Rennes in Brittany, France. The terrain at the release site is very flat. The second release took place on the 14th of November 1994, starting at 15 UTC, and continuing for 12 hours. The release point was the same as for the first release, but the release rate of tracer gas was higher, 11.3 grams/s. Additional information on the experiments is given in the report from the first Nordic ETEX meeting (Tveten and Mikkelsen, Eds., 1995).

During the days following the releases, three-hour tracer gas samples were taken by the instruments. The sampling tubes were shipped to the Joint Research Centre (JRC) at Ispra, Italy, for chemical analyses. The chemical analyses of the first experiment were finished in spring 1996, while none of the participants at the present meeting had information on the status of the analyses of samples from the second experiment.

While the two ETEX tracer gas experiments took place, a real-time modeling exercise was carried out. This involved 28 dispersion models making forecasts of the plume spread. Most of the models were European, but there were also participating models from USA, Canada, Israel and Japan. In advance of the releases, the participants of the real-time modeling exercise did not have any details of the releases, e.g. release rate, release duration, and coordinates of the release point. There were optional release points in UK and France.

A preliminary model evaluation based on data from 86 tracer gas samplers for the first experiment, has been carried out. At the time of writing, the results are presented only in a draft report. The final report (Klug *et al.,* 1997) is expected to appear in May 1997. A symposium will be held in Vienna, Austria, on May 13-16, 1997.

Presently, another model evaluation, the ATMES-II phase of the ETEX model evaluations, is being carried out. The deadline for submission of data for this model evaluation was October 1, 1996. This model evaluation is based on data from the first ETEX release. In this study, the tracer gas observations were available to the participants. The dispersion calculations performed were based on analyzed numerical weather prediction (NWP) data from the (ECMWF) European Centre for Medium-Range Weather Forecast. Besides, the participants were allowed to submit an additional set of model calculations based on another meteorological data set of their own choice. The ATMES-II model evaluation involves 26 participants.

At the time of writing, the ETEX data set of tracer gas observations is confidential, and will remain so until the report following the second phase (ATMES-II) of ETEX is completed. The data were made available to the participants in this phase of the ETEX model evaluations under the following condition from the ETEX steering committee: "You are demanded to keep the information as strictly confidential until the report will be issued".

During the first ETEX experiment, the tracer gas was observed with hourly time resolution at the National Environmental Research Institute (NERI) at Risø, Denmark, using two measurement techniques. This set of observations, which is recently reported (Ellermann and Lyck, 1995; Sørensen *et al.,* 1997), is not included in the official ETEX data set and is not confidential. During the second ETEX experiment, similar measurements were performed at Risø but tracer gas was not observed.

References

Archer G., Girardi F., Graziani G., Klug W., Mosca S. and Nodop K. (1996) The European Long Range Tracer Experiment (ETEX): Preliminary Evaluation of Model Intercomparison Exercise. In: *Proceedings of "21st ITM on Air Pollution Modeling and its Application",* Eds.: Gryning S. and Schiermeier F. A., pp. 181-190. Baltimore, USA. Plenum Press, New York, ISBN 0-306-45381-9

Archer G., Girardi F., Graziani G., Klug W., Mosca S., Nodop K. and Stingele A. (1997) The European Long Range Tracer Experiment ETEX, a Data Base for Comparing Model Results and for Harmonisation. "4th Workshop on Harmonisation within Atmospheric Dispersion Modelling for Regulatory Purposes", Oostende, Belgium. To be published in *Int. J. of Environ. and Pollution*

Ellermann T. and Lyck E. (1995) ETEX-1 Tracer Measurements at Risø. In: *Report of the Nordic Dispersion/Trajectory Model Comparison with the ETEX-1 Full-scale Experiment,* Eds.: Tveten U. and Mikkelsen T., pp. 11-16. *Risø-R-847(EN), NKS EKO-4(95)1,* ISBN 87-550-2118-2, ISSN 0106-2840

Klug W., Graziani G., Grippa G., Pierce D. and Tassone C. (Eds.) (1992) Evaluation of Long Range Atmospheric Transport Models Using Environmental Radioactivity DATA from the Chernobyl Accident. The ATMES Report. *Elsevier Science Publishers Ltd.* ISBN 1-85166-766-0

Klug W., Graziani G., Mosca S., Kroonenberg F., Archer G., Nodop K. and Stingele A. (1997) Real Time Long Range Dispersion Model Evaluation, ETEX first experiment. *In preparation.*

Sørensen J. H., Rasmussen A., Ellermann T. and Lyck E. (1997) Mesoscale Influence on Long-range Transport; Evidence from ETEX Modelling and Observations. Submitted for publication in *Atmos. Environ.*

Tveten U. and Mikkelsen T., Eds. (1995) Report of the Nordic Dispersion/Trajectory Model Comparison with the ETEX-1 Full-scale Experiment. *Risø-R-847(EN), NKS EKO-4(95)1,* ISBN 87-550-2118-2, ISSN 0106-2840

Figure 1.1 Locations of ETEX sampling stations.

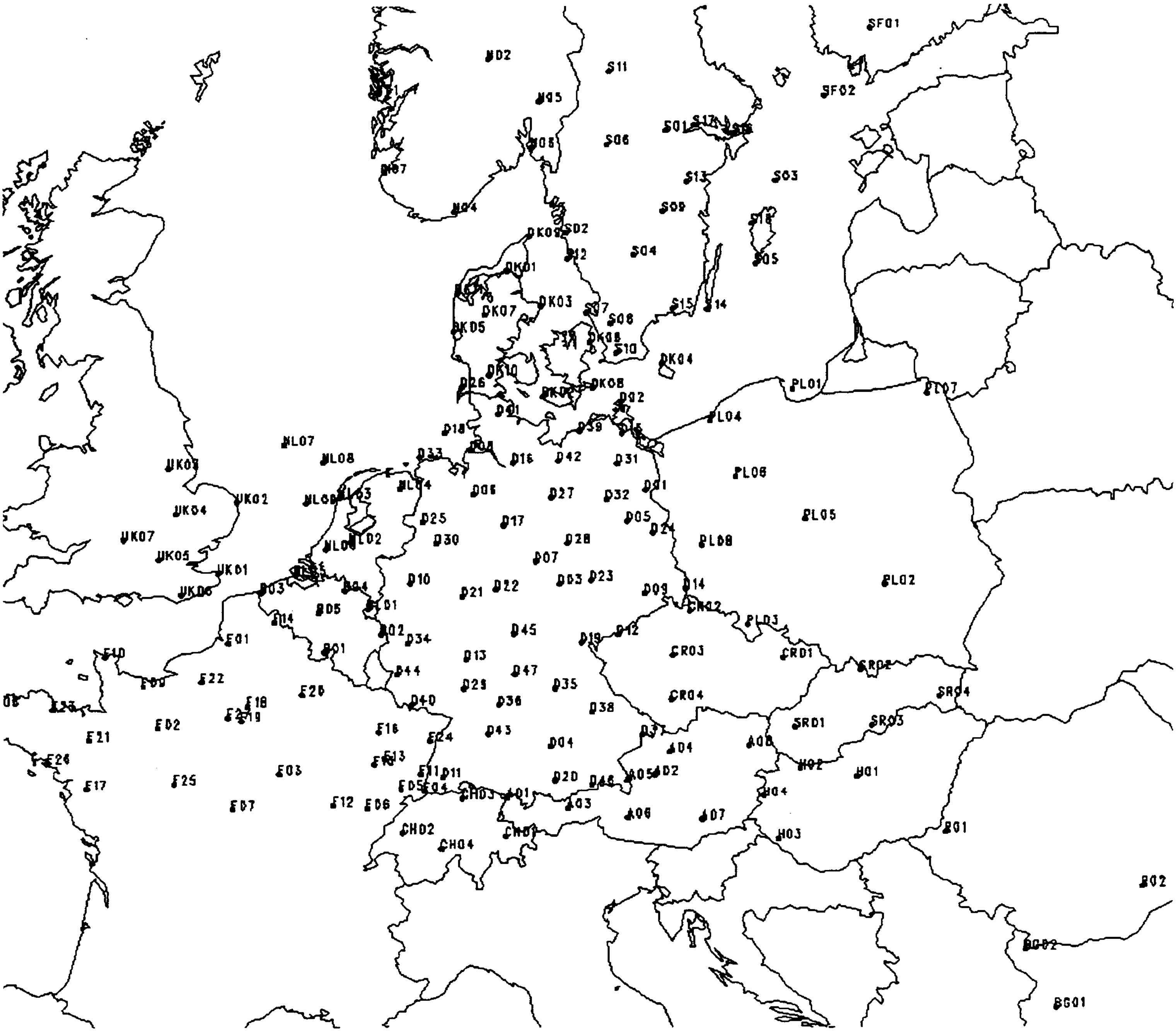

2 Quality validation of analyzed and forecast wind and temperature from the DMI-HIRLAM model

Alix Rasmussen and Jens Havskov Sørensen
Danish Meteorological Institute
Copenhagen, Denmark

2.1 Introduction

A sensitivity study is performed of vertical profiles from the DMI-HIRLAM. The study involves profiles of horizontal wind, temperature, and humidity, in the lower troposphere up to 2500 meters. Detailed comparisons of analyzed, as well as forecast, profiles are made with high-resolution radio-sonde data from Copenhagen (WMO station no. 06181). In general, the resemblance between measurements and DMI-HIRLAM profiles at Jægersborg is quite good, with a mean absolute error (MAE) for temperature around 1.5°K and for wind velocity about 2 m/s. However, especially in unstable and convective conditions, there is a tendency to underestimate the strength of the mixing and thereby large errors in the temperature profiles can occur.

In the present operational version of DMI-HIRLAM the vertical diffusion scheme is based on a local approach (so-called K theory), i.e., the flux of the quantity is proportional to the local gradient of the quantity. Moreover, the proportionality factor (eddy diffusivity) depends on local gradients of mean wind and mean virtual temperature. This applies in the ABL under neutral and stable conditions, while the local approach is not appropriate under unstable and convective conditions. This is due to the nonlocal transport of the convective plumes. Therefore, a nonlocal diffusion scheme has been developed according to (Troen and Mahrt, 1986) and (Holtslag *et al.*, 1990). In the nonlocal scheme, the eddy diffusivity is described by a profile on the basis of diagnosed boundary layer height and a turbulent velocity scale.

This new boundary layer parameterization, together with a new physical package, was implemented in a parallel version of the DMI-HIRLAM in the autumn of '96, resulting in significant improvements in the general weather forecast parameters and especially producing more realistic profiles and deeper unstable boundary layers (Gollvik *et al.*, 1995) and (Woetman-Nielsen, 1996).

2.2 Results

Figures 2.1a-b show verification results for a HIRLAM-test-run for the time period November 11 to November 28, 1996, comparing "new physics" (DKZ) with "old physics" (DKS). For the mean sea level pressure (mslp) the rms-error increases from about 1 hPa to 4 hPa during the forecast up to +36 hour. During the first 12 hours there are only minor differences in the two runs, but for forecastlengths from 18-36 hour the new physics gives about 0.8 hPa lower rms. For the wind velocity at 850 hPa the rms-error increases from about 4 m/s to nearly 8 m/s during the forecast up to +36 hour. In general the difference between the two runs is rather small, but for forecastlength from 18-36 hour the new physics gives about 0.5 m/s lower rms. The verification is based on observation from the about 60 EWGLAM-stations (EWGLAM: European Working Group for Limited Area Modelling) around Europe.

Figures 2.2a-b show the vertical profiles of temperature, dew point temperature and wind observed at the radisonde station Jægersborg and calculated by DMI-HIRLAM (analysis) from July 1, 1994 at 00 UTC and 12 UTC respectively. The observed temperature profiles have a well-defined boundary layer up to about 800 meters, while the height of the boundary layer from the HIRLAM-profile is about 600 meters at 00 UTC and about 700 meters at 12 UTC. The agreement between measurements and the modeled temperature near ground is very good in this case. For the dew point temperature the agreement is fairly good below the inversion. Above the inversion the observed profile is very dry (high pressure with sinking motion), while the HIRLAM not correctly describes this. For the wind direction and velocity the agreement is fairly good for the 00 UTC, while the differences are more pronounced for the 12 UTC case.

Figures 2.3a-b show the mean profiles of the temperature at 00 and 12 UTC, for the period April to June, 1994, respectively the corresponding mean error (ME) and mean absolute error (MAE). Near the ground the HIRLAM mean temperature is too low during day, and almost correct during night. Above about 500 meters the HIRLAM temperature is slightly too high, both during day and night. The MAE near ground is around 1.7°C during night and about 1.2 °C during day, decreasing to about 1.0 °C above 400 meters. The ME near ground is around -1.7 °C during night and about -0.2°C during day, becoming positive above 3-500 meters, indicating that the model profiles are too stable.

Figures 2.4a-b show the mean profile of wind velocity at 00 and 12 UTC for the period July to September, 1994, respectively the corresponding ME and MAE. Generally the HIRLAM mean wind velocity is too high near ground, and the diurnal variations is not correctly described, so the gradient of the model wind velocity can be erroneous. This is especially important if one uses local gradients of, e.g., the Richardson number. The MAE near ground is 2-3 m/s decreasing to about 1.5 m/s higher up.

Table 2.1 summarizes the ME and MAE of the temperature profiles at the 50-meter level for 1994 and 1995. The errors are generally largest for the day-time temperature during summer, with MAE around 2.2°C in 1994 and 1.7°C in 1995, but during the cold weather in the autumn of '95 the model gave too-high temperatures, compared with reality, resulting in a positive bias of 2.4 °C at night and a corresponding MAE of 2.5 °C.

Table 2.1 ME and MAE of the HIRLAM temperature profiles at 50-meter height for Jægersborg, 1994-95.				
Period \ Error	ME (°C) 00 UTC	ME (°C) 12 UTC	MAE (°C) 00 UTC	MAE (°C) 12 UTC
Jan.-Mar., 1994	0.4	-0.7	1.2	1.3
Apr.-June, 1994	0.1	-2.1	1.4	2.4
July-Sept., 1994	1.1	-1.2	1.7	2.0
Oct.-Dec., 1994	1.7	0.3	1.8	1.0
Jan.-Mar., 1995	0.4	-0.5	0.8	1.0
Apr.-June, 1995	0.3	-1.1	1.4	1.7
July-Sept., 1995	0.9	-1.4	1.6	1.7
Oct.-Dec., 1995	2.4	0.6	2.5	1.5

References

Gollvik, S., Bringfeldt, B., Perov, V. and A.A.M. Holtslag "Experiments with nonlocal vertical diffusion in HIRLAM," *Technical Report No. 18*, SMHI (1995).

Holtslag, A.A.M.,. de Bruijn, E.I.F and H.L-Pan, "A high resolution air mass transformation model for short-range weather forecasting,'' *Monthly Weather Review*, **118**, 1561-1575 (1990).

Holtslag, A.A.M., Boville, B.A. and C.-H. Moeng, "Eddy Diffusivity and Countergradients Transport in the Convective Atmospheric Boundary Layer," *J. Atmos. Sci.,* **48**, 1690-1698, (1991).

Källen, E. (Ed.), "HIRLAM documentation manual, System 2.5.'' *Available from SMHI* (1996).

Mahrt, L. "Modelling the depth of the stable boundary-layer," *Boundary-Layer Met.,* **21**, 3-19 (1981).

Rasmussen, A., Svensmark, H. and J.H. Sørensen, "Forecasting Atmospheric Boundary Layer Height," *In preparation.* DMI, Denmark (1997).

Sass, B. H., "The DMI Operational HIRLAM Forecasting System, Version 2.3,'' *DMI Technical Report 94-8*, DMI, Denmark (1994).

Troen, I. and L. Mahrt, "A simple model of the atmospheric boundary layer. Sensitivity to surface evaporation", *Boundary-Layer Meteorol.,* **37**, 129-149, (1986).

Vogelsang, D.H.P. and A.A.M. Holtslag, "Evaluation and model impacts of alternative boundary-layer height formulations," *Submitted for publication in Boundary-Layer Meteorol.*, (1996).

Woetman-Nielsen, N., "Nonlocal versus local vertical diffusion in HIRLAM: An intercomparison study." HIRLAM Newsletter, No. 25, (1996).

Figures 2.1a-b Verification results for mean sea level pressure (mslp) respectively wind at the 850 hPa level for a HIRLAM-test-run for the period Nov 11 to Nov 28, 1996, comparing "new physics" (DKZ) with "old physics" (DKS). The x-axis is forecast length in hours

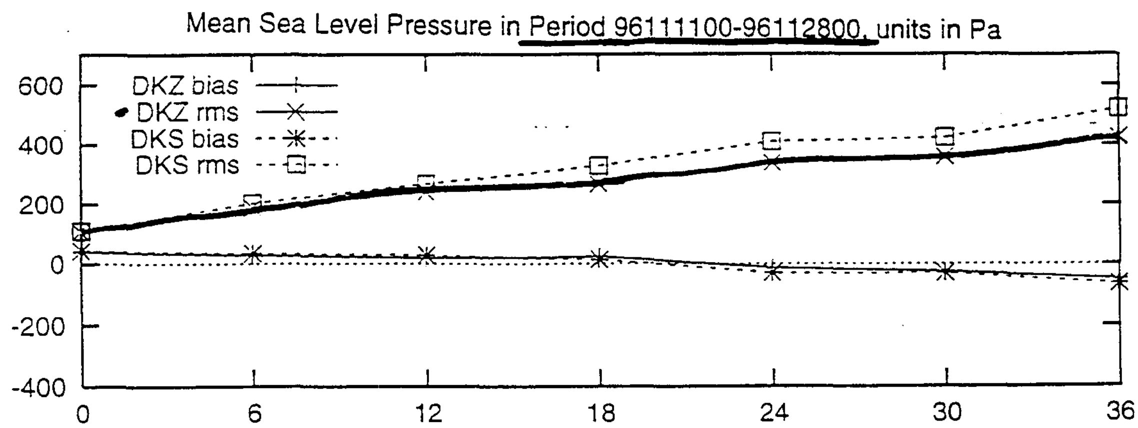

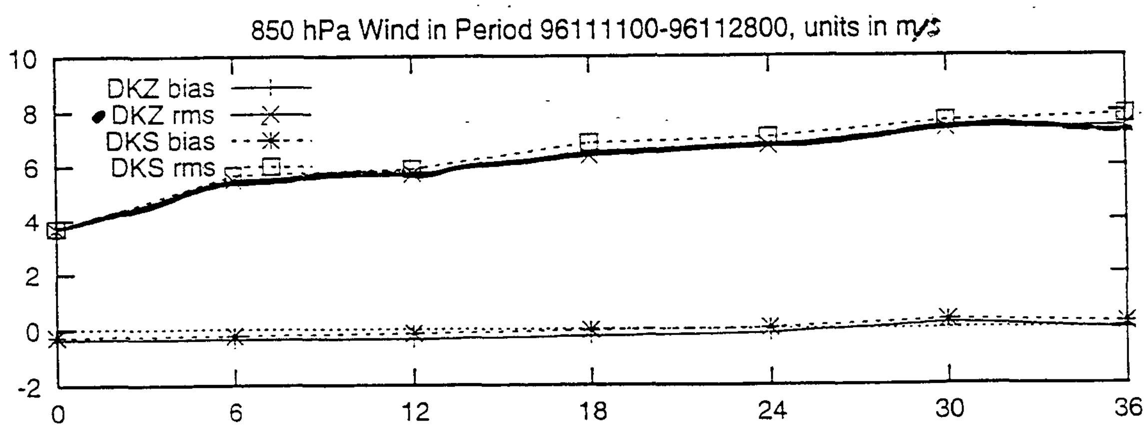

Figures 2.2a-b Profile from July 1, 1994, 00 UTC respectively 12 UTC of temperature (TT), dew point temperature (Td) and wind (WMO-standard) observed at Jægersborg and calculated by DMI-HIRLAM

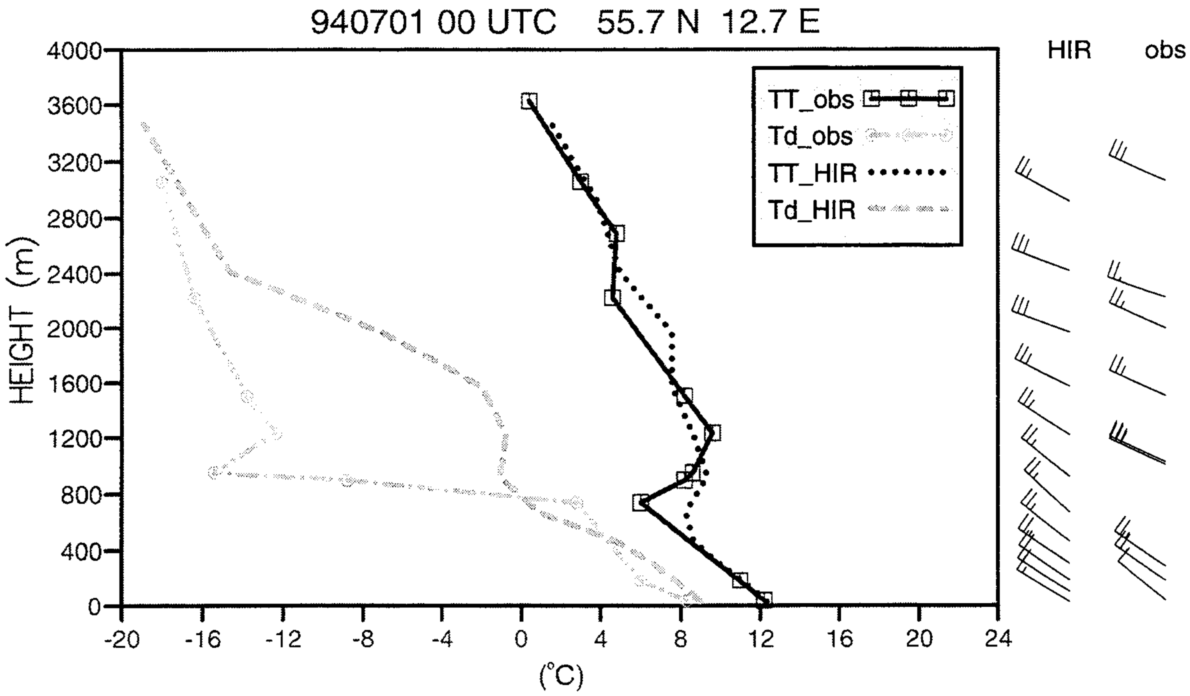

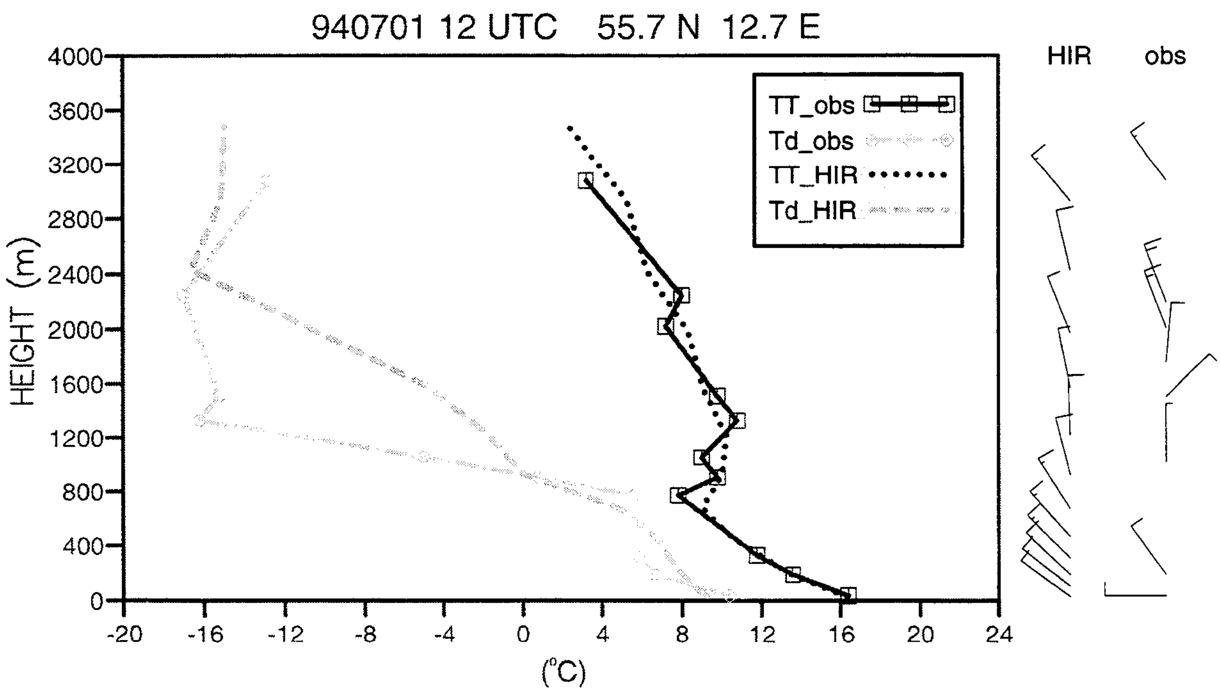

Figures 2.3a-b Mean profiles of the temperature at 00 and 12 UTC, for the period April to June, 1994, respectively the corresponding mean error (ME) and mean absolute error (MAE)

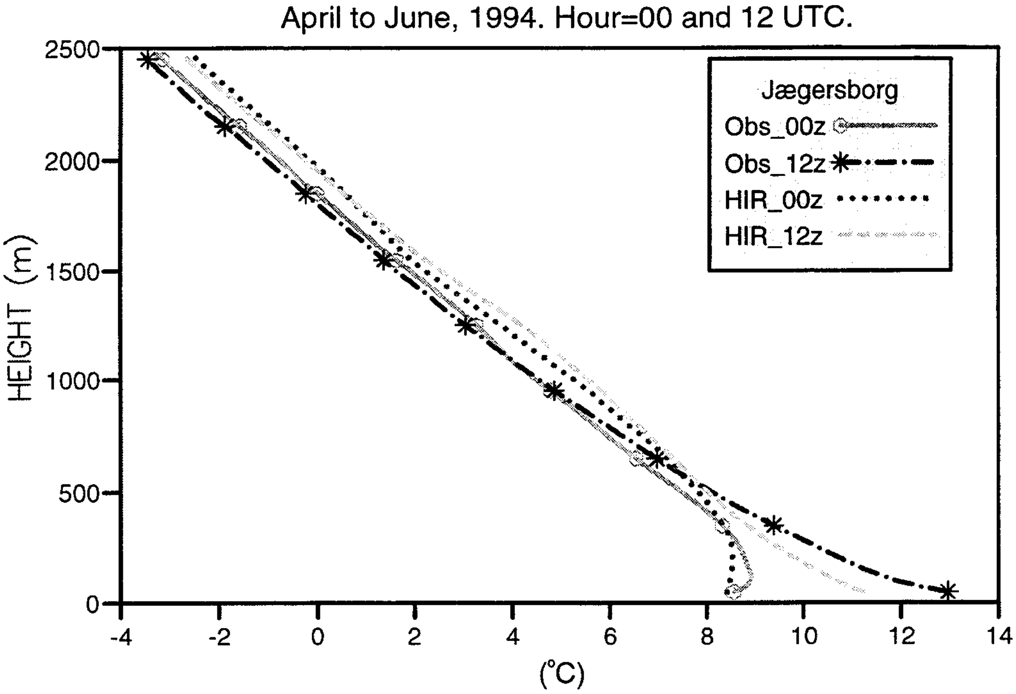

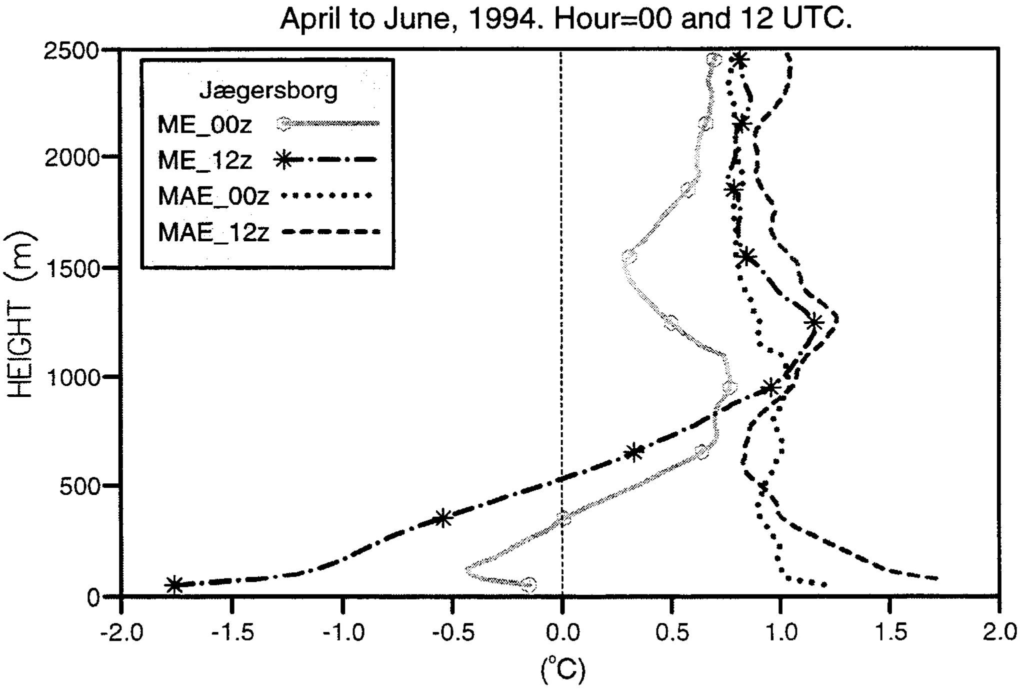

Figures 2.4a-b Mean profile of wind velocity at 00 UTC and 12 UTC for the period July to September, 1994, respectively the corresponding mean error (ME) and mean absolute error (MAE)

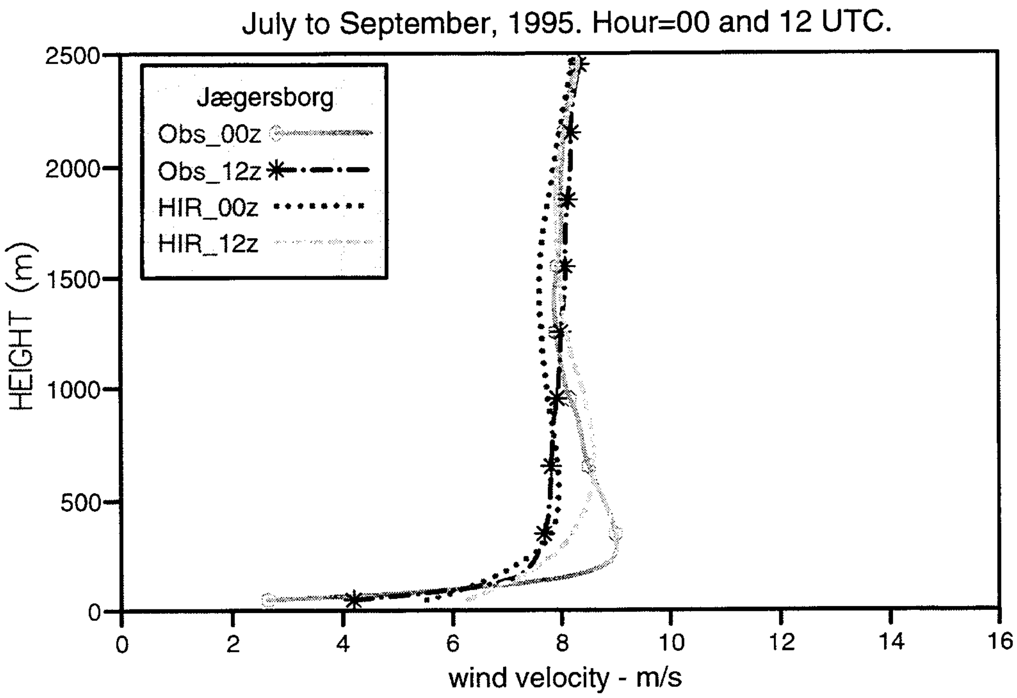

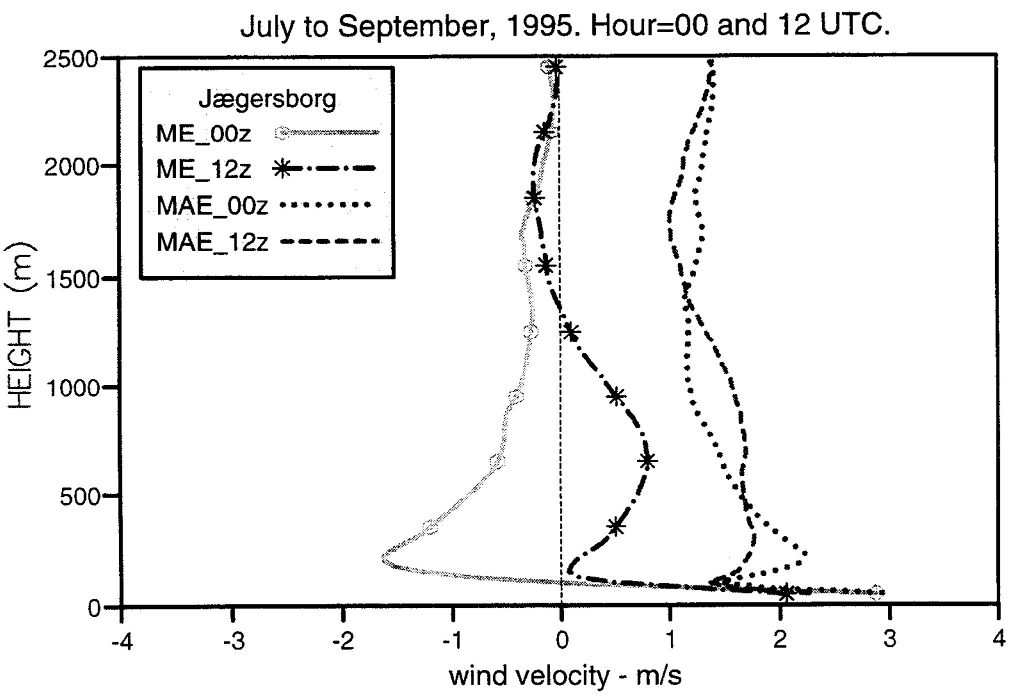

3 Evidence for mesoscale influence on long-range transport obtained from DERMA, DMI-HIRLAM and ETEX observations by NERI

Jens Havskov Sørensen
Danish Meteorological Institute
Copenhagen, Denmark

Atmospheric dispersion calculations corresponding to the ETEX releases are performed by using the Danish Emergency Response Model of the Atmosphere (DERMA) (Sørensen and Rasmussen, 1995; Sørensen *et al.,* 1997).

DERMA uses numerical weather prediction (NWP) model data from the DMI-HIRLAM model (Sass, 1994; Källén, 1996) or from the global ECMWF model. Presently, the version of the operational DMI-HIRLAM model covering most of Europe has a horizontal resolution of about 23 km, and 31 layers in the vertical. Meteorological analyses are performed each 6 hours, and forecast fields are produced with 3-hour time resolution.

DERMA is a three-dimensional long-range transport model using a multi-level puff parametrization assuming complete mixing in the Atmospheric Boundary Layer (ABL). The ABL height is estimated by a bulk Richardson number approach. This is a robust and fairly accurate method which is suited for use in situations with limited vertical resolution, e.g. output from NWP models. The bulk Richardson number at height z above ground is calculated by

$$\mathrm{Ri_B} = \frac{gz(\theta_v - \theta_s)}{\theta_s(u^2 + v^2)}.$$

The top of the ABL is given by the height at which the bulk Richardson number reaches a critical value (0.25).

In the horizontal, a Gaussian distribution of the concentration is assumed for each puff. From Gifford's random-force theory we obtain

$$\sigma_y^2 = 2K_y t_L \left\{ \tau - \left(1 - e^{-\tau}\right) - \frac{1}{2}\left(1 - e^{-\tau}\right)^2 \right\}.$$

This expression has the following well-known asymptotic behavior,

$$\sigma_y^2 = \begin{cases} 2K_y t & \text{for} \quad t >> t_L, \\ \frac{2}{3} K_y t_L^{-2} t^3 & \text{for} \quad t << t_L. \end{cases}$$

The quantity τ is the travel time in units of the Lagrangian time scale, t_L, for which a value of 10^4 s was used. For the horizontal eddy diffusivity, K_y, a value of 6×10^4 m^2/s was used in the ETEX real-time exercise. This value was suggested by (Hanna *et al.,* 1991). However, as this value applies to the total plume width, it is influenced by inhomogeneities in the wind field within the spatial extent of the plume as well as orographic distortion effects. For a multi-puff model like DERMA a smaller value should be used.

In the ATMES-II phase of ETEX the results of DERMA were fitted to the measured tracer gas concentrations from the first experiment. The best fit was, in fact, obtained by using a ten-fold lower value.

Regarding vertical diffusion for puffs inside the ABL, the assumption of complete mixing is employed while for puff centers above the ABL, a Gaussian distribution is assumed for the vertical spatial distribution with

$$\sigma_z^2 = 2K_z t_L \left\{ \tau - \left(1 - e^{-\tau}\right) - \frac{1}{2}\left(1 - e^{-\tau}\right)^2 \right\} = \left(K_z / K_y\right) \sigma_y^2 .$$

For the ETEX simulations the value of the vertical eddy diffusivity, K_z, was set to 1 m^2/s in the DERMA program.

In *Figures 3.1 and 3.2* results of calculations with DERMA for the first ETEX release are presented. 1 m^2/s in DERMA. The calculated surface concentrations were not sensitive to this parameter.

Figure 3.1 shows the tracer gas surface concentrations at 24, 48 and 72 hours after the start of the release, and in *Figure 3.2* the gas cloud 48 hours after the start of the release is represented by a concentration isosurface corresponding to the tracer gas background concentration.

During the first ETEX experiment, the National Environmental Research Institute (NERI) in Denmark performed two sets of measurements at Risø near Roskilde by using two different techniques (Ellermann and Lyck, 1995; Sørensen *et al.,* 1997). Although the ETEX data have not yet been cleared for publication, the measurements by NERI are not part of the official ETEX data set, and they can accordingly be presented here. These measurements are one-hour average concentrations whereas the ETEX measurements are three-hour averages. The accuracy of the measurements are ±25%.

The calculations of DERMA using low-resolution meteorological data from ECMWF are shown in comparison with the measurements by NERI in *Figure 3.3*. The arrival time is a few hours too late but the duration of the cloud passage and the maximum concentration agree well with the observations. The double-peak structure, however, is not represented by the calculations. Using high-resolution data from DMI-HIRLAM instead, the agreement with the measurements is very much better, as can be seen in *Figure 3.4*, and the double-peak structure is nicely reproduced.

According to DERMA in combination with DMI-HIRLAM high-resolution data, the double peak is explained by the influence of a small horizontal eddy on the tracer gas plume between one and two days before the plume arrived at Risø. The anti-cyclonic mesoscale eddy, which was superimposed on the general flow, was confined to the ABL. It was relatively short-lived with a lifetime of about 9 hours. The eddy implied a toroidal perturbation of the plume, and the double peak in the concentration time series at Risø is due to this ring-shaped structure of the plume passing over Risø. The eddy had a similar effect at 9 of the official ETEX sampling stations. A closer study of the background of the double-peak structure is presented by Sørensen *et al.* (1997).

References

Ellermann T. and Lyck E. (1995) ETEX-1 Tracer Measurements at Risø. In: *Report of the Nordic Dispersion/Trajectory Model Comparison with the ETEX-1 Full-scale Experiment,* Eds.: Tveten U. and Mikkelsen T., pp. 11-16. *Risø-R-847(EN), NKS EKO-4(95)1,* ISBN 87-550-2118-2, ISSN 0106-2840

Hanna S. R., Gifford F. A. and Yamartino J. (1991) Long range radioactive plume transport simulation model/code - phase I. Technical Report NRC-04-90-374. *Available from the U.S. Nuclear Regulatory Commission*

Källén E., Ed. (1996) HIRLAM documentation manual, System 2.5. *Available from the Swedish Meteorological and Hydrological Institute (SMHI)*

Sass B. H. (1994) The DMI Operational HIRLAM Forecasting System, Version 2.3. *DMI Technical Report* **94-8**, ISSN 0906-897X

Sørensen J. H. and Rasmussen A. (1995) Calculations Performed by the Danish Meteorological Institute. In: *Report of the Nordic Dispersion/Trajectory Model Comparison with the ETEX-1 Full-scale Experiment,* Eds.: Tveten U. and Mikkelsen T., pp. 16-27. *Risø-R-847(EN), NKS EKO-4(95)1,* ISBN 87-550-2118-2, ISSN 0106-2840

Sørensen J. H., Rasmussen A., Ellermann T. and Lyck E. (1997) Mesoscale Influence on Long-range Transport; Evidence from ETEX Modelling and Observations. Submitted for publication in *Atmos. Environ.*

Figure 3.1 One-hour average tracer gas concentrations calculated by DERMA based on DMI-HIRLAM data. The sub-figures show concentrations at 24, 48 and 72 hours after the start of the first ETEX release

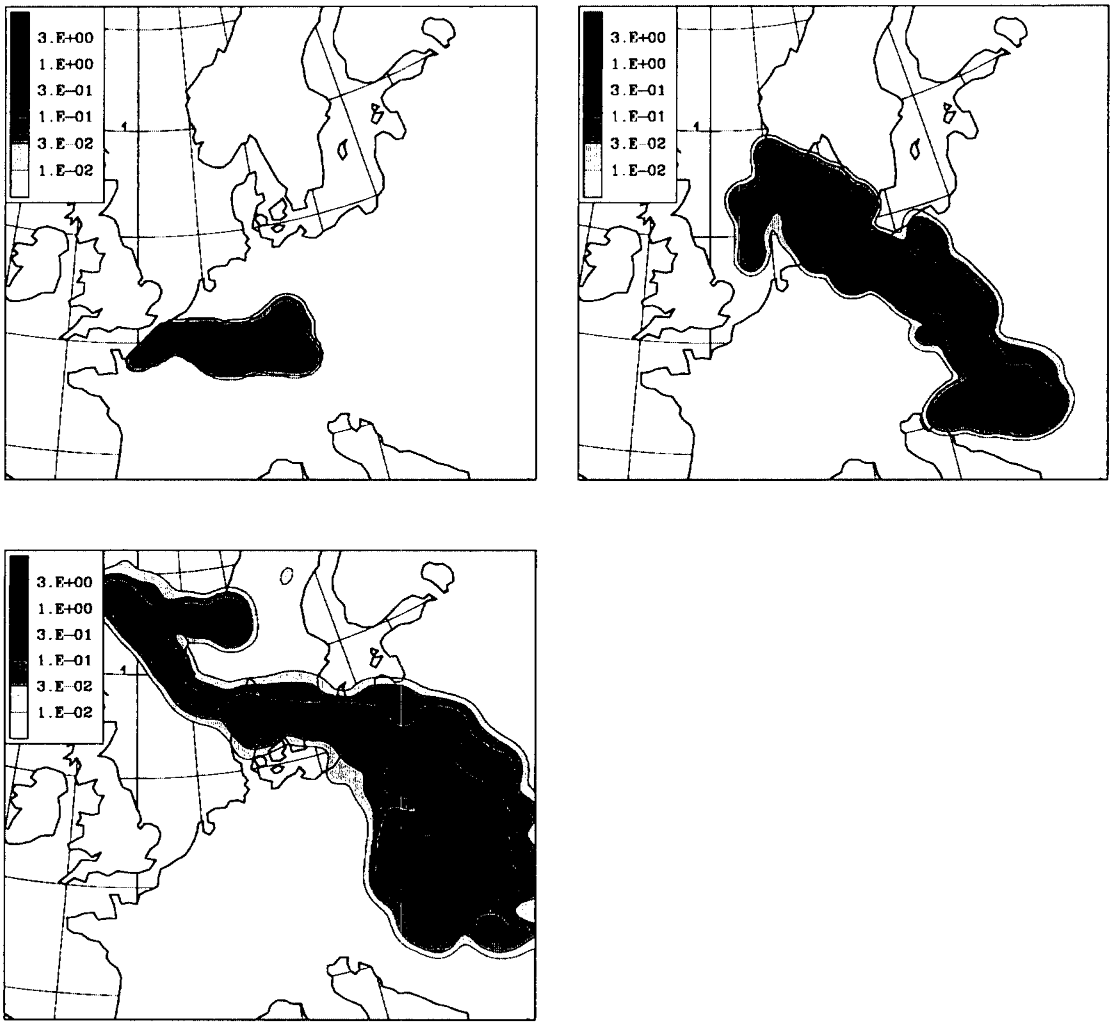

Figure 3.2 The DERMA tracer gas cloud 48 hours after the start of the first ETEX release shown as a concentration isosurface corresponding to the background concentration

Figure 3.3 Tracer gas concentrations at Risø as calculated by DERMA based on ECMWF data (thick curve) in comparison with measurements by NERI (thin curve).

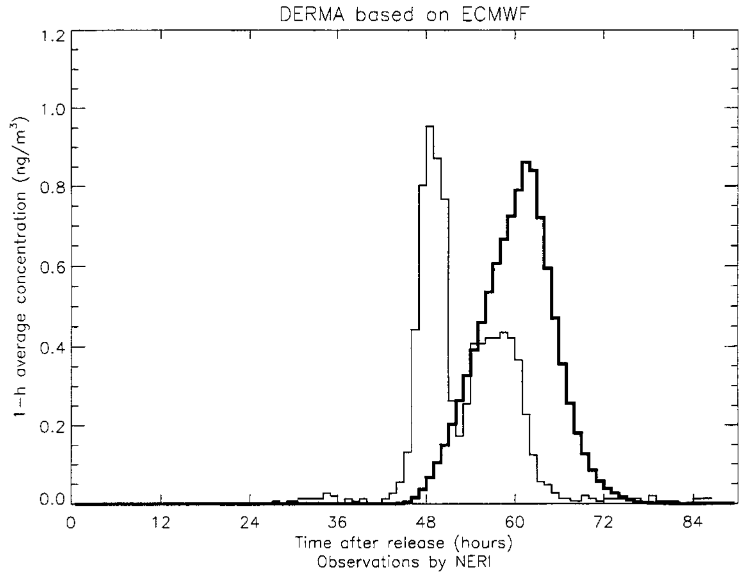

Figure 3.4 Tracer gas concentrations at Risø as calculated by DERMA based on DMI-HIRLAM data (thick curve) in comparison with measurements by NERI (thin curve).

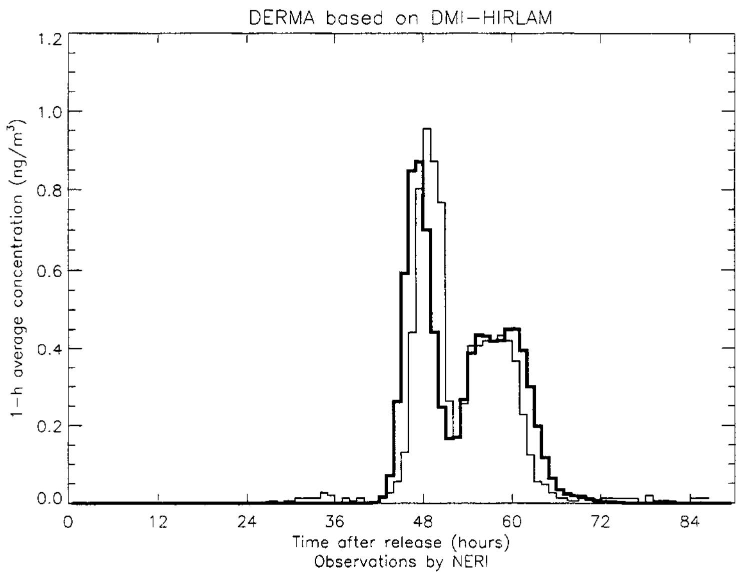

4 The Danish Rimpuff and Eulerian Accidental release Model (the DREAM) - Results with ETEX-1

Jørgen Brandt[1) 2)]
Zahari Zlatev[1)]
Torben Mikkelsen[2)]
Søren Thykier-Nielsen[2)]

[1)] **National Environmental Research Institute**
[2)] **Risø National Laboratory**

A tracer model for studying transport and dispersion of accidental releases from a single, but strong source, is under development. The model is a combination of the Lagrangian meso-scale model, RIMPUFF (RIsø Meso-scale PUFF model) (Thykier-Nielsen and Mikkelsen, 1993), and the Eulerian long-range transport model, DEM (the Danish Eulerian Model) (Zlatev, 1995). The combined model is called the DREAM (the **D**anish **R**impuff and **E**ulerian **A**ccidental release **M**odel) (Brandt et al., 1996a, 1996b, 1996c). The meteorological meso-scale model MM5V1 (Grell et al., 1995) is used as a meteorological driver for the transport model. Coupling of the transport model with MM5V1 gives a better spatial and temporal resolution of the input data, which is used in the transport model. Especially the better description of the planetary boundary layer is essential for modeling the transport and dispersion of air pollutants. Different parameterizations of the mixing height and of the vertical dispersion can be used in the model. Some results from ETEX-1 (the European Tracer Experiment) are shown.

The DREAM model is a combination of two models, DEM and RIMPUFF, where the latter two have the characteristics shown in the Table below.

DEM	**RIMPUFF**
Eulerian	Lagrangian
Finite element scheme used for solving the advection and dispersion	Puff model
Dispersion: K-approach, with different parameterizations for K in the vertical	Dispersion: Karlsruhe-Jülich $\tilde{\sigma}_{xy} = a\, x^b$, where a and b are stability dependent parameters
Long-range	Meso-scale
Horizontal resolution: 25 km	Horizontal resolution: 5 km

The model system flow chart is shown schematically in *Figure 4.1*.

The TERRAIN/LANDUSE, DATAGRID and INTERP modules are preprocessors for interpolation of analyzed data to the meteorological meso-scale model MM5V1. Output from MM5V1 is given to the transport model, DREAM. The analyzed data can also be given directly as input to the transport model. Source data are given to RIMPUFF, which calculates the initial dispersion of the release in the area around the location of the source. The Eulerian model is operating in the whole model area. Different techniques have been developed and employed for visualization and animation of output data from MM5V1 and DREAM, both one- and two-dimensional (UNIRAS) and three-dimensional (VIS5D).

Transport and dispersion in the Eulerian model is described by the equation and applied on a polar-stereographic projection

$$\frac{\partial C}{\partial t} = -\left(u\frac{\partial C}{\partial x} + v\frac{\partial C}{\partial y} + \dot{\sigma}\frac{\partial C}{\partial \sigma}\right) + \left(K_x\frac{\partial^2 C}{\partial x^2} + K_y\frac{\partial^2 C}{\partial y^2} + \frac{\partial}{\partial \sigma}(K_\sigma\frac{\partial C}{\partial \sigma})\right) + E(x, y, \sigma, t)$$

$$\sigma = \frac{P - P_t}{P_s - P_t}$$

where the vertical discretization is in σ-coordinates with 16 vertical σ-levels. The top of the model domain is at pressure P_t = 100 hPa, but can have different values, depending on the limitations of the input data. The horizontal dispersion coefficients are constant

$$K_x = K_y = 10000 \text{ m}^2/\text{s}$$

Different parameterizations of K_σ are available in the model:

- Parametrization based on Monin-Obukhov similarity theory with different flux-profile relations (Hass, 1991, Christensen, 1995)
- Louis parameterization (Louis, 1979)
- Parameterization based on the critical Richardsons number (Grell et al., 1995)

Eddies may not be resolved in the horizontal because the horizontal grid-size is normally much larger than the size of the eddies. The vertical grid-size is, however, much smaller than the horizontal grid-size and vertical mixing from these eddies is resolved. In the unstable boundary layer, local K-theory neglects the influence of large eddy transport. Some of the larger eddies in a turbulent region can advect air parcels across large vertical distances before smaller eddies mix the parcels with the environment. Such a process is non-local rather than diffusive. A scheme for simulating this non-local dispersion is under development, and will be included in the future.

Transport and dispersion in the Lagrangian model is described by releasing a series of Gaussian shaped puffs. Each puff is advected and dispersed individually along trajectories. The concentration at a given location x,y,σ is given by a sum over all puffs P.

$$C_{x,y,\sigma} = \sum_{p=1}^{P} \frac{M_p\, g\,(\sigma_{c_p} + \phi)}{(2\pi)^{3/2}\, \tilde{\sigma}_{xy_p}^{2}\, \tilde{\sigma}_{\sigma_p}\, R\, T}$$

$$\times \exp\left(-\frac{1}{2}\left(\left(\frac{x - x_{c_p}}{\tilde{\sigma}_{xy_p}} \right)^2 + \left(\frac{y - y_{c_p}}{\tilde{\sigma}_{xy_p}} \right)^2 \right) \right)$$

$$\times \left[\begin{array}{l} \exp\left(-\dfrac{1}{2}\left(\dfrac{\sigma_{c_p} + \phi}{\tilde{\sigma}_{\sigma_p}} \ln\left(\dfrac{\psi_{c_p}}{\psi} \right) \right)^2 \right) \\ + \exp\left(-\dfrac{1}{2}\left(-\dfrac{\sigma_{c_p} + \phi}{\tilde{\sigma}_{\sigma_p}} \ln\left(\psi\, \psi_{c_p} \right) \right)^2 \right) \\ + \exp\left(-\dfrac{1}{2}\left(\dfrac{\sigma_{c_p} + \phi}{\tilde{\sigma}_{\sigma_p}} \ln\left(\dfrac{\psi\, \psi_{c_p}}{2\psi_H} \right) \right)^2 \right) \end{array} \right]$$

where M_p is the mass in the puff p, (x_{c_p}, y_{c_p}, σ_{c_p}) is the center coordinate of the puff p and $\tilde{\sigma}_{xy_p}$ and $\tilde{\sigma}_{\sigma_p}$ are the horizontal and vertical standard deviations, respectively.

The first term at the right side is the concentration in the center of a given puff p. The second term represents the horizontal distribution, and the last three terms the vertical distribution with reflection from the ground and from the mixing height ψ_H. ψ is defined as

$$\psi = \frac{\sigma(P_S - P_t) + P_t}{P_S}, \quad \phi = \frac{P_t}{P_S - P_t}$$

where P_s is the surface pressure.

The puffs are Gaussian distributed in the horizontal, but in vertical they have been transformed from z-coordinates to σ-coordinates, so that the puffs are not Gaussian in the σ-coordinate system.

The individual puffs are incorporated individually into the Eulerian model when the puffs reach the boundary of the Lagrangian model area (Brandt et al., 1996a), which is illustrated in *Figure 4.2* for a single puff.

Parameterization of the planetary boundary layer is performed using a revised version of the Blackadar high-resolution PBL scheme (Grell et al., 1995). The mixing height can be parameterized by three different methods:

- Parameterization by dry parcel method (Hass, 1991)
- Parameterization based on the energy balance for the internal boundary layer (Christensen, 1995)
- Parameterization based on the bulk Richardson number (Robertson *et al.,* 1996)

The height of the planetary boundary layer is an important parameter for modeling transport of air pollutants. Different parameters, which are needed for calculating the mixing height are shown in *Figures 4.3 - 4.6.* The roughness length is dependent on the landuse. *Figure 4.3* shows some of the landuse categories in the model domain. There are 13 different landuse categories:

1 = urban land, 2 = agriculture, 3 = range-grassland, 4 = deciduos forest,
5 = coniferous forest, 6 = mixed forest and wet land, 7 = water, 8 = marsh or wet land,
9 = desert, 10 = tundra, 11 = permanent ice, 12 = tropical or sub tropical forest and
13 = savanna.

Examples of the friction velocity, surface temperature and surface heat flux, at the time of the release of ETEX-1, are given in *Figures 4.4 - 4.6.* High values of the friction velocity are found in areas of high wind speeds and high values of the roughness lengths. The surface heat flux (*Figure 4.6*) is calculated as a function of the difference between the temperature of the ground (shown in *Figure 4.5*) and the temperature at the lowest model level. Negative heat fluxes corresponds to downward fluxes (i.e. from the air to the ground), as seen over large parts of Europe in *Figure 4.6,* and positive heat fluxes means upward flux as seen over large parts of the Atlantic Ocean and the Mediterranean.

Different examples of the mixing height, at the time of release of ETEX-1, are shown in *Figures 4.7 - 4.10.* In *Figures 4.7 and 4.8* input data from MM5V1 have been used and in *Figures 4.9 and 4.10* data from ECMWF (with 0.5 degree resolution) have been used. Two different parameterizations of the mixing height are shown for comparison. In *Figures 4.7 and 4.9* the energy balance scheme is used and in *Figures 4.8 and 4.10* the parameterization based on the bulk Richardson number is used. The meteorological data from ECMWF do not cover the whole model domain. In the outer areas, where ECMWF data are missing, the MM5V1 data are implemented. The two types of parametrizations show, on large scale, similar patterns. There are, however, large differences on the local scale in different parts of Europe. The method based on the bulk Richardson number seems to give sharper gradients and higher extremes, while the parametrization based on the energy balance for the internal boundary layer is more smooth. Major differences, between the calculations where MM5V1 data have been used and the calculations where ECMWF data have been used, are seen in Central Europe, where the mixing height calculated with data from ECMWF is much lower. This is mainly due to the smaller wind velocities in these regions compared to MM5V1.

Surface concentrations from ETEX-1, 12 and 48 hours after start of release, using input data from MM5V1 and from ECMWF, are shown in *Figures 4.11 - 4.14*. The square in the Figures indicates the area where the Lagrangian model is operating. In all four figures are the mixing height parameterized using the energy balance scheme and the vertical dispersion in the Eulerian model is parameterized based on Monin-Obukhov similarity theory. Large differences are seen in the general distribution of the plume, especially in the situation 48 hours after start of release. The results, where MM5V1 data have been used, show a more detailed structure compared to the simulations where ECMWF data have been used. This is also clearly seen in *Figures 4.15 and 4.16*, which show three-dimensional iso-surfaces (surface of constant concentration at 0.01 ng/m^3) of the plumes, 48 hours after start of release (notice, that the top of the model domain is different in the two Figures).

Comparison of model results with measurements at Risø is shown in *Figures 4.17 and 4.18*. Measurements are performed by Thomas Ellermann and Erik Lyck, National Environmental Research Institute, Denmark (Brandt et al., 1996b). Both of the model results (both input data from MM5V1 and ECMWF) seem to miss the first peak in the measurements, but according to Jens Havskov Sørensen, Danish Meteorological Institute (pers. comm.), the first peak is a result of small scale effects, which is not included in the meteorological input data used in this study.

Future research in the following areas is planned:

- Dry and wet deposition will be implemented in the model.

- Non-local dispersion, large eddy simulation (under convective conditions).

- Vertical discretization (the present calculation has been performed with 16 layers. The model will be extended to 30 layers in the future)

- Precise land-use data are important for proper parameterizations of the planetary boundary layer (roughness length, deposition velocities, etc.).

Some additional calculations from ETEX-1 were also shown for the locations Risø and Jægersborg, that are only about 20 km apart. The results of the calculations were very different; much more than would be expected for positions so close together. It was remarked that it is important to remember that such large differences over short distances can occur, in the calculations. It really means that, in an emergency context, the predictions for a specific geographic position have a corresponding uncertainty.

It was mentioned that there is a land-use data base at Cologne University and also at RIVM in the Netherlands (used by the HIRLAM group). Some figures (from Cologne) were shown, but it was evident both for Finland and Norway that there were obvious disagreements with local knowledge on where there is agriculture and forest.

References

Brandt, J., T. Mikkelsen, S. Thykier-Nielsen and Z. Zlatev, 1996a: "Using a combination of two models in tracer simulations". Mathematical and Computer Modelling. Vol. 23, No. 10, pp. 99-115, 1996.

Brandt, J., T. Ellermann, E. Lyck, T. Mikkelsen, S. Thykier-Nielsen and Z. Zlatev, 1996b: "Validation of a combination of two models for long-range tracer simulations". Proceedings of the 21st NATO/CCMS International Technical Meeting on Air Pollution Modelling and its Application, held in Baltimore, Maryland, USA, November 6-10, 1995. Air Pollution Modelling and Its Application XI. Edited by S. Gryning and F. A. Schiermeier, Plenum Press, New York, 1996, pp. 461-469.

Brandt, J., T. Mikkelsen, S. Thykier-Nielsen and Z. Zlatev, 1996c: "The Danish Rimpuff and Eulerian Accidental release Model (The DREAM)". Proceedings from the European Geophysical Society XXI Assembly, Hague, Netherlands, May 6-10, pp. 4. In print.

Christensen, J. H., 1995: Transport of Air Pollution in the Troposphere to the Arctic. Ph.D. thesis. National Environmental Research Institute, Roskilde, Denmark. September 1995, pp. 377.

Grell, G. A., J. Dudhia and D. R. Stauffer, 1995: A Description of the Fifth-Generation Penn State/NCAR Mesoscale Model (MM5). NCAR/TN-398+STR. NCAR Technical Note. June 1995, pp. 122. Mesoscale and Microscale Meteorological Division. National Center for Atmospheric Research. Boulder, Colorado.

Hass, H, 1991: Description of the EURAD Chemistry-Transport-Model, Version 2 (CTM2). Mitteilungen aus dem Institut für Geophysik und Meteorologie der Universität zu Köln. Herausgeber: A. Ebel, F.M Neubauer, P. Speth. Heft 83.Köln 1991, pp. 100.

Louis, J. F., 1979: A Parametric Model of Vertical Eddy Fluxes in the Atmosphere. Boundary Layer Meteorology, 17, 1979, pp. 187-202.

Robertson, L., L. Langner and M. Engardt, 1996: MATCH - Meso-scale Atmospheric Transport and Chemistry modelling system. Basic transport model description and control experiment with ^{222}Rn. Swedish Meteorological and Hydrological Institute, S-601 76 Norrköping, Sweden, RMK No. 70, pp. 37, September 1996.
Thykier-Nielsen, S. and T. Mikkelsen, 1993: RIMPUFF, Users Guide, Version 33 (PC version). Report, Risø National Laboratory, Roskilde, Denmark, 1993, pp. 60.

Zlatev, Z., 1995: Computer Treatment of Large Air Pollution Models. Environmental Science and Technology Library. Volume 2. Published by Kluwer Academic Publishers, P.O. Box 17, 3300 AA Dordrect, The Netherlands, 1995, pp. 358.

Figure 4.1 Main modules for MM5V1 and DREAM and flow chart for the whole model system

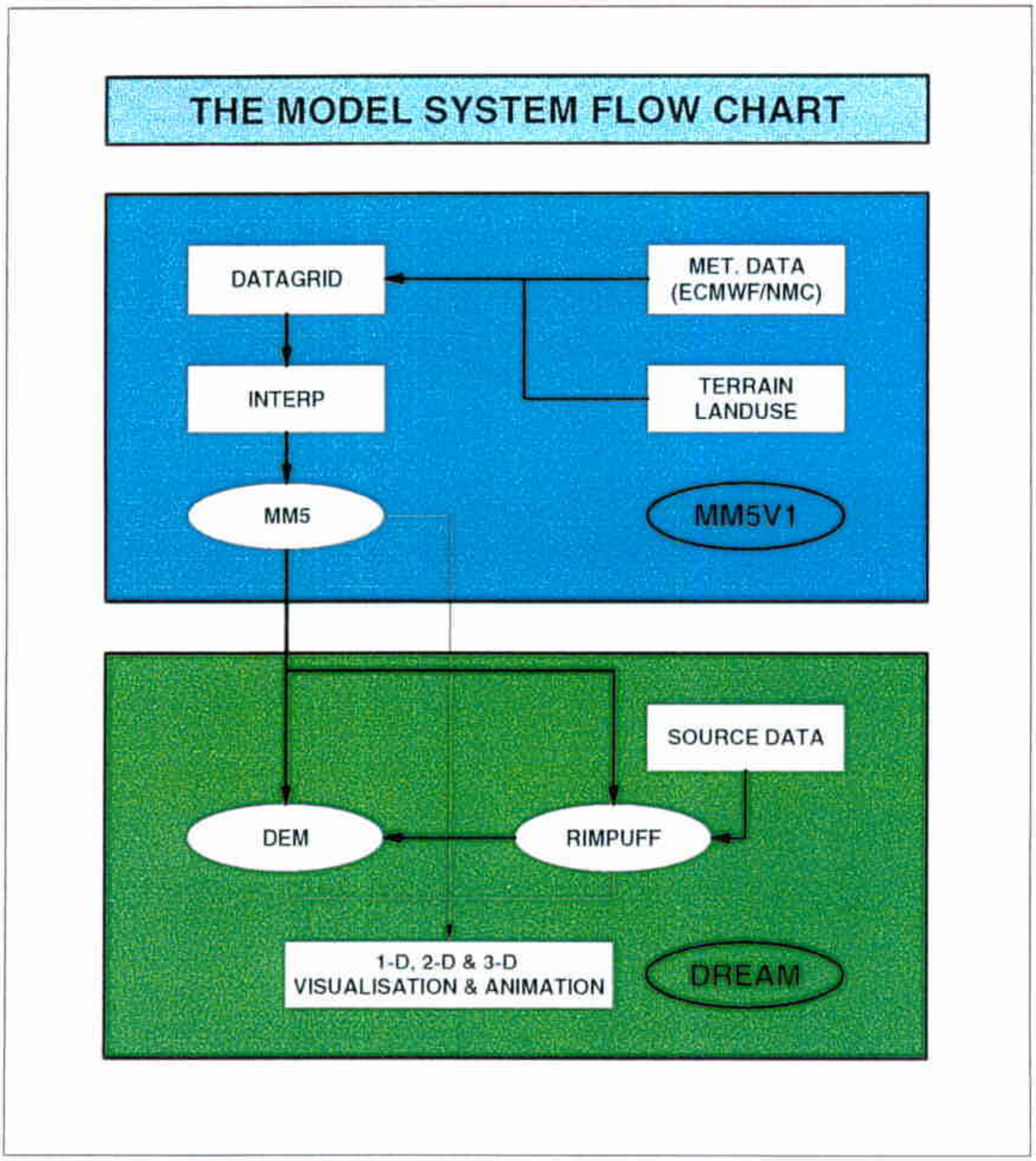

Figure 4.2 Illustration of the coupling between the Lagrangian model and the Eulerian model

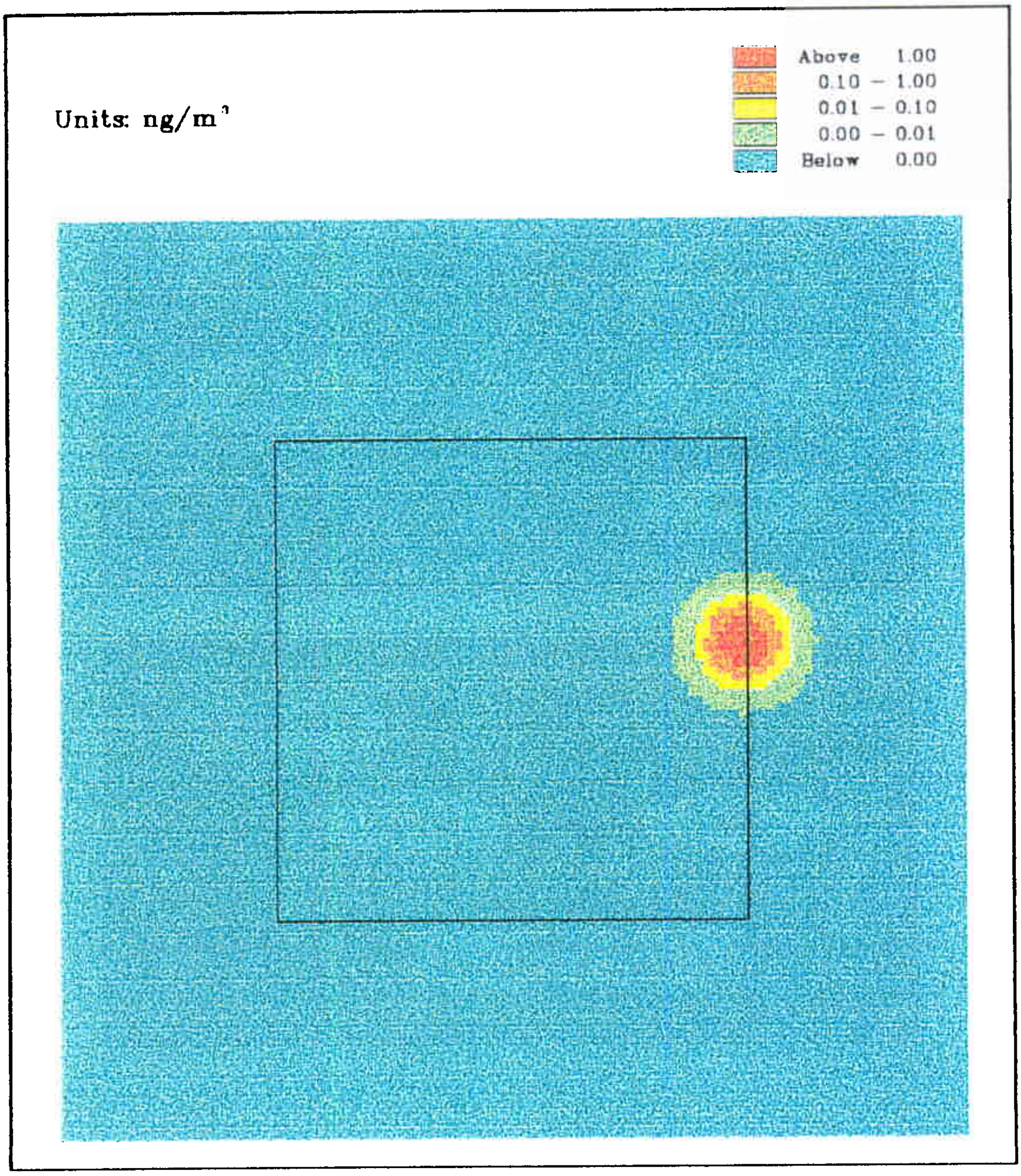

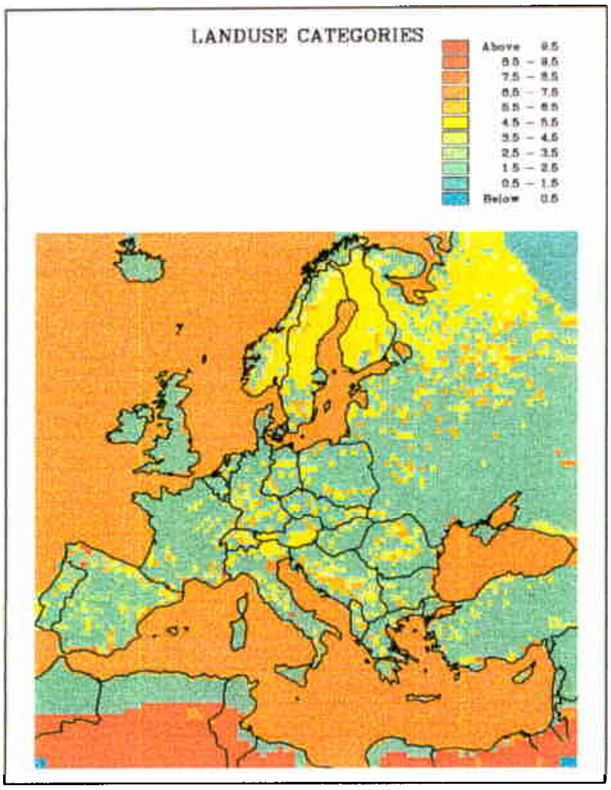

Fig. 4.3. Landuse categories used in the model system. See text for explanation.

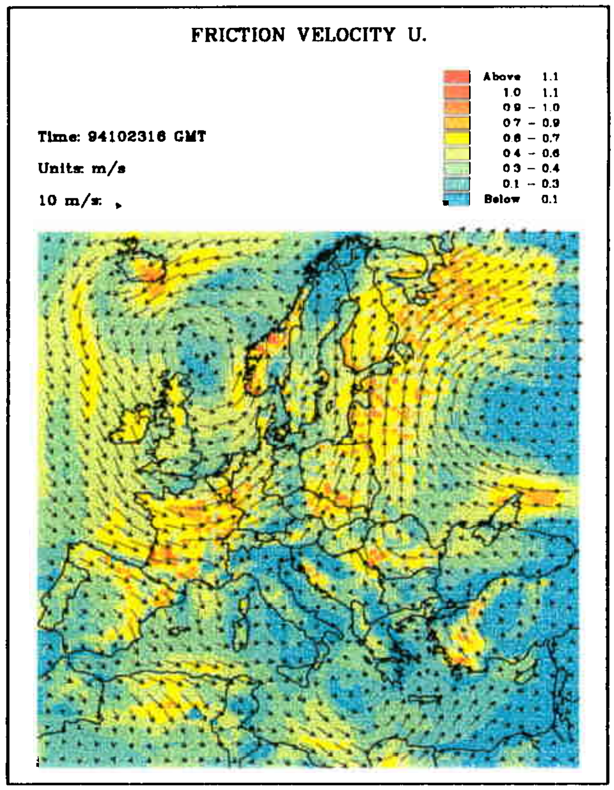

Fig 4.4. Friction velocity U* at the time of release of ETEX-1.

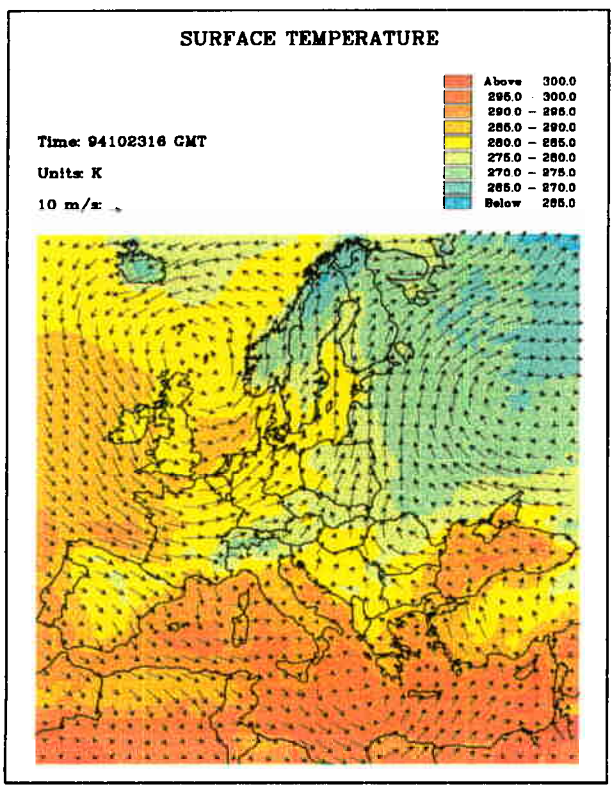

Fig. 4.5. Surface temperatures at the time of release of ETEX-1.

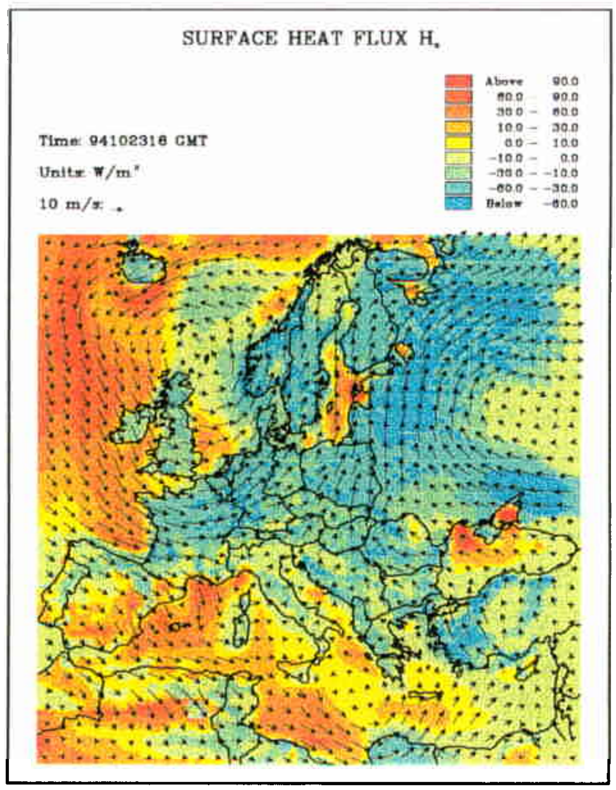

Fig 4.6. Surface heat flux at the time of release of ETEX-1.

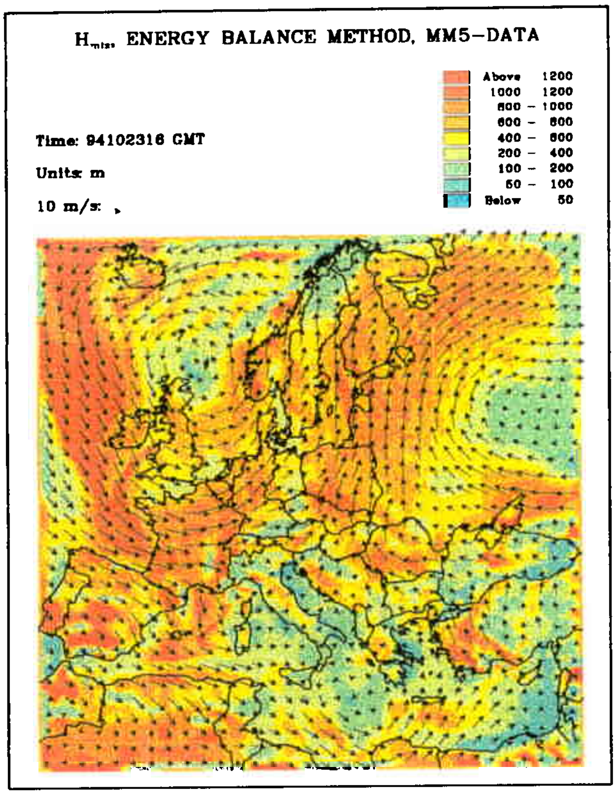

Fig. 4.7. Mixing height, calculated from energy balance and MM5-data.

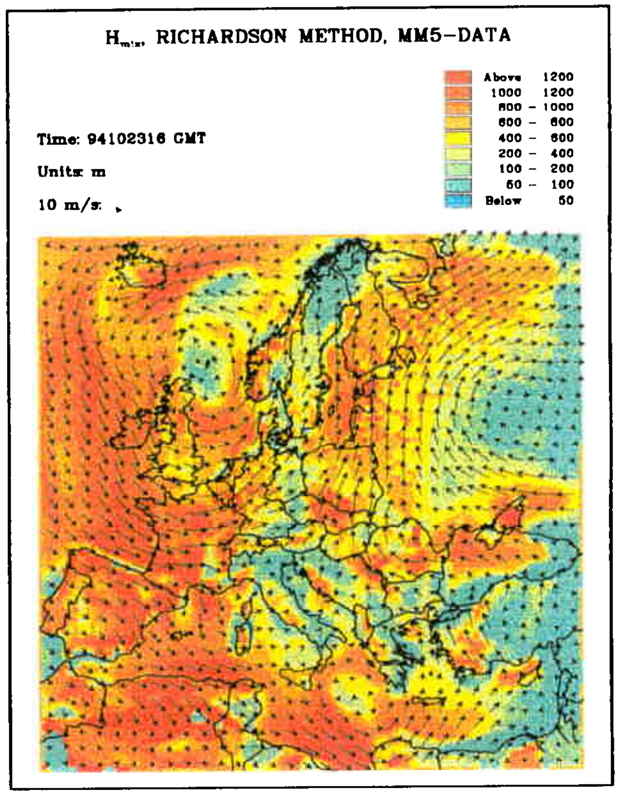

Fig. 4.8. Mixing height, calculated from bulk Richardson number and MM5-data.

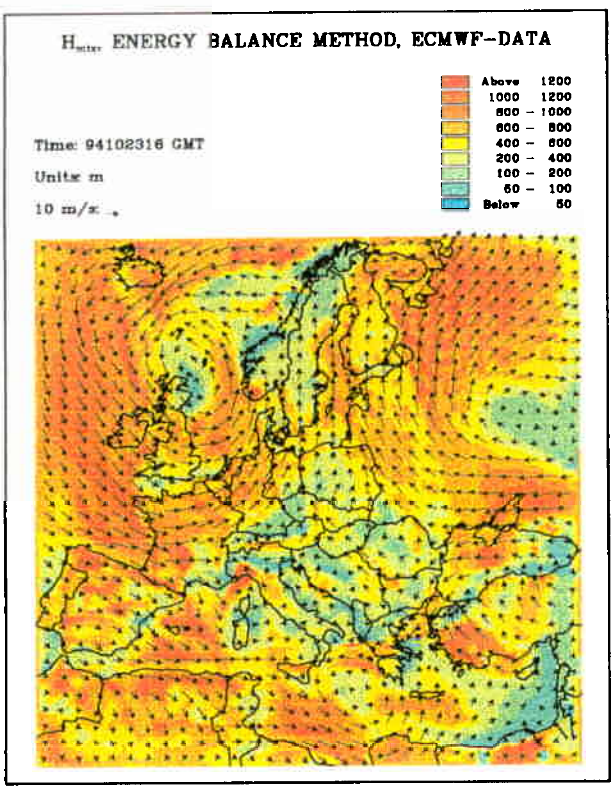

Fig. 4.9. Mixing height, calculated from energy balance and ECMWF-data.

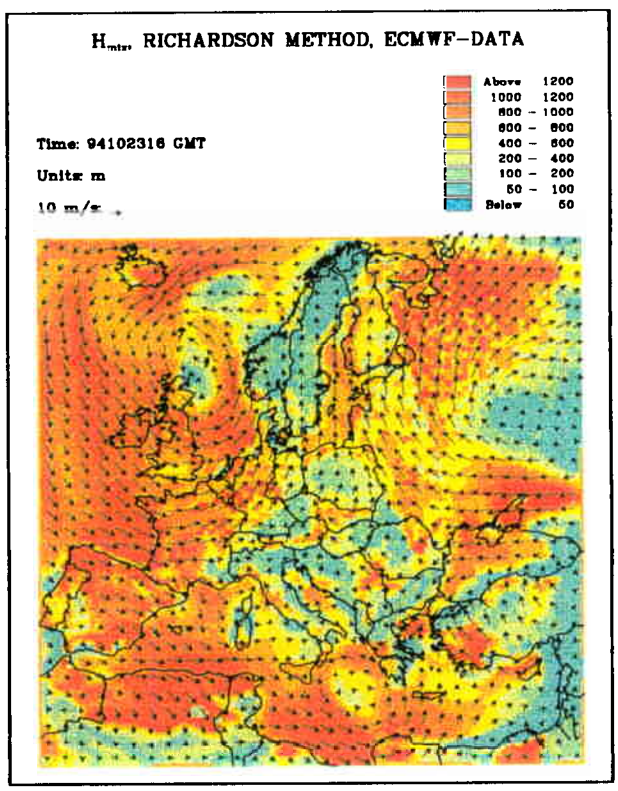

Fig. 4.10. Mixing height, calculated from bulk Richardson number and ECMWF-data.

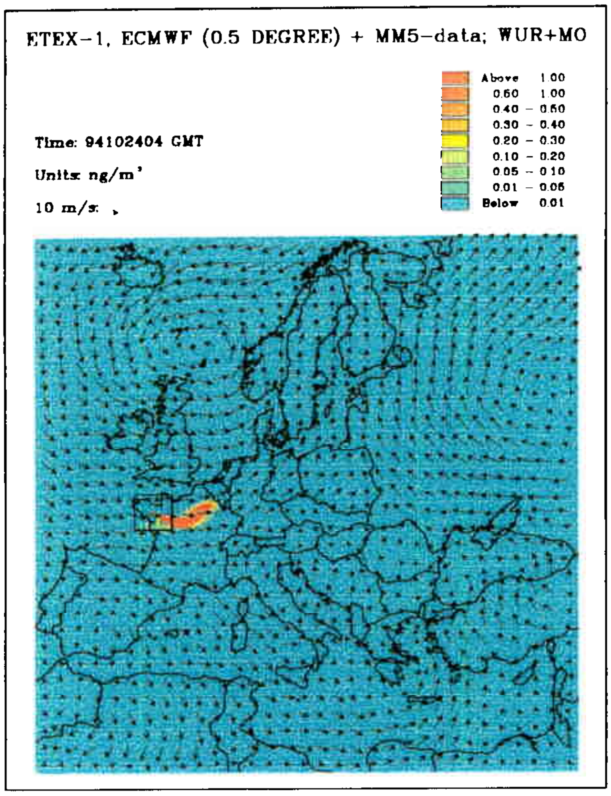

Fig 4.11. ETEX-1, with input data from ECMWF, 12 hours after start of release.

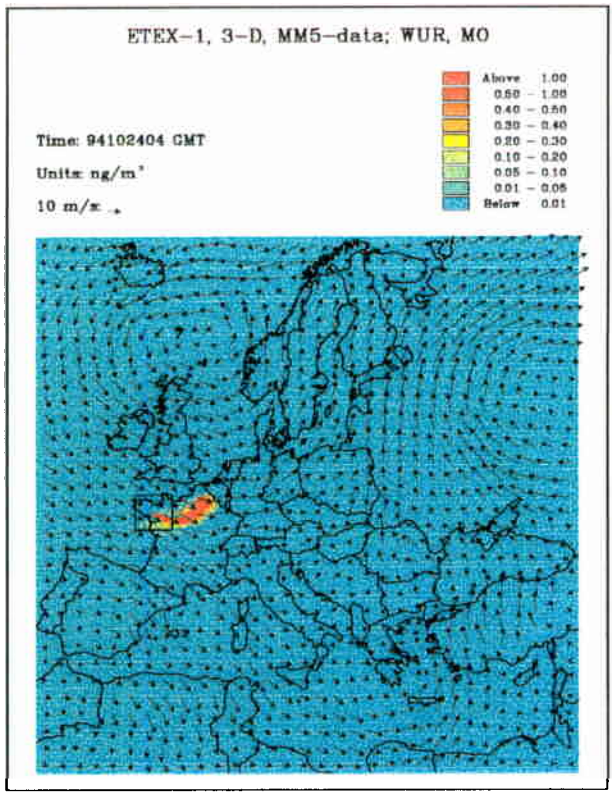

Fig. 4.12. ETEX-1, with input data from MM5V1, 12 hours after start of release.

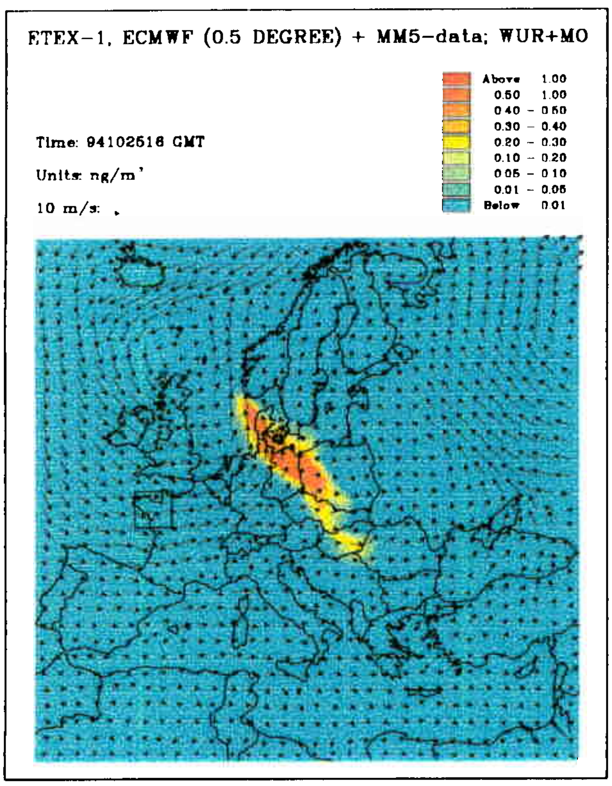

Fig. 4.13. ETEX-1, with input data from ECMWF, 48 hours after start of release.

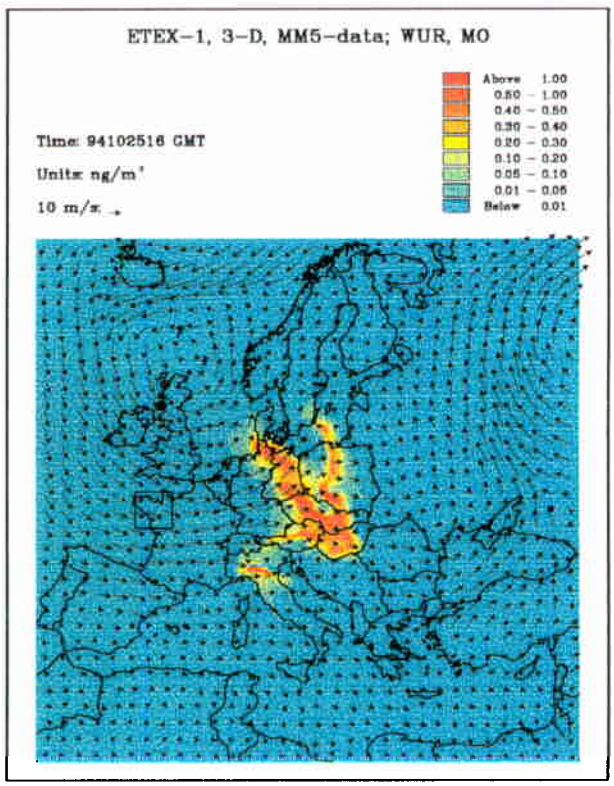

Fig. 4.14. ETEX-1, with input data from MM5V1, 48 hours after start of release.

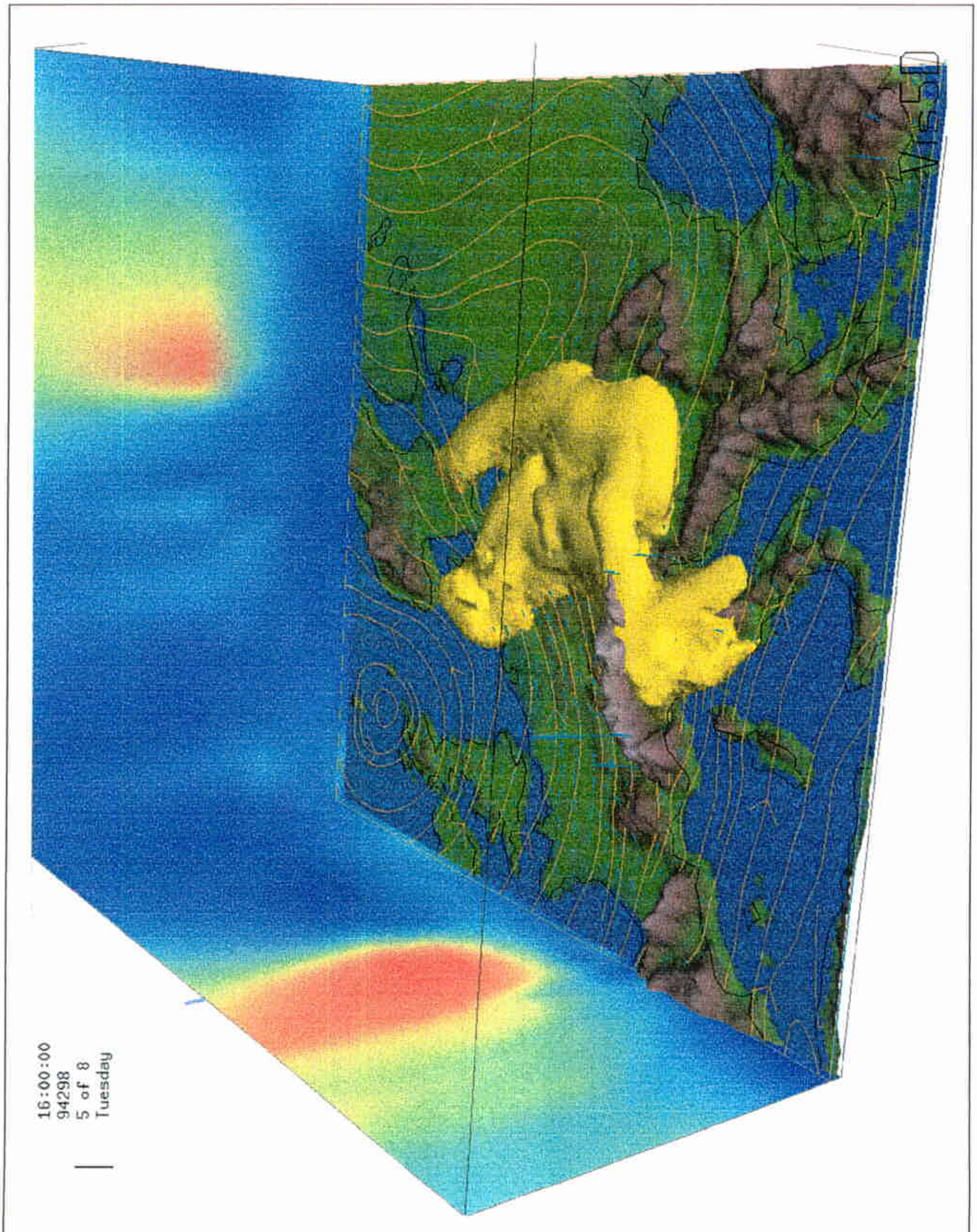

Fig 4.15. Iso-surface (constant at 0.01 ng/m^3) of the concentrations, 48 hours after start of release of ETEX-1, calculated with input data from MM5 (compare with figure 4.14). Top of model domain is at 100 hPa.

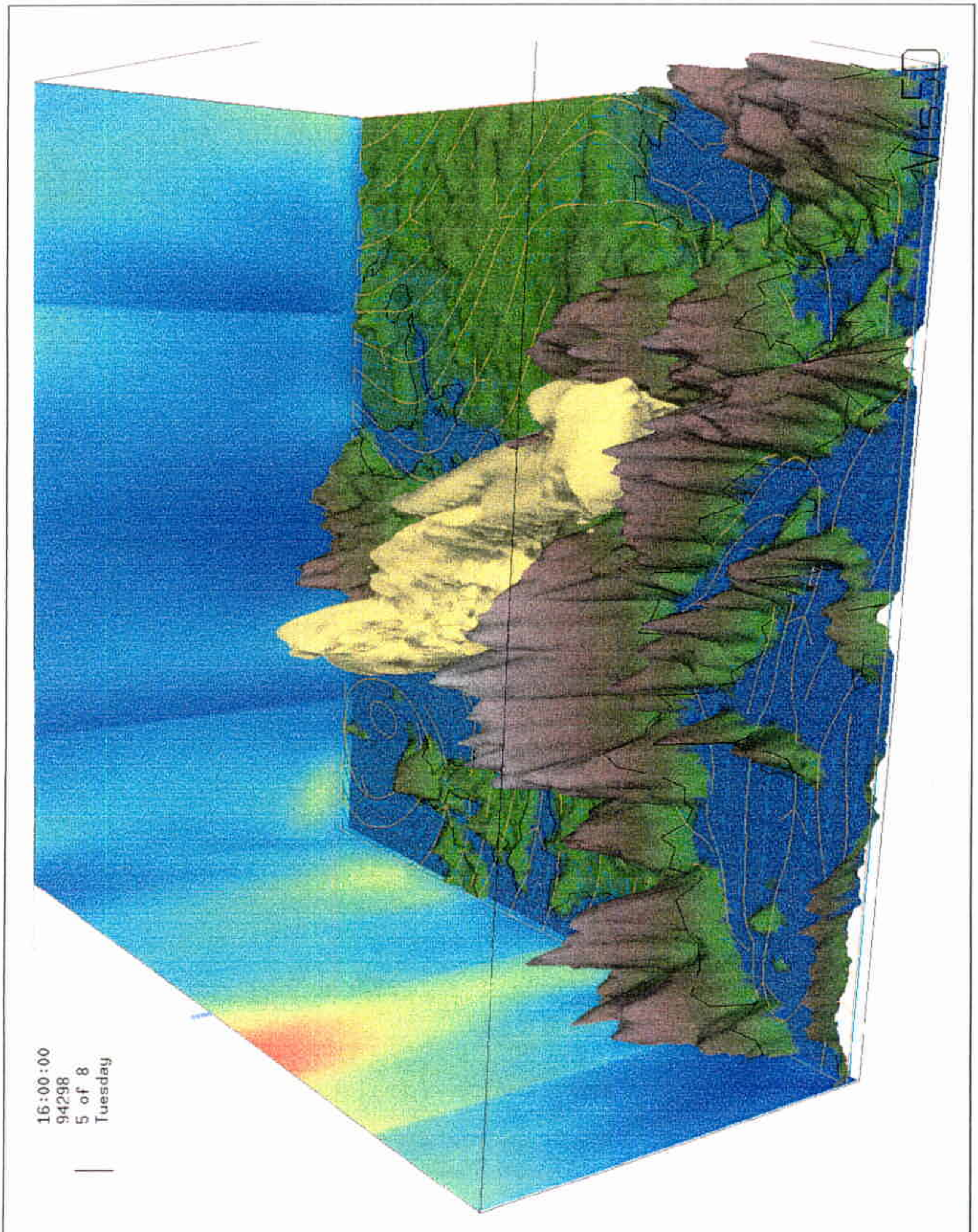

Fig 4.16. Iso-surface (constant at 0.01 ng/m^3) of the concentrations, 48 hours after start of release of ETEX-1, calculated with input data from ECMWF (compare with figure 4.13). Top of model domain is at 600 hPa.

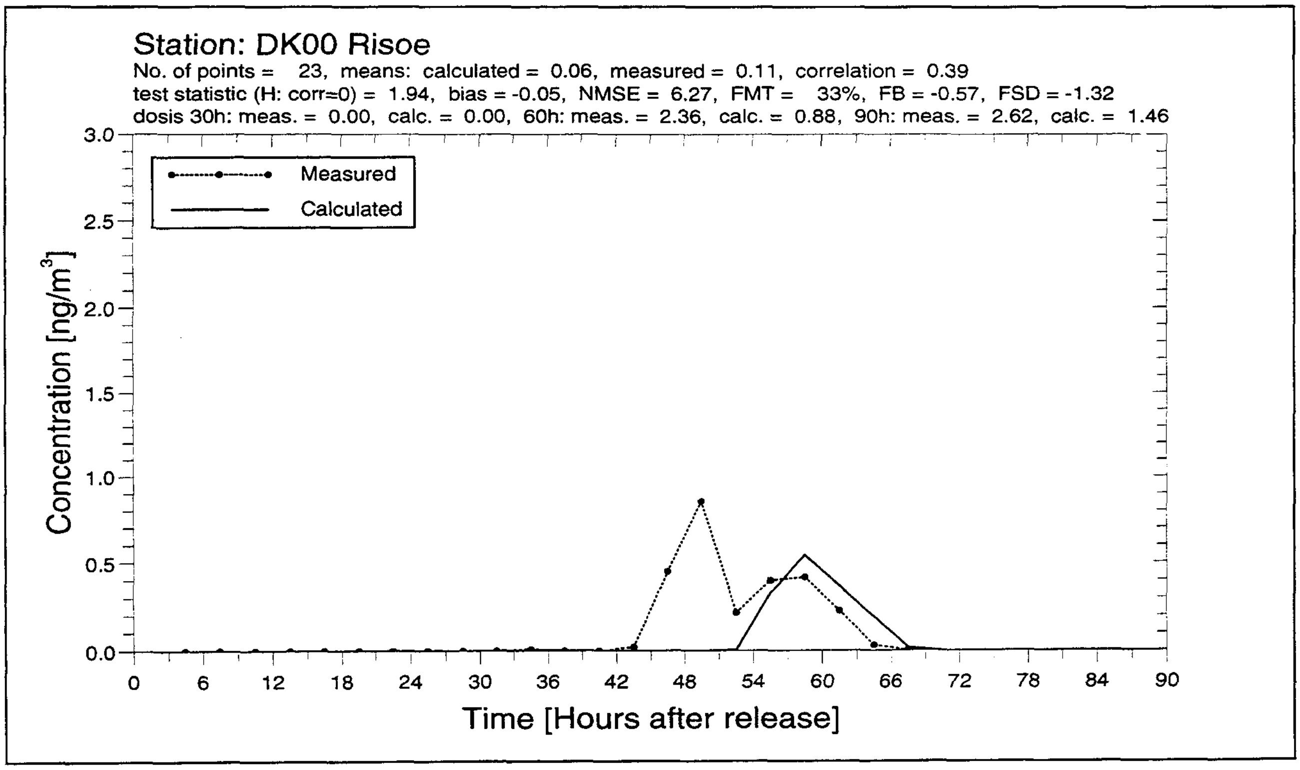

Fig. 4.17. Comparison of model results with measurements at Risø. The calculations has been performed using input data from MM5V1.

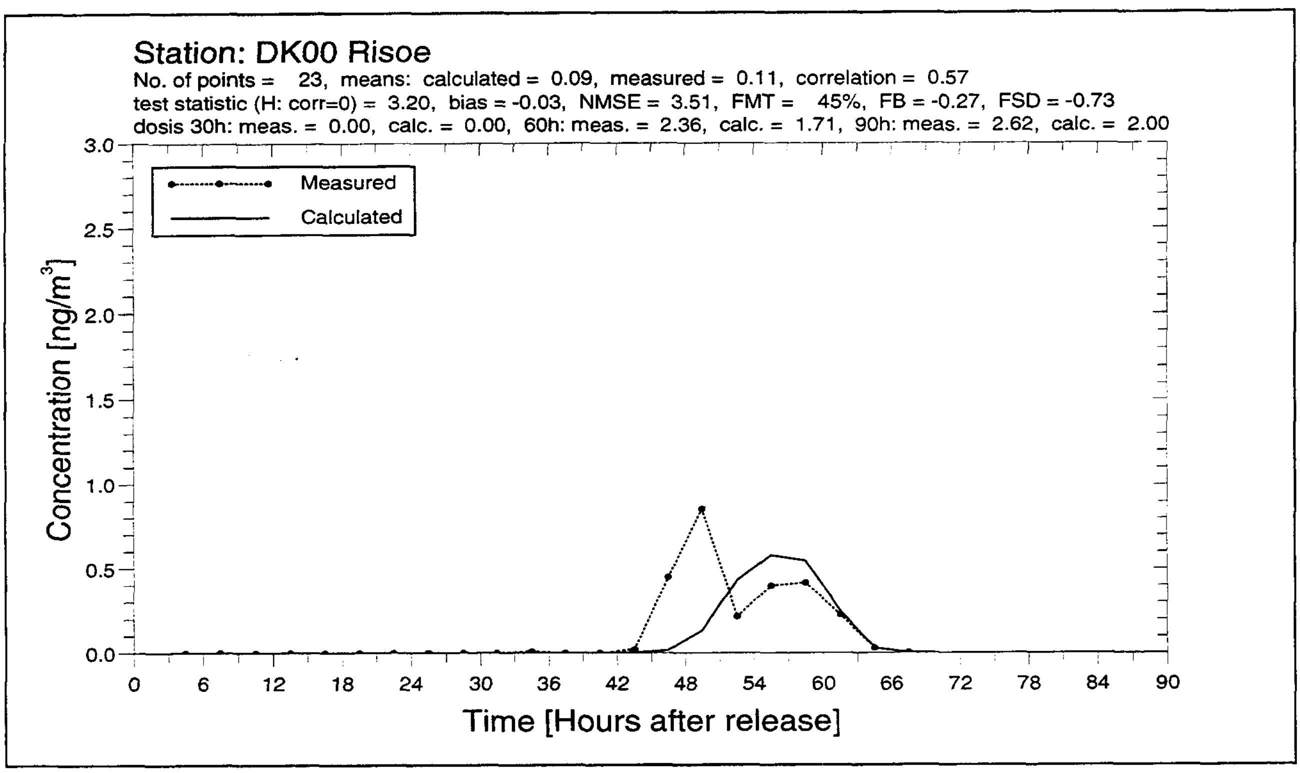

Fig. 4.18. Comparison of model results with measurements at Risø. The calculations has been performed using input data from ECMWF.

5 The ETEX experiment - The Finnish results and conclusions

Ilkka Valkama
Finnish Meteorological Institute
Helsinki, Finland

The Finnish Meteorological Institute (FMI) maintains an operational long range trajectory model for dispersion forecasting during nuclear accidents and other emergencies. The current accident model is the TRADOS model (TRajectory, Dispersion and dOSe model). The first version of this model was already available at the time of the Chernobyl accident. At that time the model was run on rather low resolution (150 km mesh) meteorological data. After the ATMES study (Klug et al., 1992) some major modifications were made, and in the beginning of the 1990's the HIRLAM meteorological model was implemented. The updated version of TRADOS was used in the European Tracer EXperiment (ETEX) calculations in 1994.

The preliminary results showed that while the HIRLAM implementation improved the horizontal (a 55 km mesh) and vertical resolutions as well as the wet deposition parametrization, many of the basic formulations, most notably the atmospheric boundary layer height and boundary layer stability, are still rather inadequately described. Solutions used are stable and work well, but are too rigid and also somewhat dependent on the source of the weather data (the NWP model). This developed some problems with the ECMWF data during ETEX-II (the ATMES-type analysis).

The ETEX first phase can be summarized by the following conclusions. Comparing the TRADOS computed temporal and spatial concentration patterns with the measurements shows that the overall evolution of the dispersion is realistic. The similarity between our concentration fields and those of the more advanced dispersion models in ETEX is reasonable. The arrival of the plume at the monitoring stations is adequately described.

On the other hand the TRADOS plume is usually much narrower, in the direction of plume advection (x-direction), than that given by the other models, as shown in *Figures 5.1a and 5.1.b*, where TRADOS results are compared to results from the other Nordic models. As a result, the modeled plume passes the monitoring stations too quickly, and consequently the air concentrations fall too fast. The concentration fields have also very steep gradients at the perimeters of the plume. These two factors also account for the large number of null (or below detection level) values in our ETEX, phase I, simulations. It must be pointed out that the results from the other Nordic models, that are presented in these two figures, are preliminary results prepared some time ago, and more recently generated results are now available. The conclusions from a comparison, however, will be the same.

The long release time (12 hours) showed the relative sensitiveness of our trajectory model to choices of the transport level, in connection with the vertical extent of the plume. The vertical dispersion is determined by the gradient transfer approach (Kz-model), where the vertical extent of the plume (i.e. the mixing height or the upper boundary of Kz-profile) is equated to the ABL top (z_i) as described in *Figure 5.2*. The mass flux across the ABL top is assumed to be zero, which means that the exchange of material between the mixed layer and the free atmosphere is solely due to variations of the ABL height. The ABL height is not based upon a "proper" turbulence parametrization, but is a function of Pasquill categories, and can only have discrete values (*Table 5.1*). Moreover, in order to reduce the computation time, the model is simplified by using precomputed steady-state concentration profiles (Kz-profiles) for stable (z_i =250 m), neutral (z_i =500 m) and unstable (z_i =1500 m) stratification, only.

Our main conclusions are, that little advantage can be gained by modifying existing TRADOS formulations and that the ETEX could be best utilized to indicate what is the state-of-art in long range dispersion modeling today. The assessment was based upon the preliminary results revealed to the participants (see e.g. Archer et al, 1996). Out of the 12 modeling approaches that worked "best" in the exercise, 50% were used in Eulerian and 50% in Lagrangian framework. Out of the Lagrangian models 80% were multi-particle dispersion models. The gradient transfer approach (K-theory) was used in some 55% (K_x,K_y) to 65% (K_z) of all models.

As a consequence, a new random-walk type particle dispersion model development project was initiated at the FMI in 1995. Because of this work, and because the preliminary test runs on the ECMWF data showed that no improvement in TRADOS concentration patterns were to be expected without major changes in the model, it was decided that the old model should be withdrawn from the ATMES-type exercise.

References

Archer, G., F. Girardi, G. Graziani, W. Klug, S. Mosca and K. Nodop, 1995. The European long range tracer experiment (ETEX). Preliminary evaluation of model intercomparison exercise. Proceedings of The 21st NATO/CCMS International Technical Meeting on Air Pollution Modeling and its Applications, Baltimore, USA, November 6-10, 1995 (pp. 100-107).

Klug, W., Graziani, G., Grippa G., Pierce D. and Tassone, C., 1992. Evaluation of Long-range Atmospheric Transport Models Using Environmental Radioactivity Data from the Chernobyl Accident ; The ATMES Report. Elsevier, New York, 365 pages.

Table 1 : The mixing layer height (ABL height z_i) in TRADOS

Stability	Pasquill A	Pasquill B	Pasquill C	Pasquill D	Pasquill E	Pasquill F	Pasquill G
TRADOS ABL height (m)	1200	1500	1800	1500	500	250	200 over land/ 100 over sea

Figure 5.1a *Comparison on the ETEX forecasts by the Nordic dispersion models. Location of the cloud after 24 hours.*

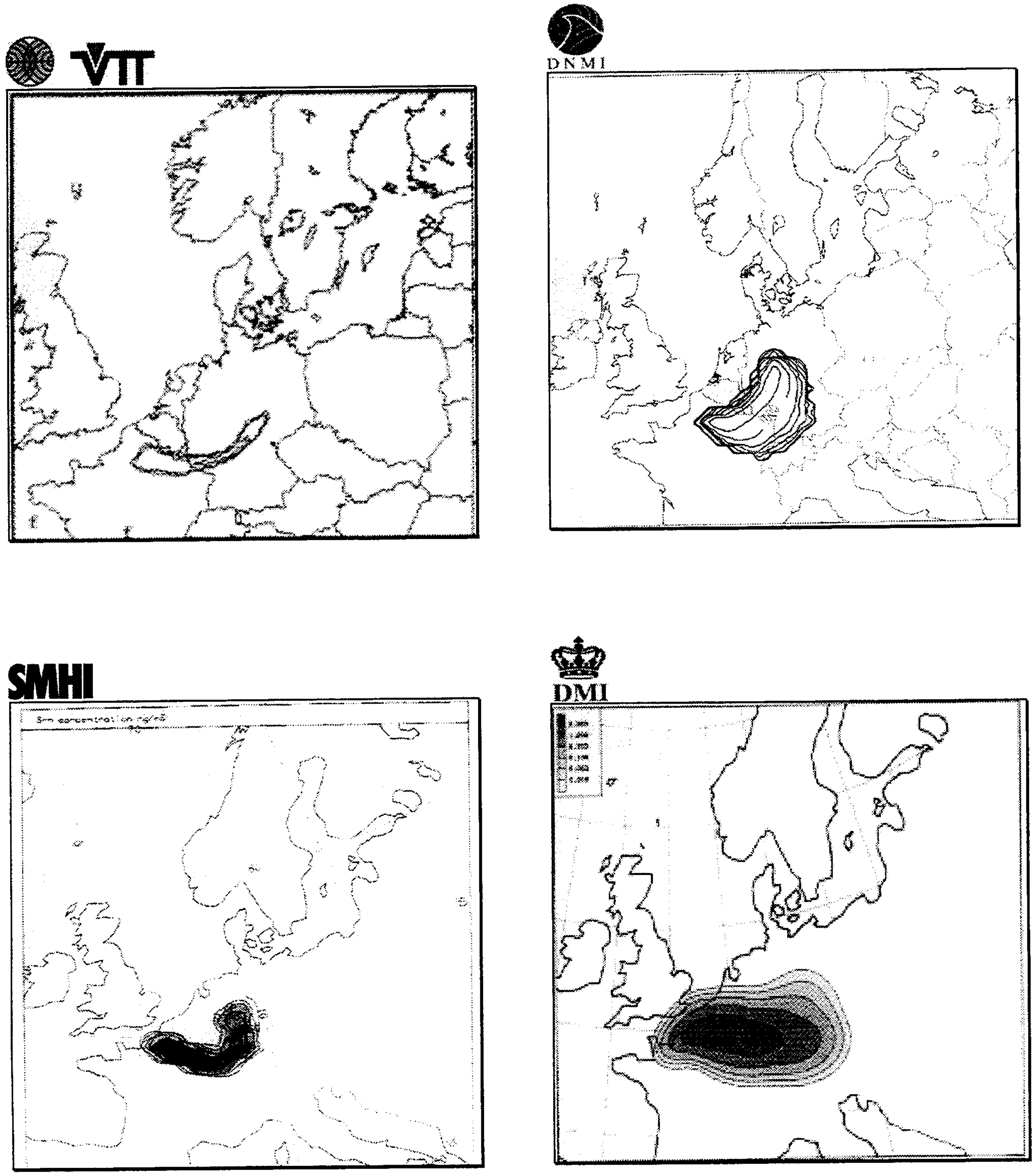

Figure 5.1b *Comparison on the ETEX forecasts by the Nordic dispersion models. Location of the cloud after 48 hours.*

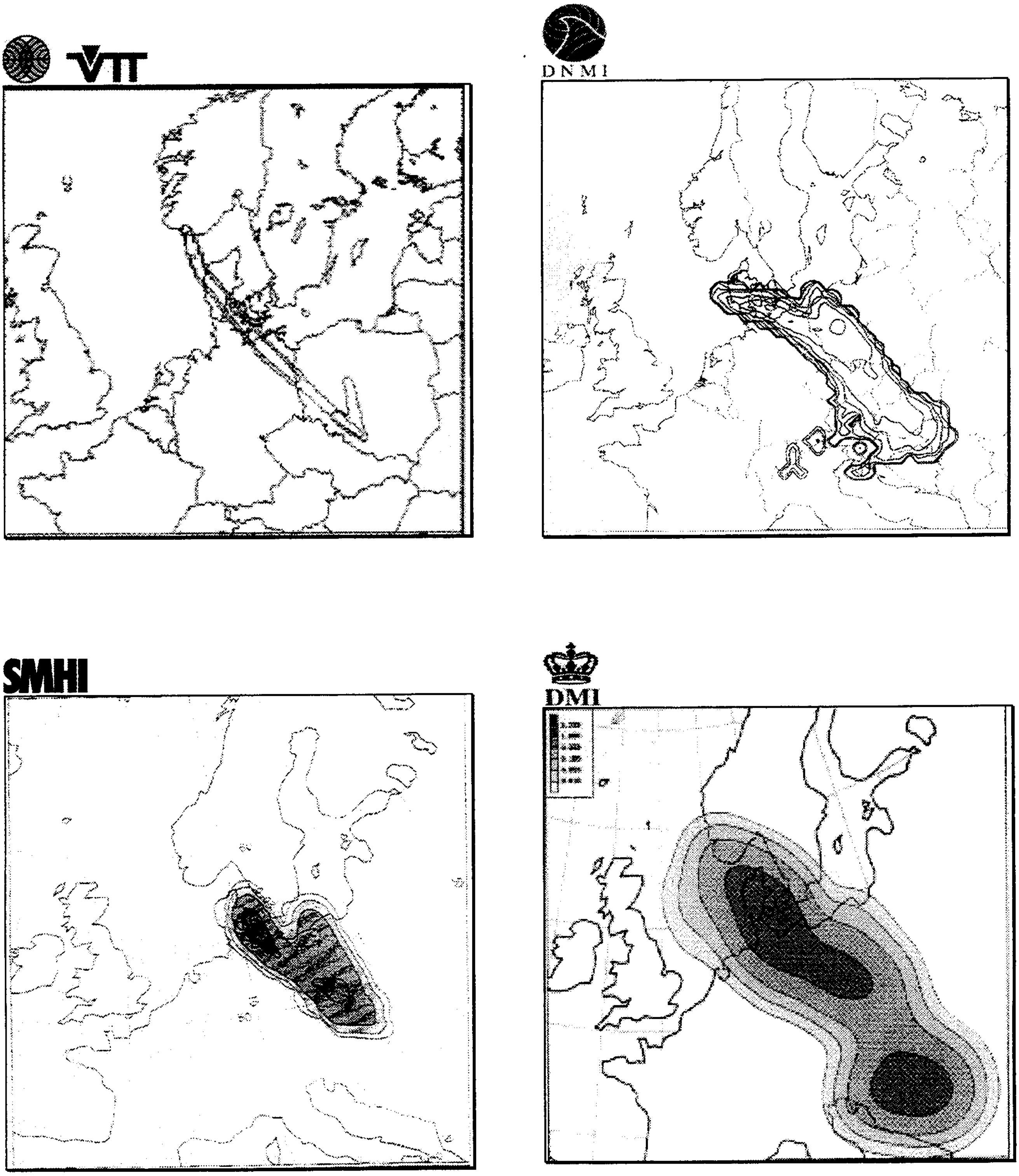

Figure 5.2 The two layer approach of the TRADOS model

free atmosphere

——— mixing height (ABL top z_i) ———

mixed layer

——— ground surface ———

6 ATMES II - ETEX runs using SNAP

Jørgen Saltbones
Meteorological Institute of Norway, DNMI
Oslo, Norway

DNMI's dispersion model SNAP (Severe Nuclear Accident Program) has been used for the ETEX, phase I, calculations, submitted in October 1994 and for the ETEX, phase II (ATMES-II) calculations, submitted in September 1996. The meteorological input was taken from the numerical weather prediction model LAM50S for the phase I calculations and from ECMWF for the phase II calculations.

The versions of SNAP used in the two phases are not much different, except for the treatment of meteorological input data.

The first version of SNAP was based on the same theoretical assumptions and had the same basic architecture as the NAME model, developed by the UK Meteorological Office (Maryon et al., 1991). This was the version used by DNMI in the ETEX exercises in October and November 1994, using meteorological input data from LAM50S.

LAM50S is the abbreviation for Limited Area Model, 50 km grid resolution, (Grønås and Midtbø, 1984 and Nordeng, 1986), and was DNMI's operational Numerical Weather Prediction (NMP) model up to 1/7-1995.

The vertical structure of SNAP was made compatible with LAM50S, using data from a subset (data from 14 σ-layers, 7 layers below 1500 m) of the 31 layers available. The vertical structures of LAM50S, SNAP and ECMWF are shown in *Figures 6.1 to 6.3.*

In this version, SNAP uses σ as vertical coordinate. Concentration and deposition fields (output from SNAP) were stored and presented in the same grid as the one used for the input data. The grid system used for ETEX covers Europe and the North Atlantic. The distance between the grid points is 50 km at 60°N in the Polar Stereographic Projection.

For the ATMES II run in September 1996, a slightly updated version of SNAP was used. The main change is the ability of SNAP for direct use of the meteorological input data from the European Centre for Medium-Range Weather Forecasts (ECMWF). NOTE: We have used the "ECMWF 1995; ETEX Data Set (ATMES II) directly with no change or modification of the meteorological input data. We have instead adopted/changed the dispersion model SNAP to cope with a new input module. This gives about the same special resolution as the earlier version of SNAP used in the ETEX exercises in 1994; both horizontal (0.5 deg by 0.5 deg in a regular latitude/longitude grid) and vertical (model levels 18 to 31 of the model, up to 500 hPa). Output is given in the grid mentioned above. (There was no change in the output module).

Figure 6.4 contains information on the areas covered by the LAM50S and ECMWF data. *Figure 6.5* shows grid systems. (See the figures for detailed information).

SNAP-results for the ETEX-plume at two different times after the release are shown in *Figures 6.6 and 6.7.*

It can be mentioned that the new updated version of SNAP, used in the ATMES II (ETEX Phase II) run, uses the same hybrid vertical coordinate η as the ECMWF model and DNMI's new operational NWP model HIRLAM. This does not make a great difference in the ABL where both σ and η are "terrain-following" coordinates.

More specified technical questions or nuclear points connected to DNMI's ATMES II run through the use of SNAP, can be addressed directly to the DNMI team.

References

Grønås, S. and K.H. Midtbø: Operational multivariate analysis by successive corrections. *J. Meteo. Soc. Japan*, **65**: 61 - 74. 1984

Maryon, R.H., J.B. Smith, B.J. Conway and D.M. Goddard: The United Kingdom nuclear accident model. *Prog. Nucl. Energy*, **26**: 85 - 104. 1991

Nordeng, T.E.: Parametrization of physical processes in a three-dimensional numerical weather prediction model. DNMI Technical Report No. 65. 1986

Figure 6.1 The vertical structure(σ-layers) for the numerical weather prediction model LAM50, providing meteorological input data for SNAP in Phase I of ETEX in October and November 1995

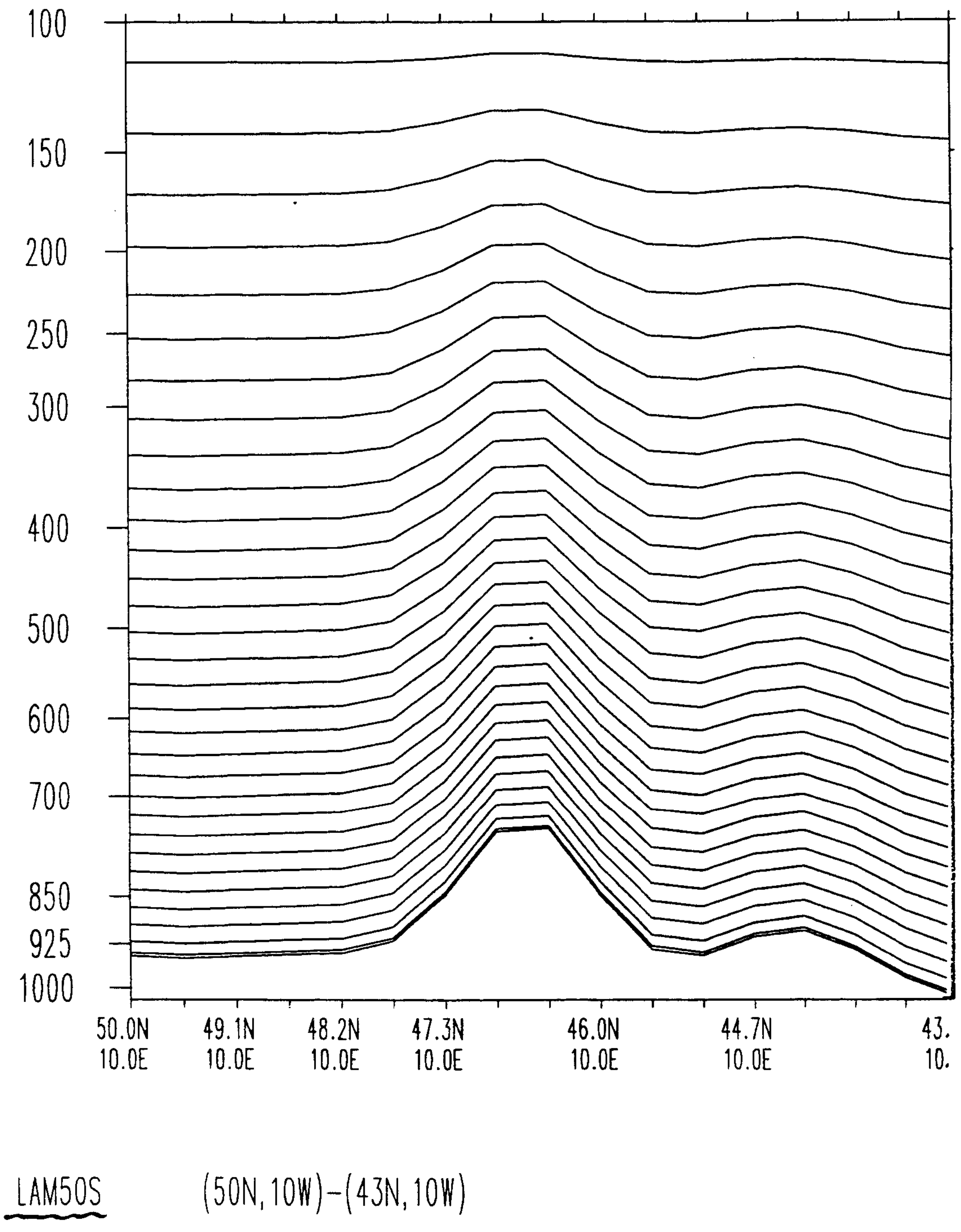

Figure 6.2 The vertical structure of SNAP, as it was in ETEX Phase I, October and November 1995 (This is a subset of the layers presented in Figure 6.1)

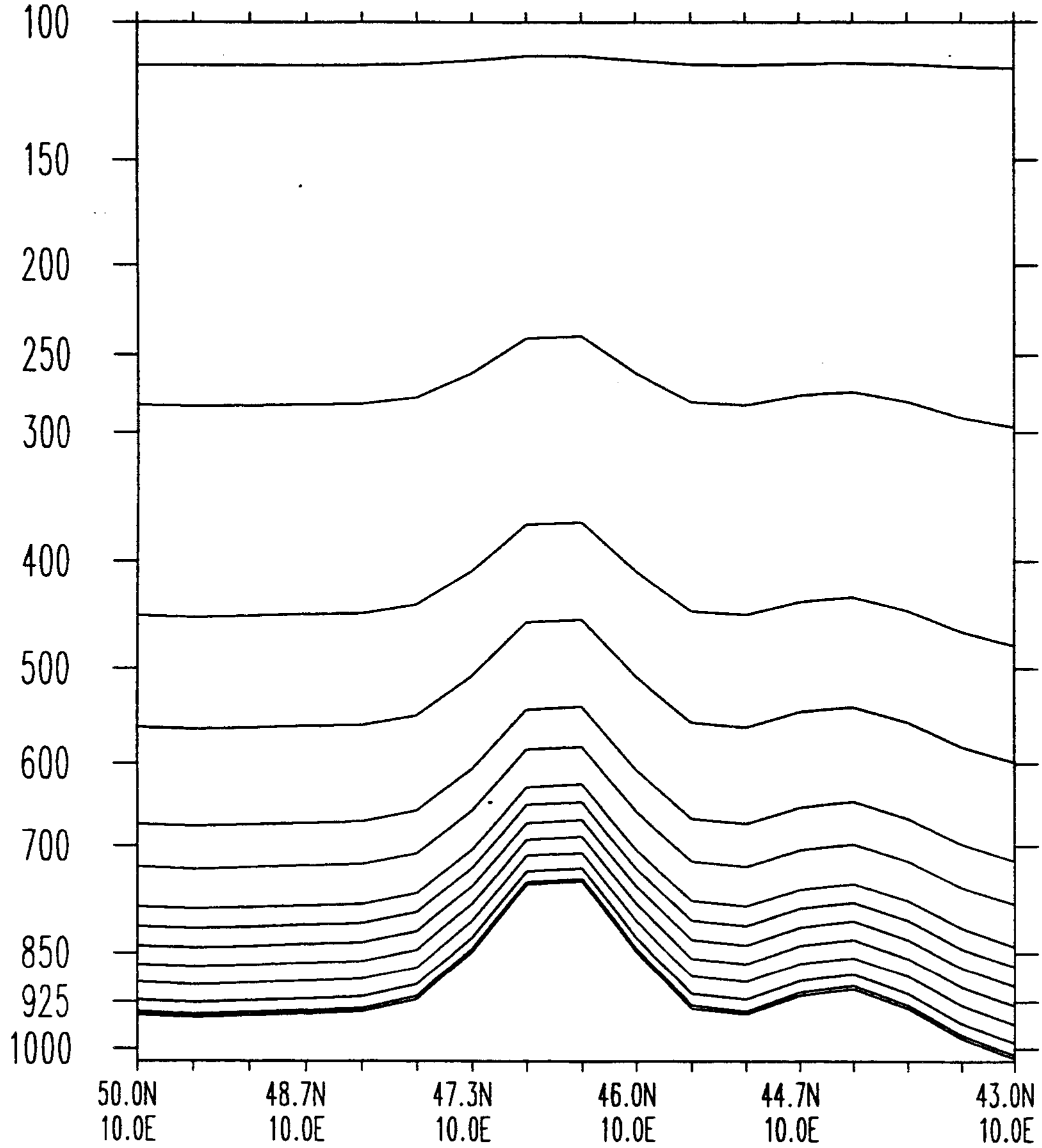

SNAP (50N,10W)-(43N,10W)

Figure 6.3 The vertical structure of SNAP, as it was used in ETEX Phase II, September 1996. (This is a subset of the η-layers used in the ECMWF-model; providing meteorological input data to ETEX Phase II)

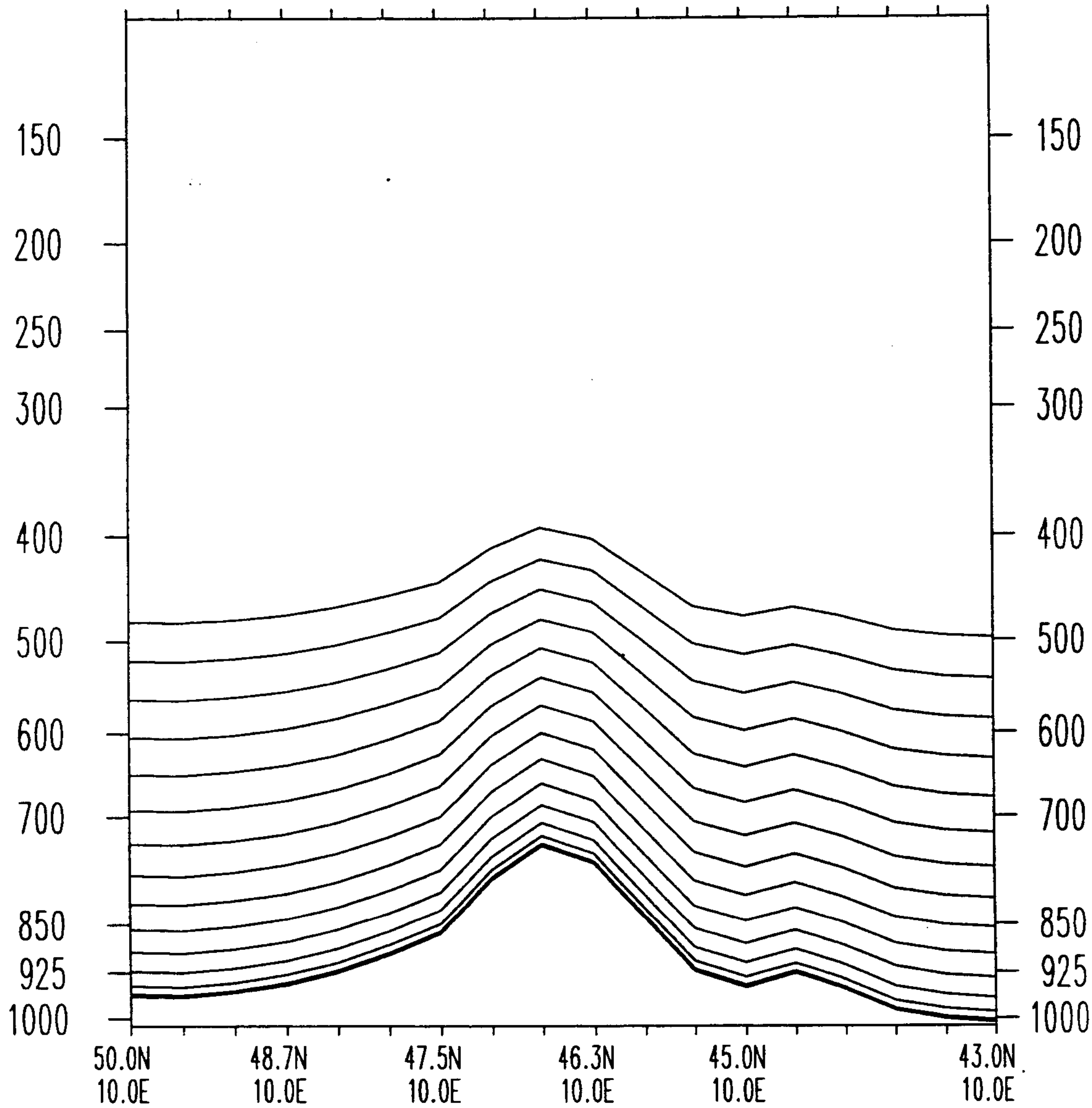

ECMWF (50N,10W)-(43N,10W)

Figure 6.4 The horizontal extent of the LAM50S data (large area) together with the extent of the ECMWF data for ETEX Phase II (the sectorial shaped subregion)

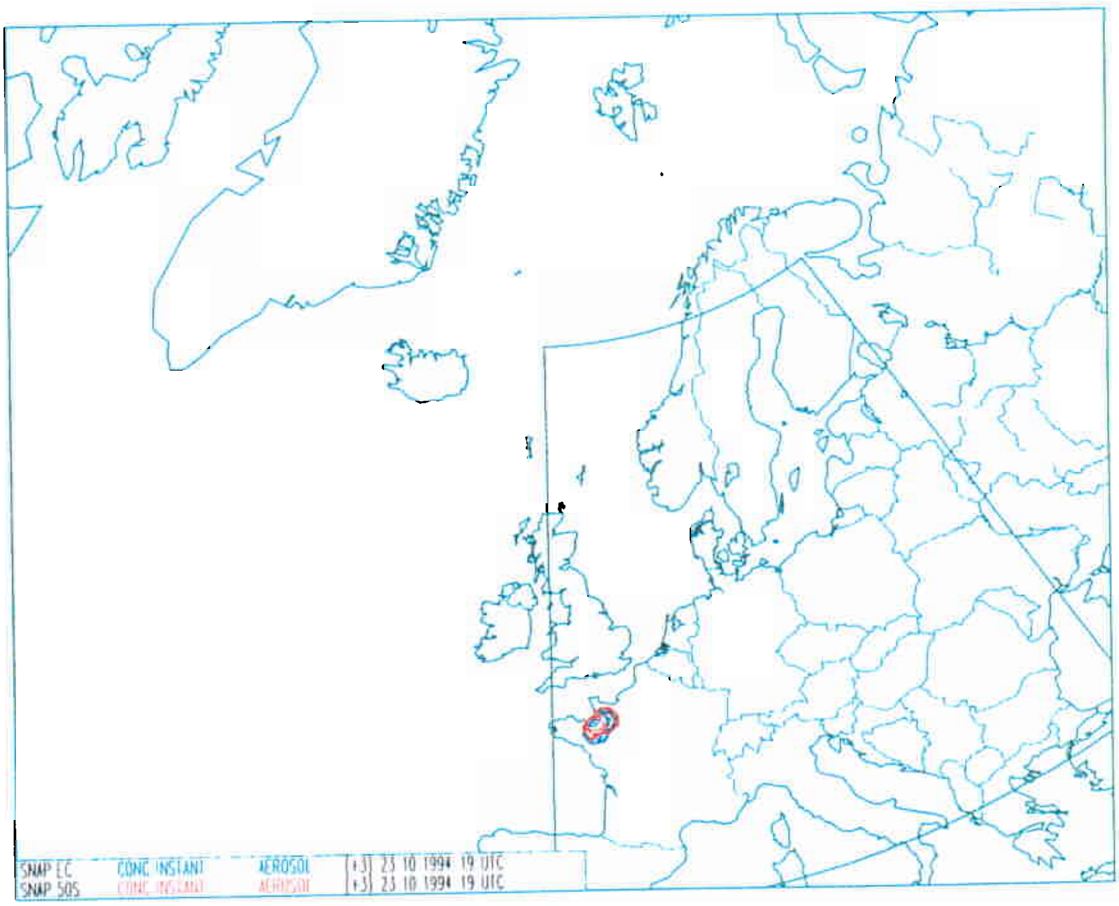

Figure 6.5 The horizontal resolution of the two gird systems providing the meteorological input data. The regular spacing shows every 5th grid square for the LAM50S-model (in red). The sectorial shaped grid shows every 5th (2.5^0) in the latitude - longitude system used by the ECMWF-model (in blue). In the Northern part of the area, this gives about double grid resolution, compared with LAM50S.

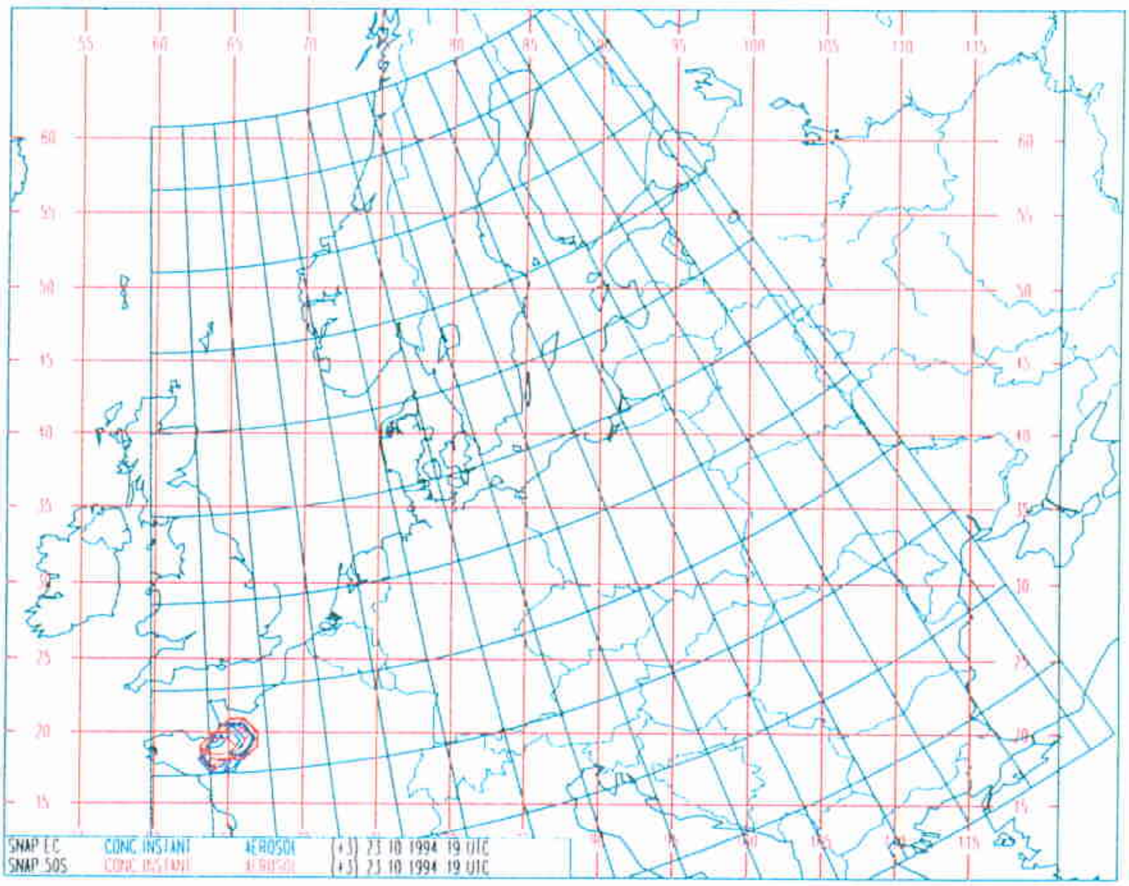

*Figure 6.6 The results of the two simulations 24 hours after start of release.
The results are very similar.
SNAP.50S is ETEX Phase I calculations (in red).
SNAP.EC is ETEX Phase II calculations (in blue).
In the ETEX Phase II calculations the plume is slightly more spread out, both behind and in front*

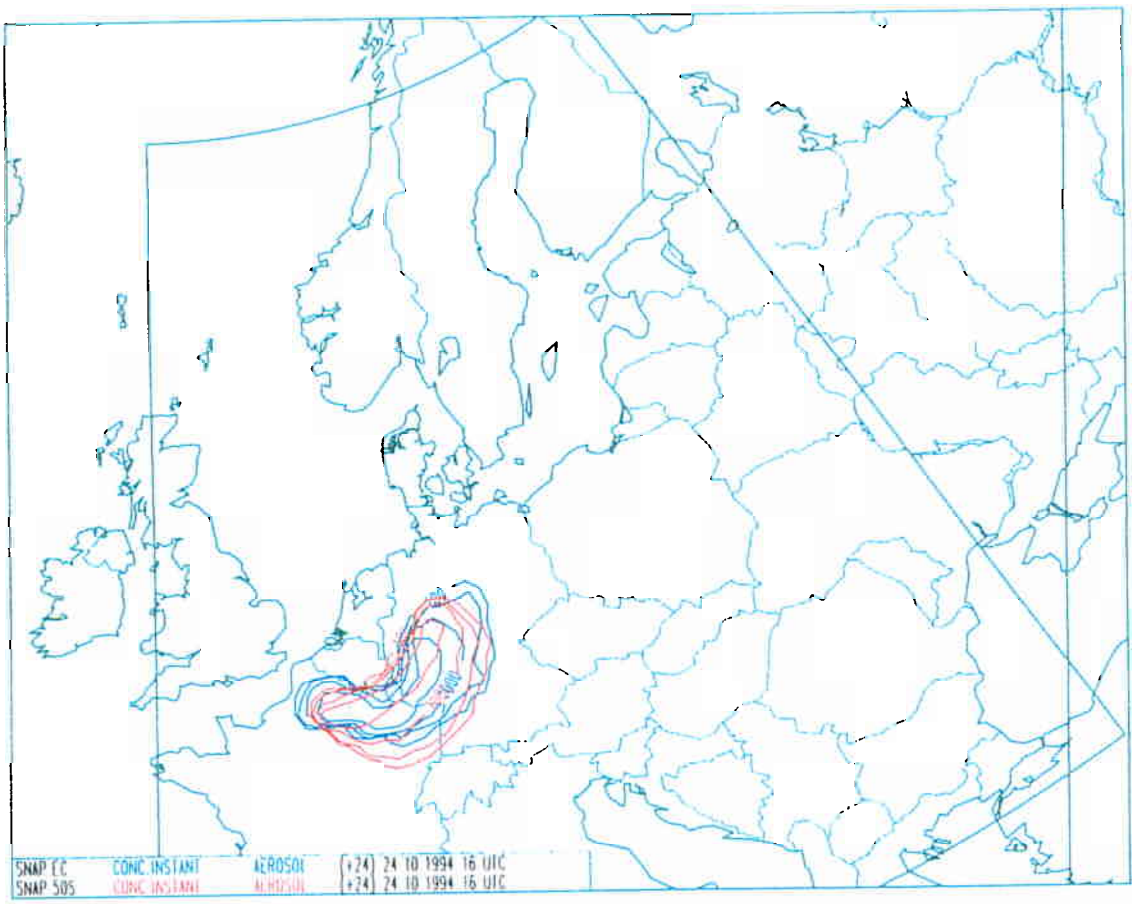

*Figure 6.7 The results of the two simulations 60 hours after start of release.
The results are very similar.
SNAP.50S is ETEX Phase I calculations (in red).
SNAP.EC is ETEX Phase II calculations (in blue).
More of the material is sent up along the Western coast of Norway in the ETEX Phase II (blue) calculations. Also more is sent down towards the Balkan region in Phase II. Apart from that, the results from these two simulations seem surprisingly similar in shape*

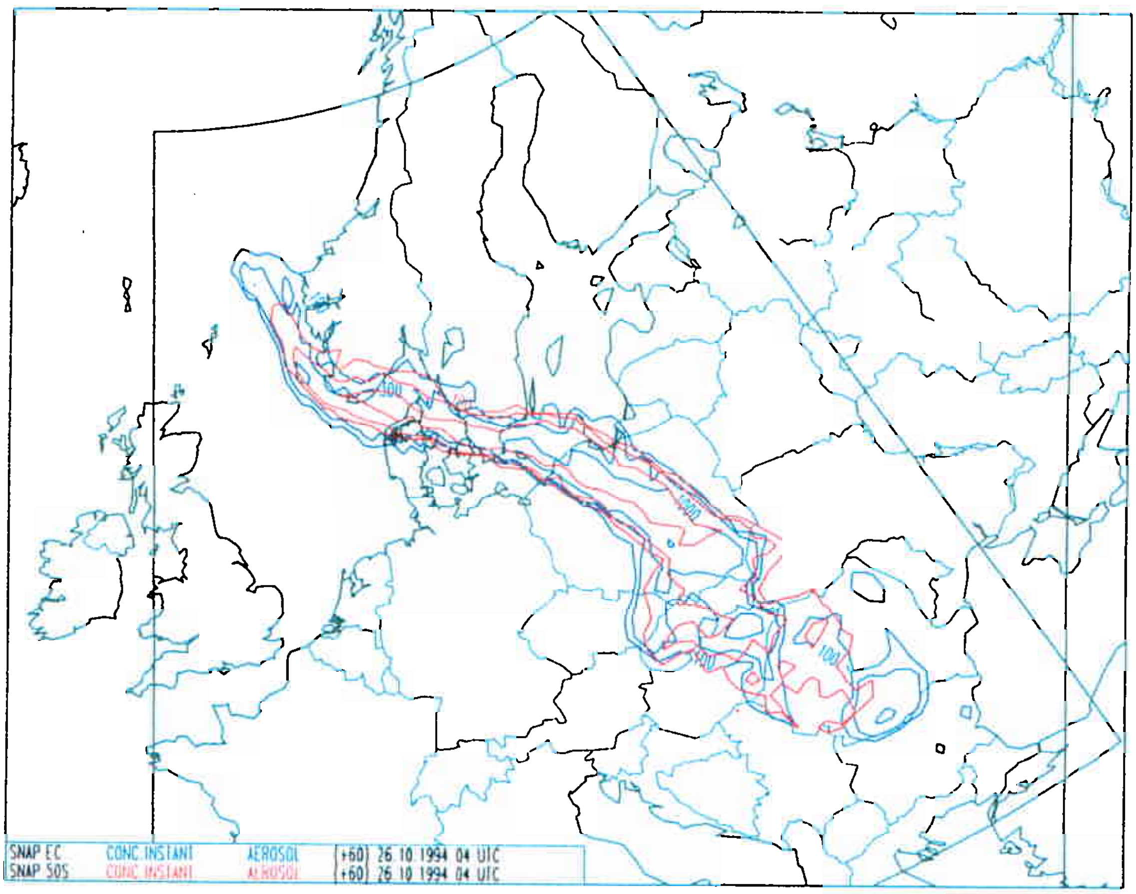

7 ETEX-1 - Measurements compared to calculations performed with the MATHEW/ADPIC model at FOA, Sweden

Lennart Thaning
National Defense Research Establishment - FOA
Umeå, Sweden

The ETEX calculations at FOA have been carried out with the MATHEW/ADPIC model, a particle model originally developed at Lawrence Livermore National Laboratory in the USA (Sherman, 1978, Lange, 1978, Foster, 1992). The model, developed in the late 1970's, has been updated and adjusted to the FOA-environment during the 90's (e.g. Thaning & Näslund, 1991, Näslund & Holmström, 1993), but nevertheless the model framework is now becoming somewhat old.

In the present calculations 41x41x15 gridpoints (63kmx63kmx100m) were used. The model was run with constant mixing height (the mixing heights are not calculated by the model, and they can not be changed in space, only in time) and under assumption of neutral, static stability.

Figure 7.1 shows the air concentrations at 2 meters height above ground at four different times after the release. *Figures 7.2 and 7.3* show comparisons between calculational results and the ETEX observations at a number of different geographical locations and for two different values of the mixing height (500 and 1000 meters). The compared values are time-integrated concentrations at two meters height. The explanation of the symbols used in these figures is as follows:

+	the calculated value > observed value
-	the calculated value < observed value
0	both the calculated and the observed values are zero
0 with a + inside	the calculated value is non-zero and the observed is zero
0 with a - inside	the calculated value is zero and the observed is non-zero

Figure 7.4 shows a comparison between the calculation results for the two mixing height values. Here a +sign indicates that the 500-meter-value is larger than the 100-meter-value etc. The comparison shows that the shape of the cloud is almost the same in the two cases, but a 500 meter mixing height tends to keep more of the pollutant in the North-Westerly part of the cloud than a 1000 meter mixing height.

Figure 7.4 also demonstrates that an increased mixing height does not everywhere result in a decrease in the concentration at ground. When the winds at higher altitudes become available for the advection of the cloud, the horizontal spread, and consequently, the affected area will be enlarged. Therefore, the concentrations in the outer parts of the affected area will increase. This fact emphasizes the importance of having a good description of the mixing height, especially in emergency response models, for which a main task is to predict which areas will be affected and which will not.

References

Forster, C. S., Editor, 1992. User's guide to the MATHEW/ADPIC models. UCRL-MA-103581 Rev 1, Lawrence Livermore National Laboratory (LLNL), USA.

Lange, R., 1978. ADPIC - a three dimensional particle-in-cell model for the dispersal of atmospheric pollutants and its comparison to regional tracer studies. **J. Appl. Meteorol.**, **17,** 320-329.

Näslund, E. and Holmström, H., 1993. Inclusion of a three-dimensional washout coefficient in ADPIC, UCRL -ID-114054, Lawrence Livermore National Laboratory, Livermore, CA.

Sherman C.A., 1978: MATHEW: A Mass-Consistent Model for Wind Fields Over Complex Terrain. **J. Appl. Meteorol.**, **17**, 312-319.

Thaning, L. and E. Näslund, 1991. A Simulation of radioactive fallout using the MATHEW/ADPIC model. FOA Report, December 1991, National Defence Research Establishment (FOA), Umeå, Sweden, 22 p.

Figure 7.1 MATHEW/ADPIC results for ETEX. Surface concentrations.

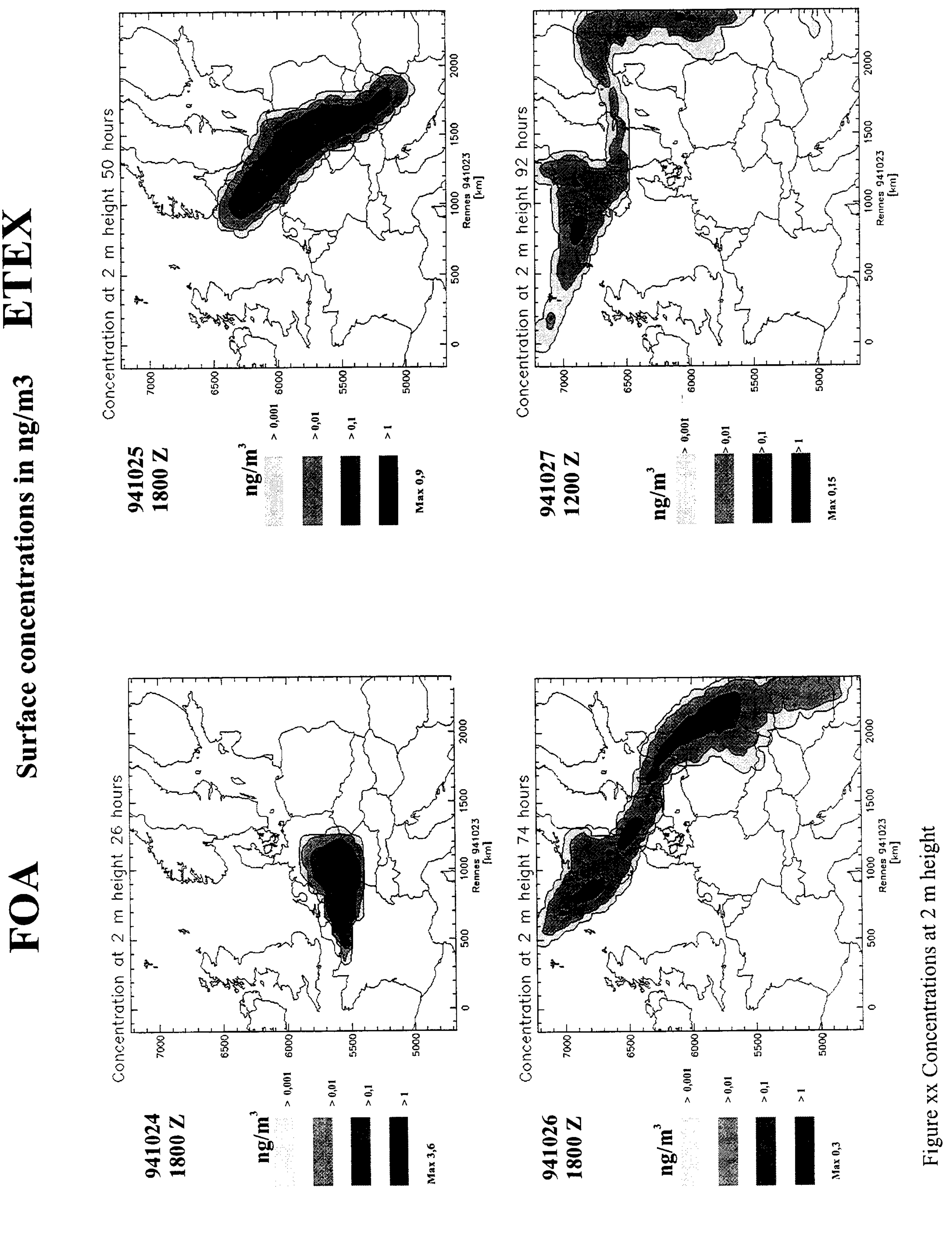

Figure 7.2 Differences between predicted and observed integrated concentrations.
+ means predicted > observed. - means predicted > observed
0 means either predicted or observed or both are zero.
Mixing height = 500 meters

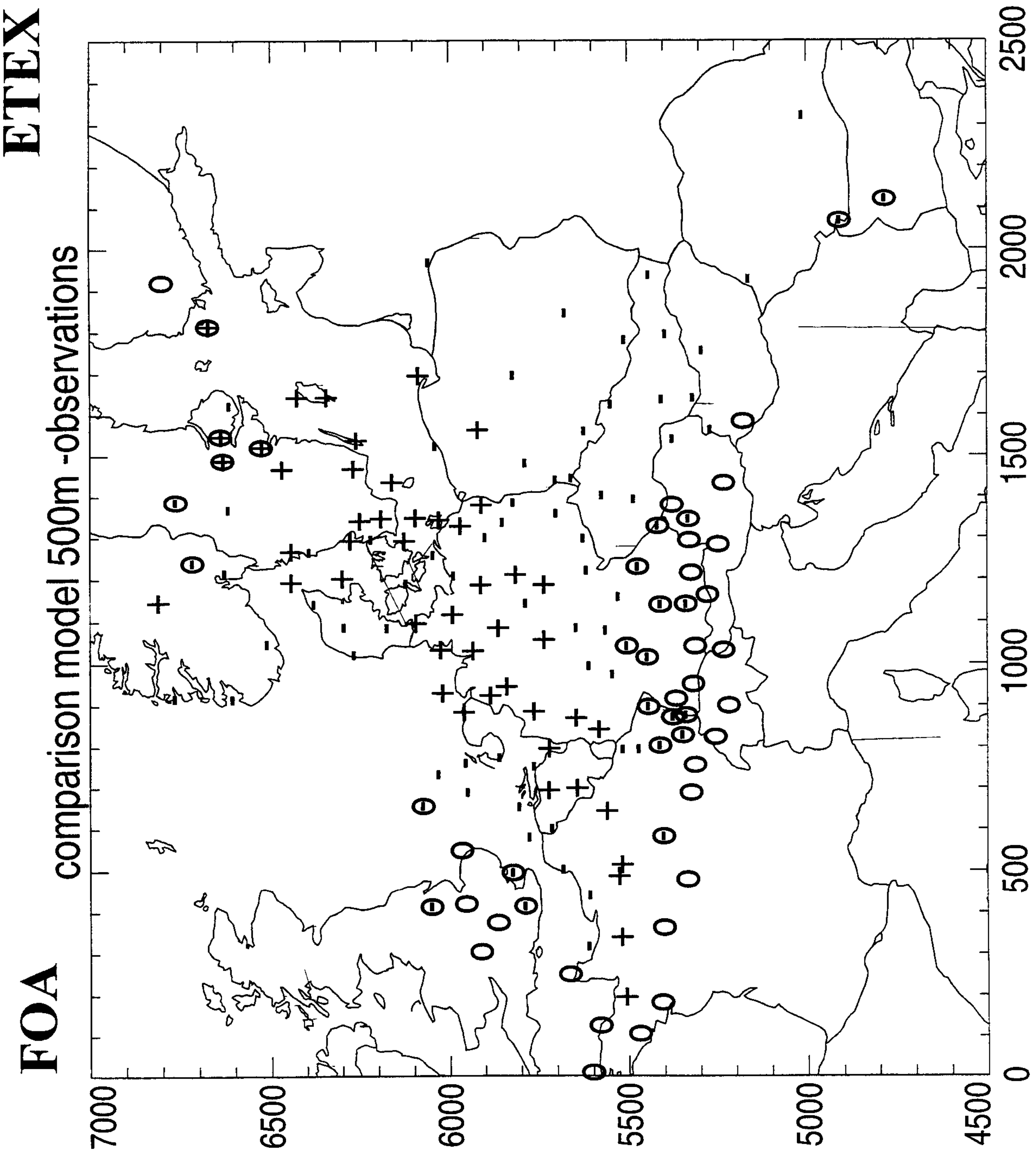

Figure 7.3 Differences between predicted and observed integrated concentrations.
+ means predicted > observed. - means predicted > observed
0 means either predicted or observed or both are zero.
Mixing height = 1000 meters

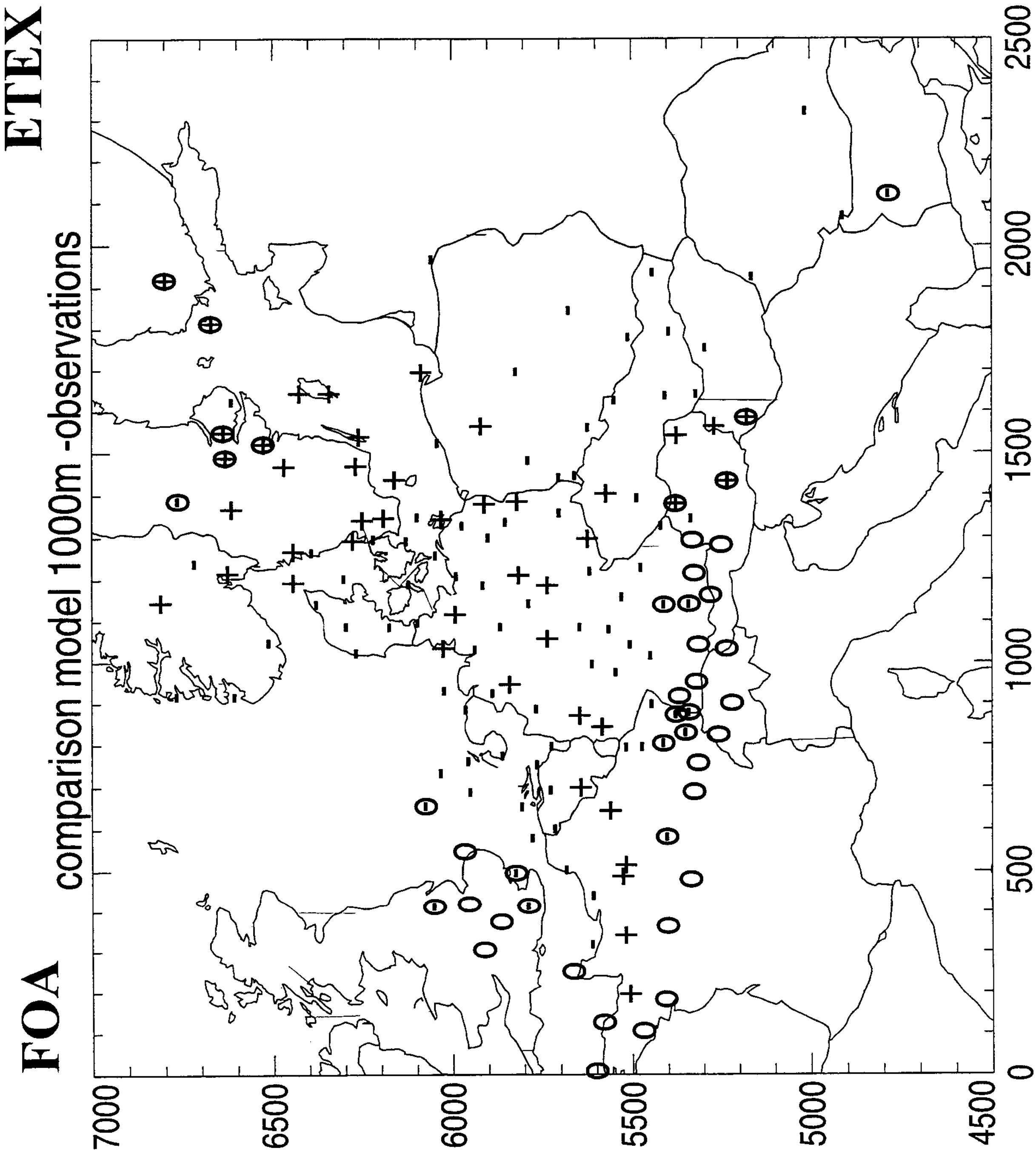

Figure 7.4 Differences between integrated concentrations predicted with mixing heights 500 and 1000 meters.
+ means predicted (500 m) > predicted (1000 m)   - means the opposite.
0 means either one prediction or both are zero.

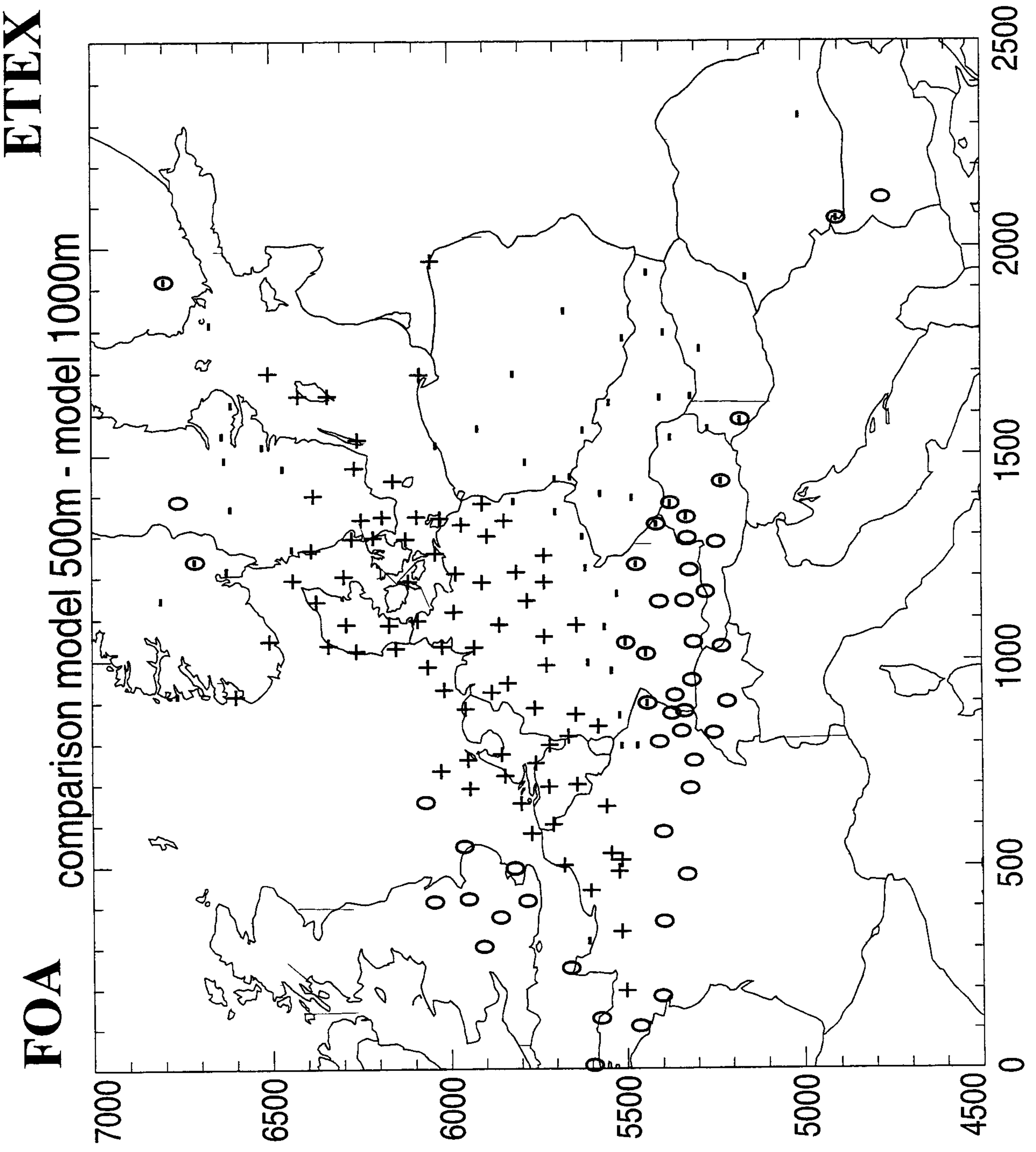

8 MATCH - A regional transport model. The ETEX-1 validation

Christer Persson, Lennart Robertson and Joakim Langner
Swedish Meteorological and Hydrological Institute - SMHI
Nyköping, Sweden

The MATCH (Meso-scale Atmospheric Transport and CHemistry) emergency modeling system is a Eulerian off-line model. Some important characteristics:

- Hybrid vertical coordinates (sigma, p)
- Horizontal advection by 4th order shape preserving scheme (Bott, 1992)
- Vertical advection (0 or 2nd order Bott scheme)
- Mass conservative vertical diffusion:
  Convective $K_z = F(Z_i / w_*)$
  Neutral/stable $K_z = F(u_*, Z_i, H)$
- Hybrid Lagrangian-Eulerian particle model for the initial 10 hours

A detailed presentation of the model is given in (Robertson *et al.*, 1996).

Figure 8.1 shows the MATCH simulation for the first ETEX experiment, in a three-dimensional representation, at one specific time.

The calculations performed showed that proper adjustment of the unbalanced wind fields was important.

The rate of change of the surface pressure should match the vertically integrated air mass convergence. If the wind field is not in balance the calculated surface pressure tendency will become too large. Unbalances cause wrong vertical winds. Unbalance between mass and wind fields can be caused by:

- Spatial interpolation errors
- Low accuracy in stored meteorological data
- Time interpolation errors

An adjustment of the wind field can be made (Heimann and Keeling, 1989).

Test runs have been performed with meteorological data from HIRLAM and from ECMWF. Simulations are made for 48 hours. Here are some important characteristics for these runs:

	HIRLAM	**ECMWF**
Case a	No spatial and no time interpolation	Spatial but no time interpolation
Case b	Time interpolation	Spatial and time interpolation
Case c	Time interpolation with adjustment	Spatial and time interpolation with adjustment

The results of these calculations are shown in three-dimensional representations in *Figures 8.2 (a-c) and 8.3 (a-c).* Here is assumed a mixing ratio at the upper boundary of 1000 ppt and initial zero mixing ratio within the model. The isosurface for 10 ppt is shown in the figures. It can be seen that the interpolations introduce strong vertical winds in cases a and b. An adjustment scheme has been defined, and it can be seen from cases c that this reduces the vertical winds significantly, and these results seem to be more realistic.

Some model experiments with the MATCH model have been made for the ETEX-1 release. It can be concluded from the calculations that generally the model gives good agreement, but there are some aspects that are not quite satisfactory. The calculated mixing height is too low in the standard version of MATCH. The point source in the model calculations is placed close to the ground, as was the case in the experiment. Over France the model gives far too high concentrations. Arrival time to some stations is too late, and to other places too early. However, by assuming constant mixing height of 1000 meters better agreement is achieved. It may, however, be that it is not the actual calculation of mixing height that is wrong, but rather that there is some convective mixing, which is not modeled.

Figure 8.4 shows the results of some measurements from aircraft for ETEX-1 at three different time intervals after the release, at about 400 km from the release point. Also are shown MATCH-calculated values at approximately the same times. There are slight differences in altitudes between the different time intervals. The general agreement between model and measurement is good, although there is a tendency to move the cloud somewhat too far South at 10 UTC.

References

Bott, A.: Monotone flux limitation in the area-preserving flux-form advection algorithm. Monthly Weather Rev., 120, pp. 2592-2602. 1992.

Heiman, M. and C.D. Keeling: A three-dimensional model of atmospheric CO^2 transport based on observed winds. 2. Model description and simulated tracer experiments. In: Aspects of climate variability in the Pacific and the Western Americas (ed.: D.H. Peterson). American Geophysical Union. pp. 237-275. Washington, D.C. 1989.

Robertson, L., J. Langner and M. Engart: MATCH - Meso-scale atmospheric and chemistry modeling system. SMHI RMK Report no. 70. 1996.

SMHI - Swedish Meteorological and Hydrological Institute

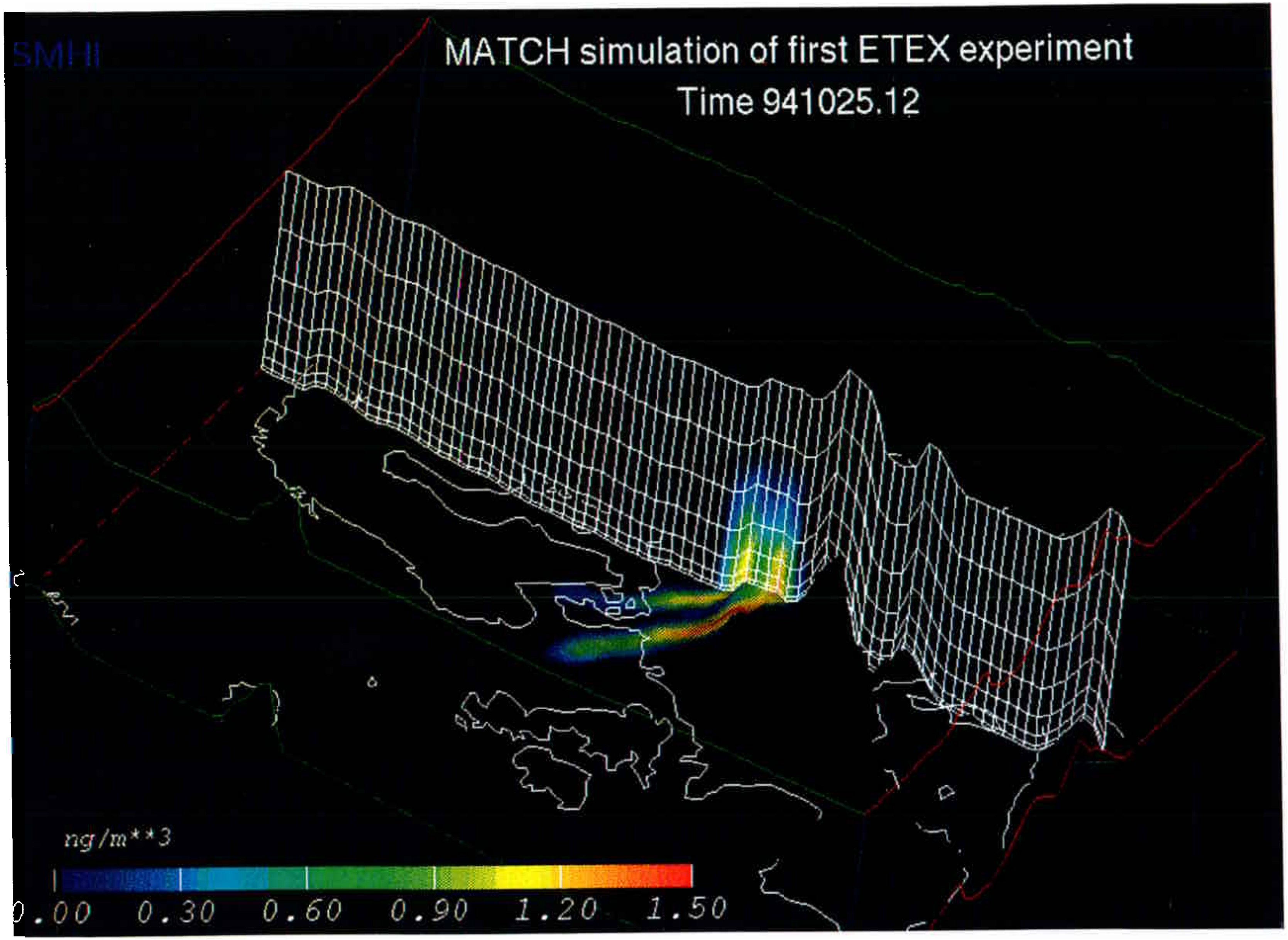

Figure 8.1 MATCH model calculated distribution of the passive tracer in the ETEX-1 experiment 45 hours after release. The MATCH coordinate system used in the standard model version is also illustrated

Figure 8.2 Calculated penetration of a passive tracer from the top of the model domain, after 48 hours of simulation, starting from a zero initial distribution using data from HIRLAM, viewed from a location slightly below and to the left of the model domain.
a) No adjustment, no time interpolation
b) No adjustment, time interpolation
c) With adjustment and time interpolation.
Isosurface for 10 ppt (m). The mixing ratio at the upper boundary was fixed at 1000 ppt(m). Units: ppt(m)

a)

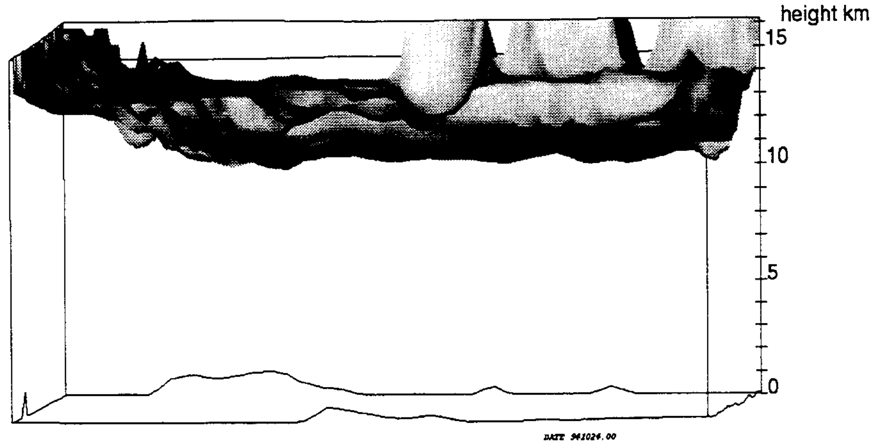

b)

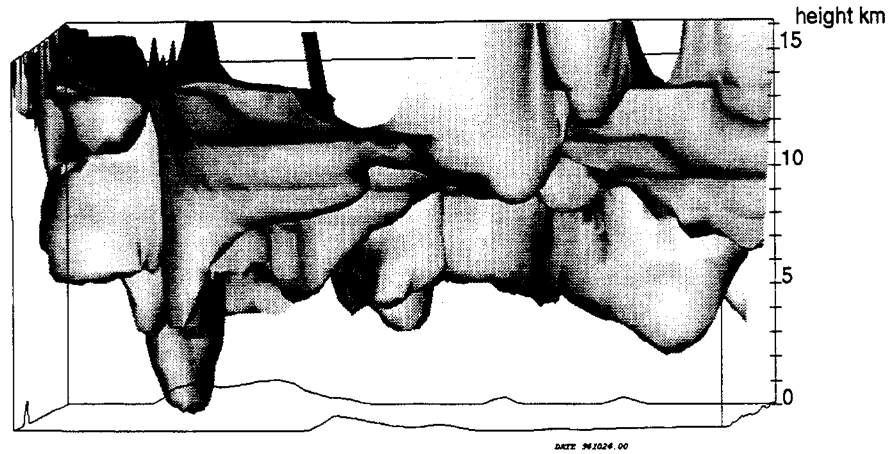

c)

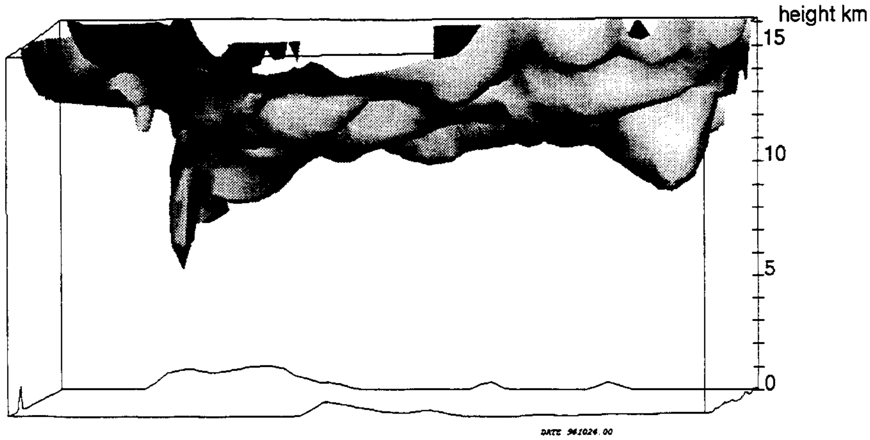

Figure 8.3 Calculated penetration of a passive tracer from the top of the model domain, after 48 hours of simulation, starting from a zero initial distribution using data from ECMWF, viewed from a location slightly below and to the left of the model domain.
a) No adjustment, no time interpolation
b) No adjustment, time interpolation
c) With adjustment and time interpolation.
Isosurface for 10 ppt (m). The mixing ratio at the upper boundary was fixed at 1000 ppt(m). Units: ppt(m)

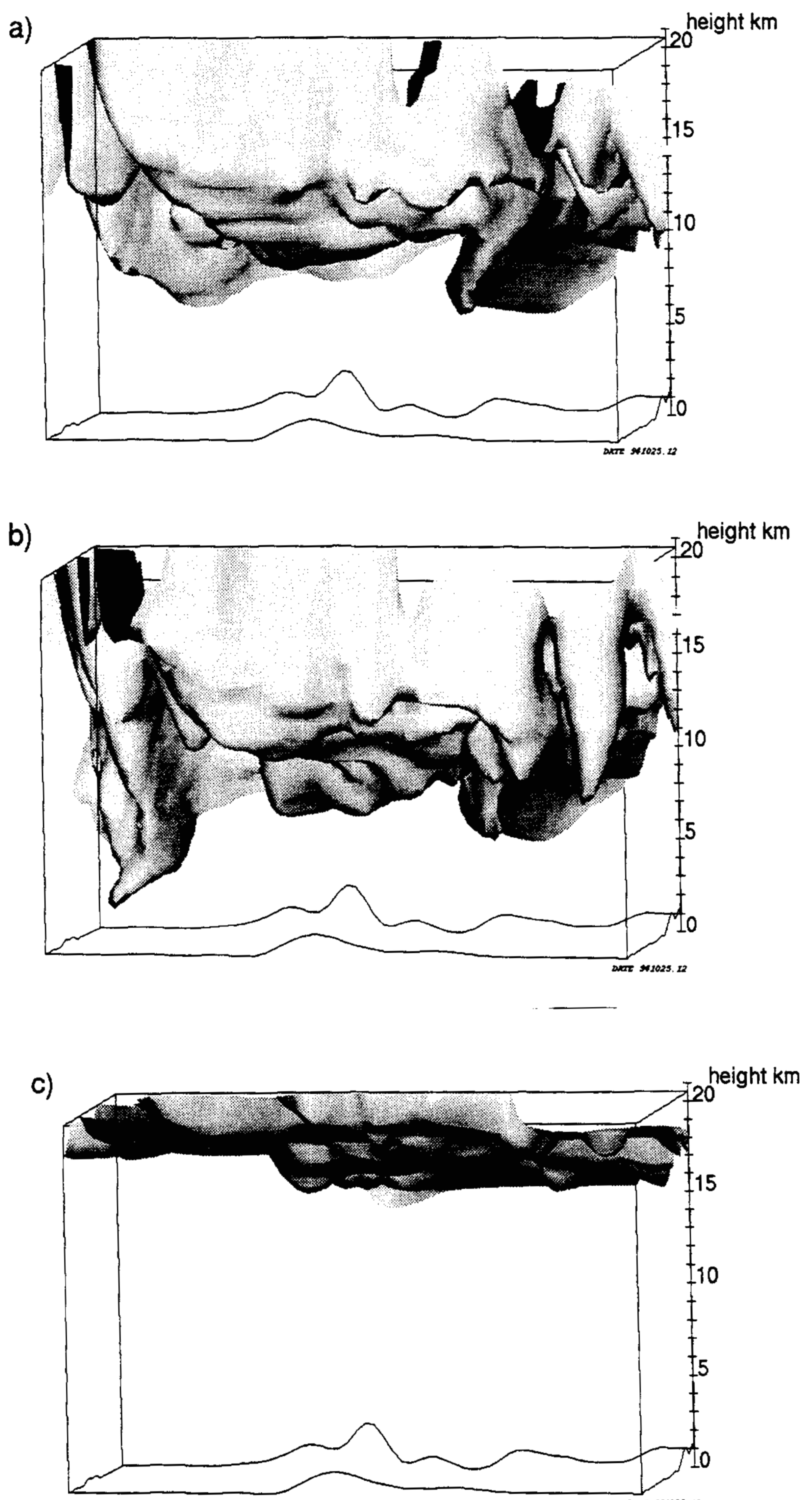

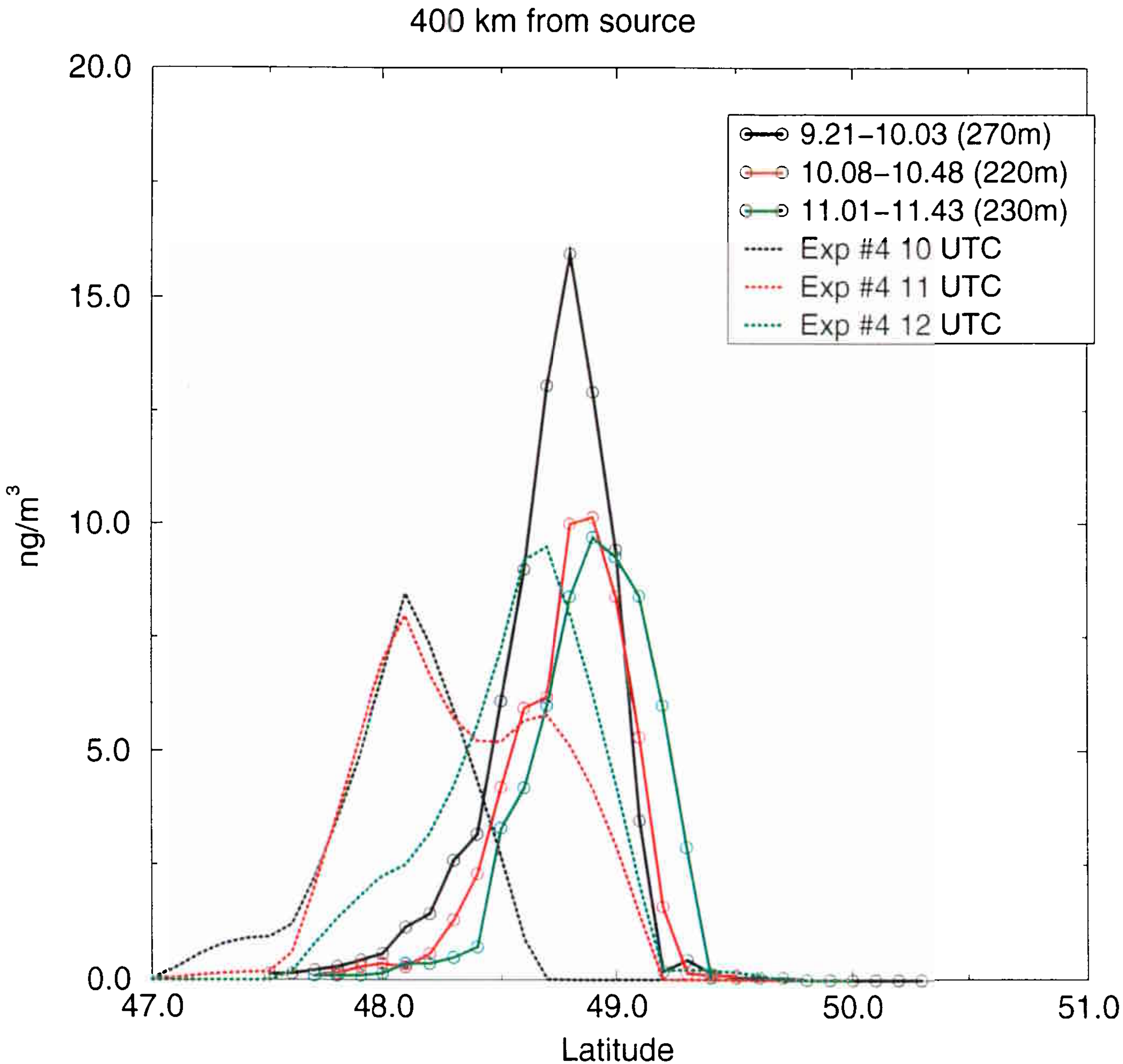

Figure 8.4 ***Measured and MATCH model calculated concentrations for ETEX-1 experiment presented as horizontal cross-sections at a height of 200-300m about 400 km from the source. Solid lines refer to aircraft measurements and dotted lines refer to MATCH calculations***

9 The sensitivity of the ETEX simulations to different diffusion schemes

Roy Maryon and Derrick Ryall
Meteorological Office
Bracknell, United Kingdom

9.1 The Diffusion Model

The UK Meteorological Office medium and long-range dispersion model, NAME, is of Lagrangian, multiple particle type, utilizing the output winds and meteorology of the UK Met Office operational numerical weather prediction model, the Unified Model. NAME now includes nested mesoscale and other high resolution grids (Ryall and Maryon, 1996), requiring diffusion schemes appropriate to the near-source situation so that the model now possesses a wide range of diffusion options---

Near-source random walk schemes:
- homogeneous vertical profiles of the turbulent velocity variances;
- inhomogeneous vertical profiles of the turbulent velocity variances;
- skewed or Gaussian statistics for the convective boundary layer; and
- for homogeneous profiles, small-scale entrainments at the inversion capping the boundary layer, or a reflection condition (entrainments are implicit in the inhomogeneous scheme).

Far-field Wiener-type diffusion schemes (allowing larger timesteps):
- homogeneous vertical turbulence profiles and entrainments;
- a basic *K*-diffusion scheme with its own specific entrainment parametrization.

Available as required are schemes for low-frequency wind meandering, venting of aerosols by large cumulus, and plume rise.

9.2 Advection and Near-source Diffusion

Particles are advected each timestep using

$$\mathbf{x}_{t+\Delta t} = \mathbf{x}_t + [\mathbf{u}(x_t) + \mathbf{u}'(x_t)]\Delta t\,,$$

where $\mathbf{x}$ is the particle position vector, $\mathbf{u}$ and $\mathbf{u}'$ the wind and turbulent wind velocity vectors, and Δt the timestep. Then for the u-component

$$u'_{t+\Delta t} = u'_t\left(1 - \frac{\Delta t}{\tau_u}\right) + \left(\frac{2\sigma_u^2 \Delta t}{\tau_u}\right)^{\frac{1}{2}} r_t\,,$$

where σ_u^2 is the turbulent velocity variance, τ_u the Lagrangian timescale and r_t is a random Gaussian variable of zero mean and unit variance. The right hand terms represent damping and innovation, respectively. For the inhomogeneous vertical scheme a third term

$$\frac{\Delta t}{\sigma_w}\frac{\partial \sigma_w}{\partial z}\left(\sigma_w^2 + w_t'^2\right)$$

accounts for the "drift velocity", which prevents particles from collecting at levels of small σ_w.

Skewed Turbulence

In the convectively unstable boundary layer the top-down/bottom-up turbulence is non-Gaussian (i.e. skewed). The stochastic equation is

$$w'_{t+\Delta t} = w'_t + a\Delta t + \left(C_0 \varepsilon \Delta t\right)^{1/2} r_t,$$

where ε is the rate of dissipation of TKE and C_0 is a constant. The Fokker-Planck equation is solved (Luhar & Britter, 1989) to obtain the coefficient *a,* which allows for the memory and drift terms---the expression is cumbersome and not reproduced here.

9.3 Homogeneous and Inhomogeneous Turbulence

Figure 9.1 shows three options for the vertical profiles of σ_w^2. Profiles (a) and (b) are the NAME inhomogeneous and homogeneous options, respectively. Profile (c) is practicable, but has neither the realism of (a) nor the computational economy of (b). Inhomogeneous statistics can be diagnosed from NWP model output if available, or empirical profiles taken from field measurements. In the latter case mechanical and convective turbulence can both be taken into account---both for turbulent velocities and dissipation rate. For example, for unstable conditions---

$$\sigma_w = \left[1.2 w_*^2 \left(1 - 0.9\frac{z}{z_i}\right)\left(\frac{z}{z_i}\right)^{\frac{2}{3}} + \left(1.8 - 1.4\frac{z}{z_i}\right) u_*^2\right]^{\frac{1}{2}},$$

(Hibberd & Sawford (1994), Brost et al (1982)), with gradient

$$\frac{\partial \sigma_w}{\partial z} = \frac{1}{\sigma_w z_i}\left[w_*^2\left(\frac{z}{z_i}\right)^{-1/3}\left(0.4 - 0.9\frac{z}{z_i}\right) - 0.7 u_*^2\right],$$

$$\sigma_u = \sigma_v = \left[0.4 w_*^2 + (5 - 4z/z_i) u_*^2\right]^{\frac{1}{2}}, \qquad \tau_{u,v,w} = 2\sigma_w^2 / C_0 \varepsilon$$

where
$$\varepsilon = \left(1.5 - 1.2\left(\frac{z}{z_i}\right)^{\frac{1}{3}}\right)\frac{w_*^3}{z_i} + \frac{u_*^3 (1 - 0.8 z / z_i)}{kz}.$$

Homogeneous approximations to σ_w can be derived immediately from the inhomogeneous (e.g. mid-boundary layer values).

9.4 Diffusion at Long Range

A more economical technique is used, based upon the

Homogeneous profiles

A preliminary assumption that the model timestep $\Delta t = \tau_u$ is made so that the near-source scheme reduces to $u' = \sqrt{2}\sigma_u r_t$, i.e., the memory term is excluded. An "effective velocity variance", σ_{eff}, is chosen which preserves an appropriate diffusion coefficient K more appropriate to a fixed timestep, $\Delta t = 15\,\text{min.}$:

$$K = \sigma_u^2 \tau_u = \sigma_{eff}^2 \Delta t .$$

Then $\sigma_{eff} = \sqrt{\dfrac{\sigma_u^2 \tau_u}{\Delta t}}$, so that $u' = \sqrt{2}\sigma_{eff} r_t$.

Similarly for the other components: a Wiener-type process.

K-diffusion

Version 1.0 of NAME used for ETEX in October, 1994 possessed a simpler diffusion scheme, which has been continued as an additional option. This scheme used a constant horizontal diffusion coefficient, $K_H = 5300 m^2 s^{-1}$ in a basic perturbation of particle position, so that $\sigma_y = \sqrt{2n\Delta t K_H}$ over n timesteps. Each particle below the inversion is randomly reassigned to a new height in the vertical on the assumption that it would have "forgotten" its position at the beginning of the timestep, due to eddy motions.

9.5 Entrainment

Large scale (e.g. day-to-day) entrainments are handled by the movement of the diagnosed boundary layer top from one model timestep to the next, or by particles being advected to regions of different boundary layer depths.

Homogeneous profiles retain particles in the boundary layer during a model timestep by reflecting particles off the surface and boundary layer top. Alternatively a novel **small-scale entrainment** scheme (Thomson et al, 1997) can be used at the boundary layer top. For a particle crossing the inversion, calculate

$$Arg^2 = \left\{ \frac{w'^2(old)}{\sigma_w^2(old)} + \log_e \frac{\sigma_w^2(new)}{\sigma_w^2(old)} \right\},$$

If Arg^2 is negative, the particle is reflected at the inversion. If it is positive, the particle is allowed to cross the interface with its velocity changing to

$$w'(new) = \sigma_w(new)Arg.$$

Far field

In the far field the probability of transmission is $(K(new)/K(old))^{1/2}$, which implies

$$w'(new) = w'(old)\sqrt{K(new)/K(old)}.$$

K-diffusion

To account for small scale entrainments, each particle is in fact reassigned over a depth slightly larger than that of the boundary layer, calculated to maintain the well-mixed condition.

9.6 Wind Meandering

Two years' 10-minute mean wind data from the Met Research Unit at Cardington, England, were processed to provide a parametrization of the form $\sigma^2_{v,\ell} = cu_{10}T_F$, where $\sigma^2_{v,\ell}$ is the meander velocity variance, u_{10} the mean wind at 10m, T_F the interval between the Unified Model wind fields supplied to the NAME dispersion model, and c a constant. A suitable timescale $\tau_{u,\ell}$ was estimated from the spectra of 10 min. means, and a second random walk applied:

$$u'_{t+\Delta t} = u'_t\left(1 - \frac{\Delta t}{\tau_{u,\ell}}\right) + \left(\frac{2\sigma^2_{u,\ell}\Delta t}{\tau_{u,\ell}}\right)^{1/2} r_t .$$

9.7 Venting in Active Convection

It is likely that, during the ETEX tracer releases, material was vented from the boundary layer by vigorous convection. Pending further investigation a very basic venting scheme was adopted: given a convective cloud base below 800 hPa and a cloud thickness exceeding 300 hPa, a particle is randomly distributed between the surface and the cloud top with a probability $(\Delta t / T_C) \times$ fractional cloud amount, where T_C is a time scale for convection.

9.8 Results of the Intercomparison

'Global' statistics were used to test the different diffusion options--- i.e., they include 30 three-hourly means for 168 surface measuring stations, provided the observed concentration exceeded 0.05 ngm m^{-3}. The statistics consisted of the mean square error (MSE), normalized mean square error (NMSE), mean absolute error (MAE), bias and Pearson's correlation (r). The results are given in *Table 9.1*, in which **L**, the long range scheme, is used as the **benchmark,** and the different options are identified as follows:

I: Inhomogeneous near-source run for 1st hr, then long range scheme.

Isk: As **I**, with skewed turbulence for 1st hr.

Iem: As **I,** with meandering and (except near-source, where it is implicit in the inhomogeneous scheme) small-scale entrainment.

H: Homogeneous near-source run for 1st hr, then long range scheme.

Lm: As **L** with meandering.

Le: As **L** with entrainment.

Lc: As **L** with convective venting.

Lcm: As **Lc** with meandering.

Lcme: As **Lcm** with entrainment.

Lcm₂e: As **Lcme** with $\sigma^2_{v,\ell}$ doubled.

K: *K*-diffusion scheme.

Kc: As **K** with convective venting.

Table 9.1 Percentage improvement over the ***L*** *run for 12 ETEX runs using different diffusion options.*

	I	Isk	Iem	H	Lm	Le	Lc	Lcm	Lcme	Lcme	K	Kc
nmse	*-5*	*-5*	*-2*	< 1	3	9	*-17*	*-13*	*-4*	*-4*	39	32
mse	*-6*	*-6*	6	*-<1*	2	19	11	14	28	29	34	46
mae	*-1*	*-1*	10	*-1*	2	12	21	24	28	29	*-4*	24
bias	*-1*	*-1*	16	*-1*	*-2*	21	48	48	61	63	*-14*	40
r	*-<1*	*-<1*	*-3*	*-<1*	< 1	*-2*	*-3*	*-3*	*-5*	*-5*	2	*-<1*

9.9 Conclusions

(1) There is much variability, an improvement in one statistic often involving a deterioration in another.

(2) The near-source schemes had little impact on the statistics (predominantly for long-range dispersion). This seems to justify economies in far-field integrations.

(3) In isolation, meander led to a slight improvement, venting and small-scale entrainments to moderate improvements. As meander and entrainment options were *added* to the venting the results improved monotonically: an important result.

(4) Arbitrarily increasing the meander, $\sigma_{v,\ell}$, made a marginal improvement.

(5) The **K** scheme, in which entrainment and meandering are allowed for one way or another, gave the best results for MSE, NMSE and correlation. When venting was added it gave the best performance overall. The results may reflect the strong diffusion associated with the uniform *K*-diffusivity---often a beneficial factor when applying conventional statistics to complex dispersion situations. (5) reinforces the conclusion of (2), and throws some light on conclusion (4).

References

Brost R. A., Wyngaard J. C. & Lenschow D. H.: 'Marine stratocumulus layers' Part II: Turbulence budgets' *J. Atmos. Sc.* **39,** p.818 (1982).

Hibberd, M.F. and Sawford, B.L.: 'A saline laboratory model of the planetary convective boundary layer' *Boundary-Layer Met.*, **69**, p. 229 (1994).

Luhar, A.K. and Britter, R.E.: (1989) 'A random walk model for dispersion in inhomogeneous turbulence in a convective boundary layer' *Atmospheric Environment*, **23**, p.1911 (1989).

Ryall, D.B. and Maryon, R.H.: 'The NAME 2 Dispersion Model: A Scientific Overview', *UK Met. Office Turb. & Diff. Note 217b* (1996).

Thomson, D. J., Physick, W. L. and Maryon, R. H.: 'Treatment of interfaces in random walk dispersion models', submitted to *Jnl Applied Met* (1997).

Figure 9.1 Three options for representing the vertical profiles of the vertical velocity variance σ_w^2 --- (a) Inhomogeneous statistics, (b) homogeneous statistics, with a step change at the inversion, z_i, and (c) linear transition through the inversion

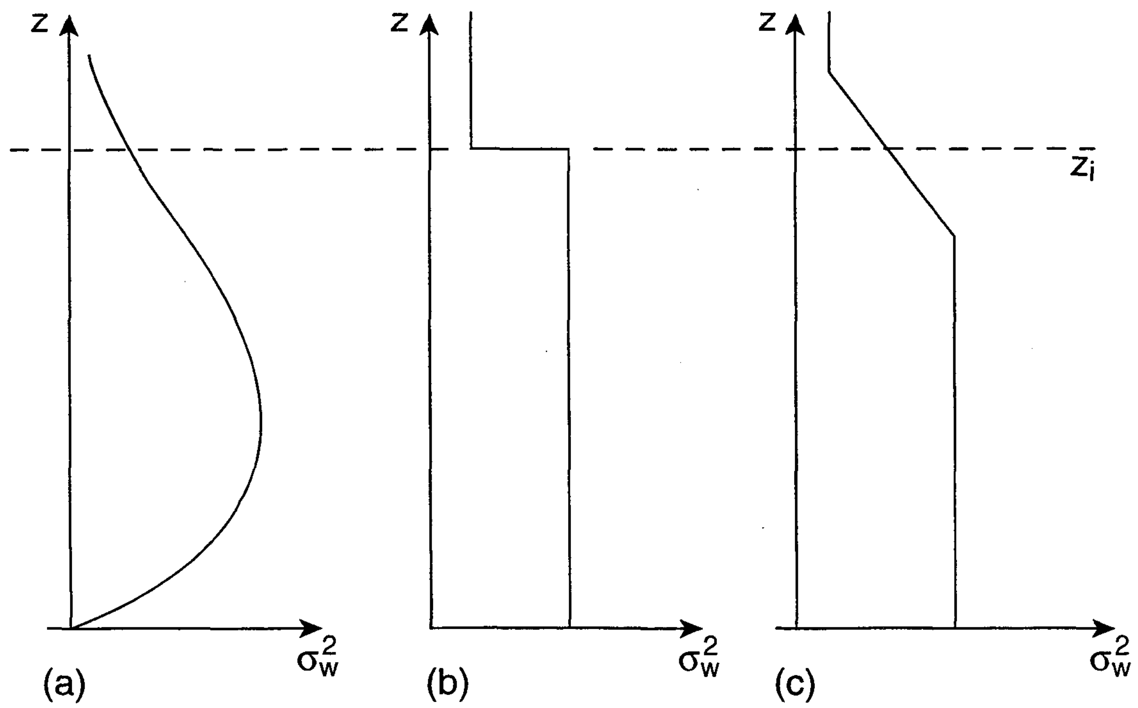

10 A summary of experiments on the dispersion of radioactive particles from the Chernobyl accident using a simple trajectory model

Ilkka Valkama
Finnish Meteorological Institute
Helsinki, Finland

The Finnish Meteorological Institute (FMI) maintains several models for dispersion forecasting during accidents and other emergencies. The current operational long range dispersion model for nuclear accidents is the TRADOS model (TRajectory, Dispersion and dOSe model). The model has two separate modules: a three dimensional trajectory model and a radiological dose model. The flow parameters are computed using numerical meteorological forecasts of the HIRLAM NWP model. The dose model and the UNIX-based graphical user interface common to both modules were developed at the Technical Research Centre of Finland (VTT).

The presentation summarized some transport simulation experiments made with the TRADOS model and how they fit the environmental findings in Europe after the Chernobyl accident, 1986. The model is described in (Valkama and Salonoja, 1995), with a special emphasis on the trajectory model characteristics. The Chernobyl accident simulation experiments have earlier been presented in two papers (Valkama et al., 1995, Valkama and Pöllänen, 1996). A third paper has been submitted for publication (Pöllänen et al., 1996).

The simulations were run on the Chernobyl HIRLAM data, specially compiled by the Danish Meteorological Institute. The same data base has earlier been utilized by (Langner at al., 1993). Some further TRADOS simulations using the same 137Cs release have been made and were presented at the first Nordic ETEX-meeting at Risø in 1995.

In the first simulations we concentrated on familiarizing ourselves with the data and on testing the model performance with it. Even after ten years, there are some uncertainties as regards the source term at the various stages of the Chernobyl accident. It was decided best to concentrate on the first 24 hours release, only. We think that a suitably well defined release scenario can be made for this period. Also the environmental effects, i.e. the deposition patterns over the Nordic countries, are much researched and well known. The first step was to test, how well the trajectories could describe the over-all dispersion during the Chernobyl accident. We begun by computing hour-by-hour air parcel trajectories for the first 24 hours of the accident, starting from 26th April 2100 UTC, and at 100 m elevation intervals from the ground level up to 4500 m. Close analysis of the resulting 1100 trajectories showed that we could find finely defined groups in them. The main features are given in *Tables 10.1 and 10.2* (adopted from (Valkama et al., 1995)). The results compare rather well both with the air-borne measurements and estimates of times of the first arrival of the plume. In particular the agreement with the picture given by (Persson et al., 1987) were excellent. The agreement between *Table 10.1 and Figure 10.1*, which gives the actually measured vertical structure of the plume over Finland (Sinkko et al., 1987) is good.

Encouraged by the results, we next made some dispersion simulations on Zirkonium. This nuclide is a good tracer, as the fall-out patterns of 95Zr over Finland suggests, that most of it originated from the very first stages of the accident. We decided to put the whole estimated released amount of Zr into the first 9 hours of the accident (Valkama et al., 1995). Using our trajectory statistics as the guide, we chose 2000 m as the maximum release height. The main result is given as *Figure 10.2*, from which it can be seen that while the agreement is not perfect, nor is it too bad. The general shape of fall-out patterns is very similar, the main difference being in that the model deposition area is narrower and a little bit too much to the south.

Having made ourselves familiar with the data, and having obtained some confidence on the model performance, we next tried Cesium. Our first simulations on 137Cs, with the release scenario taken from (Langner et al., 1995), were not very successful (see *Figure 10.3*). The agreement with the measured maximum deposition around Gävle, Sweden, is poor. This most probably is due to fact that the precipitation in the numerical data does not coincide with the plume over this region (i.e. our trajectories arrive incorrectly). Also, the fall-out trace over Finland has too elongated shape, which suggests that much of 137Cs arriving at Finland originated from later stages during the accident, as those arriving at Sweden. As the factors affecting the dispersion and deposition of the 137Cs after the accident can be considered to be well understood, explained (see e.g. (Arvela et al., 1987, Persson et al, 1987, Sinkko et al., 1987)) and modeled, we decided not to take these studies any further. Instead we searched to find some other topics not so well researched. One specific problem suggested itself, namely the fate of so called "hot particles". These are large, highly radioactive particles, which were found all over Europe in 1986. The problem was mentioned already by (Persson et al., 1987), but has received little attention since.

A thorough analyses of the literature published on the subject revealed, that indeed surprisingly large particles have been discovered hundreds of kilometers from Chernobyl, at places as far from each other as Norway and Greece (Pöllänen and Toivonen, 1996). How can these particles, large enough to have considerable gravitational settling velocities, have remained air-borne so long? Two possible explanations have been suggested, that either the effective release height must have been considerably higher than reported earlier or convective cells might account for uplift during the transport (Persson et al., 1987). By applying some simple physical approximations for the respective terminal velocities of large particles we have computed the maximum transport distances to be expected for particles of several sizes. The results are shown in *Figures 10.4* and *10.5* and in *Table 10.3* (Pöllänen et al, 1996). *Figure 10.4* shows that increased release height does indeed explain much of the findings from the first stage of accident (the Nordic counties and Poland). However, as *Figure 10.5* shows, during the latter stages of the release, things are different. The relevant release heights are then too low to carry the larger particles very far.

The second assumption has, to our knowledge, been discussed in modeling context only occasionally (Bonelli et al., 1991, Lagner et al., 1995). To test this assumption, a simple parametrization of deep convection, based on the George's lability indice (George, 1960), was implemented in the trajectory model. Preliminary results (*Figure 10.6*, from (Valkama and Pöllänen, 1996)) supported the view, that travel distances of particulate matter are considerably increased, if deep convection phenomena are included.

Having completed this experiment, which resulted in a paper offered for publication (Pöllänen et al., 1996), we returned to our original 137Cs simulation. After as re-evaluation of the source term we found that one of the main problems with the original simulation was the poor resolution of the transport. More precisely, the number of trajectories was insufficient to describe the plume advection both to Sweden and to Finland. Instead of trying to base the whole simulation on one single set of trajectories, we used our original trajectory analysis to recognize the respective transport levels most relevant for Sweden and Finland. The releases and release heights were then segmented accordingly. The total amount of 137Cs released was kept to that from (Langner et al., 1995), in order to compare our results with theirs. Preliminary results are given in *Figure 10.7.a* for Sweden and in *10.7.b* for Finland. It can be seen that, compared to *Figure 10.3*, the main features of deposition are now much better defined, and resemble the observed ones given in *Figure 10.7.c* rather well. The maximum deposition over Gävle region is still somewhat smaller than the measured one, and more to the east. This is most likely due to the inability of our model to get the plume and the precipitation simultaneously over this region. It should be noted that also (Langner et al., 1995) reported similar problems in their numerical simulation. We are going to look into this more closely in the near future.

References

Arvela, H., L. Blomqvist, H. Lemmelä, A.L. Savolainen and S. Sarkkula, 1987. Environmental gamma radiation measurements in Finland and the influence of meteorological conditions after the Chernobyl accident in 1986. STUK-A65, 1987.

Bonelli, P., Calori, G. and Finzi, G., 1991. The influence of deep convection phenomena on trajectories computed by long-range transport models. Proceedings of the 19th International Technical Meeting on Air Pollution Modeling and its Applications, CCMS/NATO, Athens 1991.

George, J.J., 1960. Weather forecasts for aeronautics. Academic Press, New York.

Langner, J., Persson, C. and Robertson, L., 1995. The Chernobyl accident : A case study of dispersion of Cs-137 using high resolution meteorological data. In : Tveten, U. (ed.) Dispersion prognoses and consequences in the environment. Final report from the NKS, Project BER-1. TemaNord 1995:544. Kjeller, Norway, December 1994.

Persson, C. and H. Rodhe and L-E. De Geer, 1987. The Chernobyl accident : A meteorological analysis of how radionuclides reached and were deposited in Sweden. Ambio 16, 20-31.

Pöllänen R. and H. Toivonen, 1996. Transport of radioactive particles from the Chernobyl accident. Submitted for publication.

Size estimation of radioactive particles released in the Chernobyl accident. Poster at the 14th International Conference on Nucleation and Atmospheric Aerosols, Helsinki, August 26-30, 1996.

Sinkko, K., H. Aaltonen, R. Mustonen, T.K. Taipale and J. Juutilainen, 1987. Airborne radioactivity Finland after the Chernobyl accident in 1986. STUK-A56, 1987.

Valkama I., M. Salonoja, J. Lahtinen, H. Toivonen and R. Pöllänen, 1995. Transport of radioactive gases and particles from the Chernobyl accident. Proceedings of the IAEA International Symposium on Environmental Impact of Radioactive Releases, Vienna, May 8-12, 1995.

Valkama I. and M. Salonoja , 1995. Experimentation with the Finnish long-range trajectory and dispersion model (TRADOS). Proceedings of the 10th IUAPPA World Clean Air Congress, Espoo, May 28 - June 2, 1995.

Valkama I. and R. Pöllänen, 1996. Transport of radioactive materials in convective clouds. Proceedings of the 14th International Conference on Nucleation and Atmospheric Aerosols, Helsinki, August 26-30, 1996.

Table 10.1 The vertical structure of the dispersion towards Finland for the first 24 hours of the Chernobyl accident, 1986 as described by 3-D trajectories.

Initial height over Chernobyl (m)	Height on arrival over Finland (m)
2500 - 4000	2000 - 2500
1600 - 2500	1500 - 1700
1500	1000 - 1300
1000 - 1400	800 - 1000

Table 10.2.a Times of arrival (UTC) over Sweden for various release heights for the initial explosion of the Chernobyl accident, 21:30 UTC 26th April, 1986.

Initial release height (m)	Time and height of arrival over Gotland	Time and height of arrival over Eastern Svealand
1300 - 1400		27.4 18:00 UTC / 800 m
1000	27.4 09:00 UTC / 300 m	27.4 12:00 UTC / 500 m
500 - 750	27.4 12:00 UTC / 400 m	27.4 20:00-23:00 UTC / 400 m

Table 10.2.b Times of arrival (UTC) over Finland for various release heights for the initial explosion of the Chernobyl accident, 21:30 UTC 26th April, 1986.

Initial release height (m)	Time and height of arrival over South-Western Finland	Time and height of arrival over Åland
2000	27.4 12:00 UTC / 1500 m	27.4 15:00 UTC / 1500 m
1500	27.4 15:00 UTC / 1000 m	27.4 16:00 UTC / 1000 m
1300 - 1400	28.4 00:00-03:00 UTC / 1000 m	27.4 18:00 UTC / 1000 m

Table 10.3 The minimum and maximum transport distances of particles release from different altitudes during the first 12 hours of the Chernobyl accident

Particle size		Trajectory length (km) for release heights 500 - 3000 meters					
d_a (μm)	d_p (μm)	500 m	1000 m	1500 m	2000 m	2500 m	3000 m
20	6.2	90 - 150	250 - 410	570 - 780	810 - 1000	1200 - 1600	1400 - 1800
30	9.3	64 - 83	140 - 200	250 - 320	400 - 480	530 - 640	650 - 800
40	12	42 - 51	94 - 120	160 - 210	220 - 280	290 - 370	350 - 470
50	15	29 - 36	67 - 81	110 - 140	150 - 200	190 - 250	240 - 310
60	19	23 - 29	47 - 60	81 - 99	110 - 140	150 - 190	180 - 230
70	22	17 - 22	38 - 44	63 - 75	88 - 110	110 - 140	140 - 170

(Pöllänen et al, 1996)
Trajectories computed with one hour intervals from 25th April 21:00 UTC to 26th April 08:00 UTC.
Particle sizes: d_a = 20 μm d_p = 70 μm
Model: TRADOS
Meteorological data base: DMI/HIRLAM

Figure 10.1 *Vertical distributions of gamma dose rates over Southern (A), Central (B) and Eastern (C) Finland according to flight measurements made by Finnish Air Forces on 29th April, 1986.*

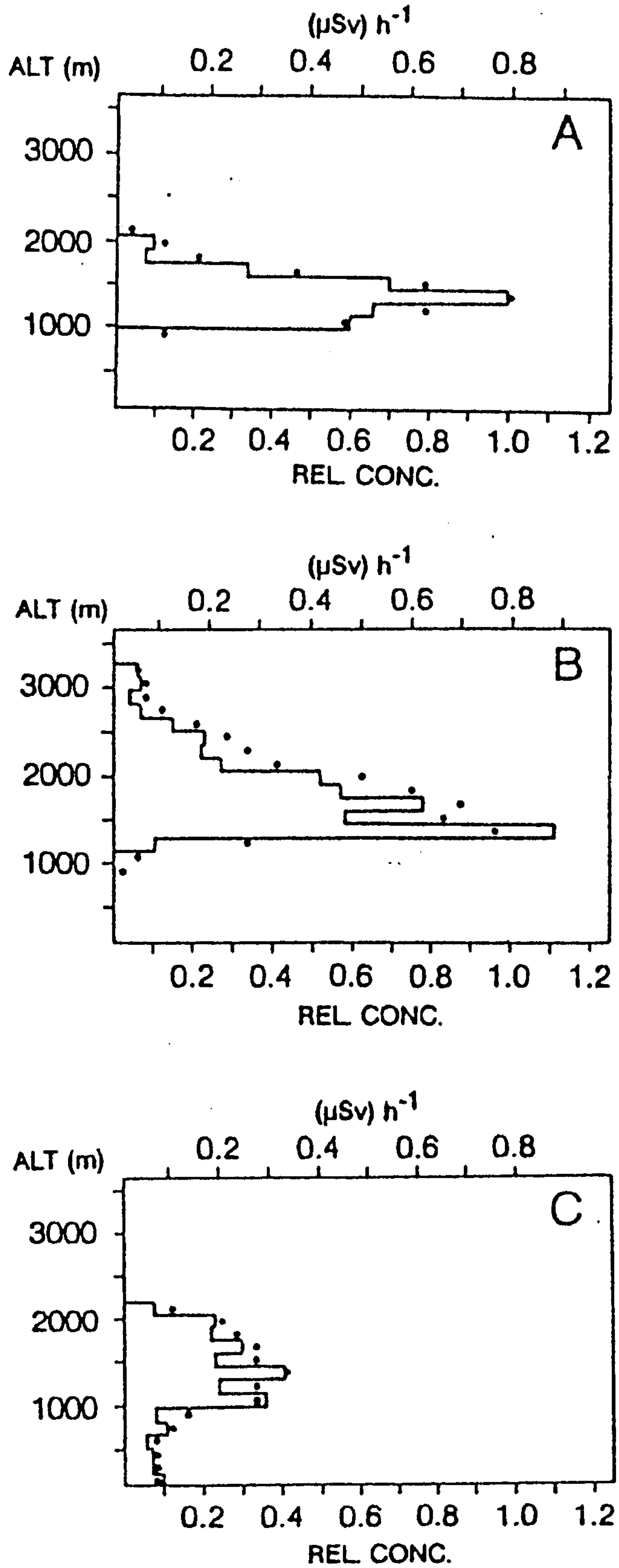

Reproduced from Sinkko, K., H. Aaltonen, R. Mustonen, T.K. Taipale and J. Juutilainen, 1987. Airborne radioactivity Finland after the Chernobyl accident in 1986. STUK-A56, 1987.

Figure 10.2 *The 95Zr fall-out patterns over Finland, a comparison of measurements to the dispersion model simulations. The solid line is the 2 kBq m-2 isoline, while the dark gray shading depicts the same area according to the soil samples. The insert shows the trajectories starting from Chernobyl at 21:00 UTC 25th April, 1986, at 750 m (A), 100 m (B), 1500 m (C) and 2500 m (D) elevations.*

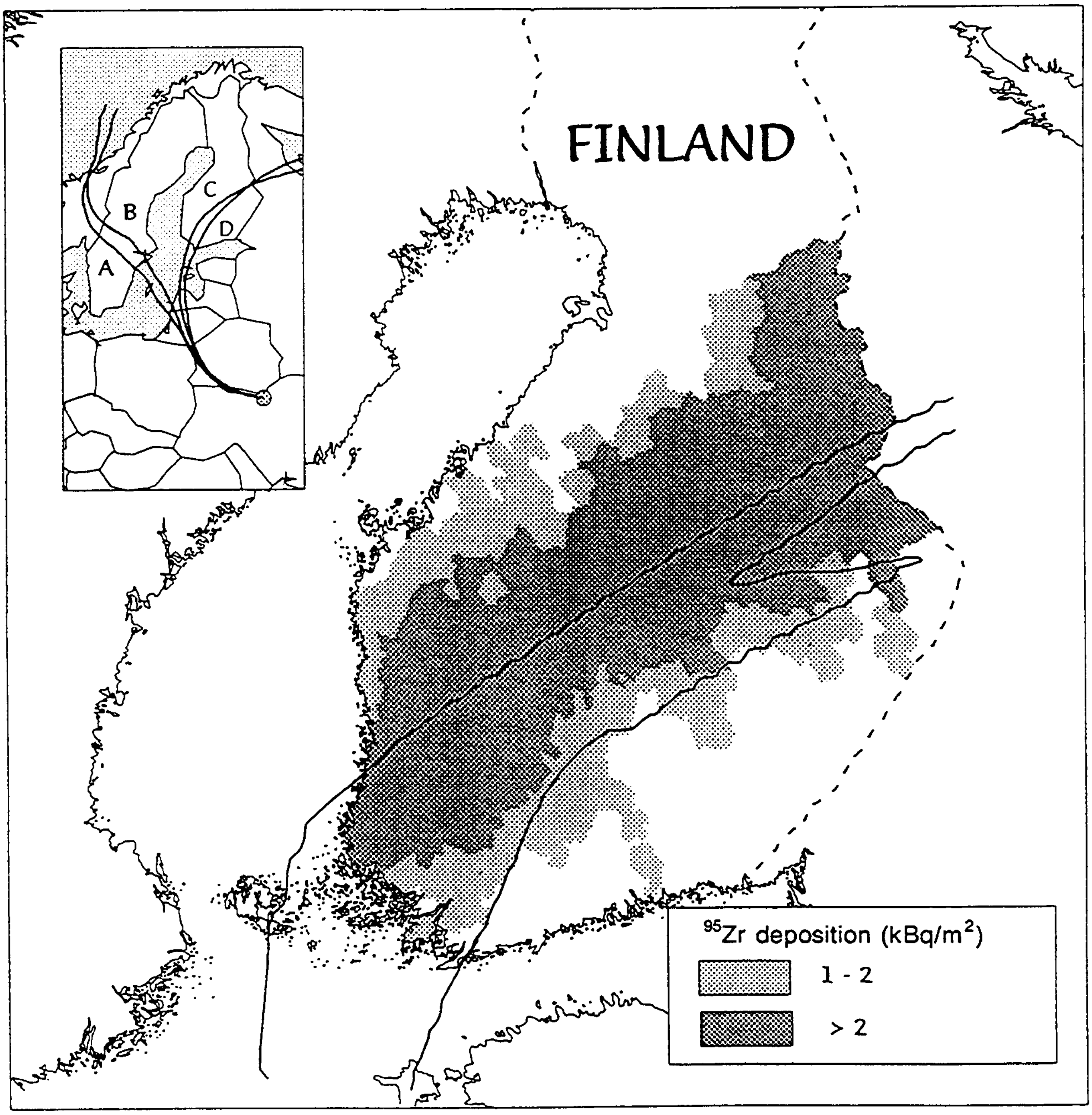

Figure 10.3 *The 137Cs deposition over Sweden and Finland as computed with TRADOS and as measured after the Chernobyl accident, 1986.*

FINNISH METEOROLOGICAL INSTITUTE

VTT

RADIOACTIVE DEPOSITION
Runtime: 21-NOV-1996 13:09 UTC
Chernobyl 1986
Model: Trados   Weather data: TRADOS_HIRLAM
tots

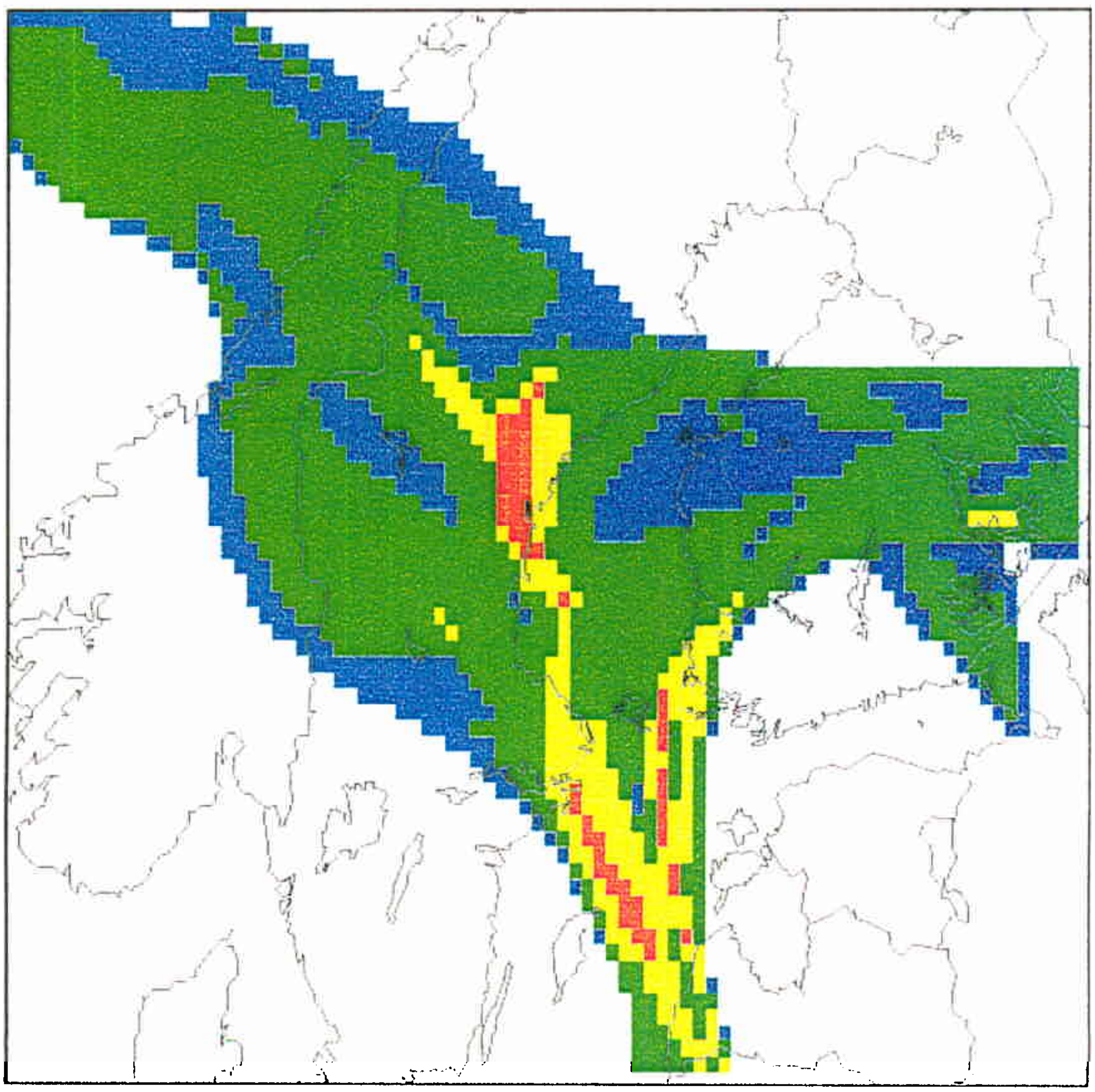

Figure 10.4 Points of impact for 20 μm particles released from various altitudes for the first 12 hours of the Chernobyl accident, 1986.

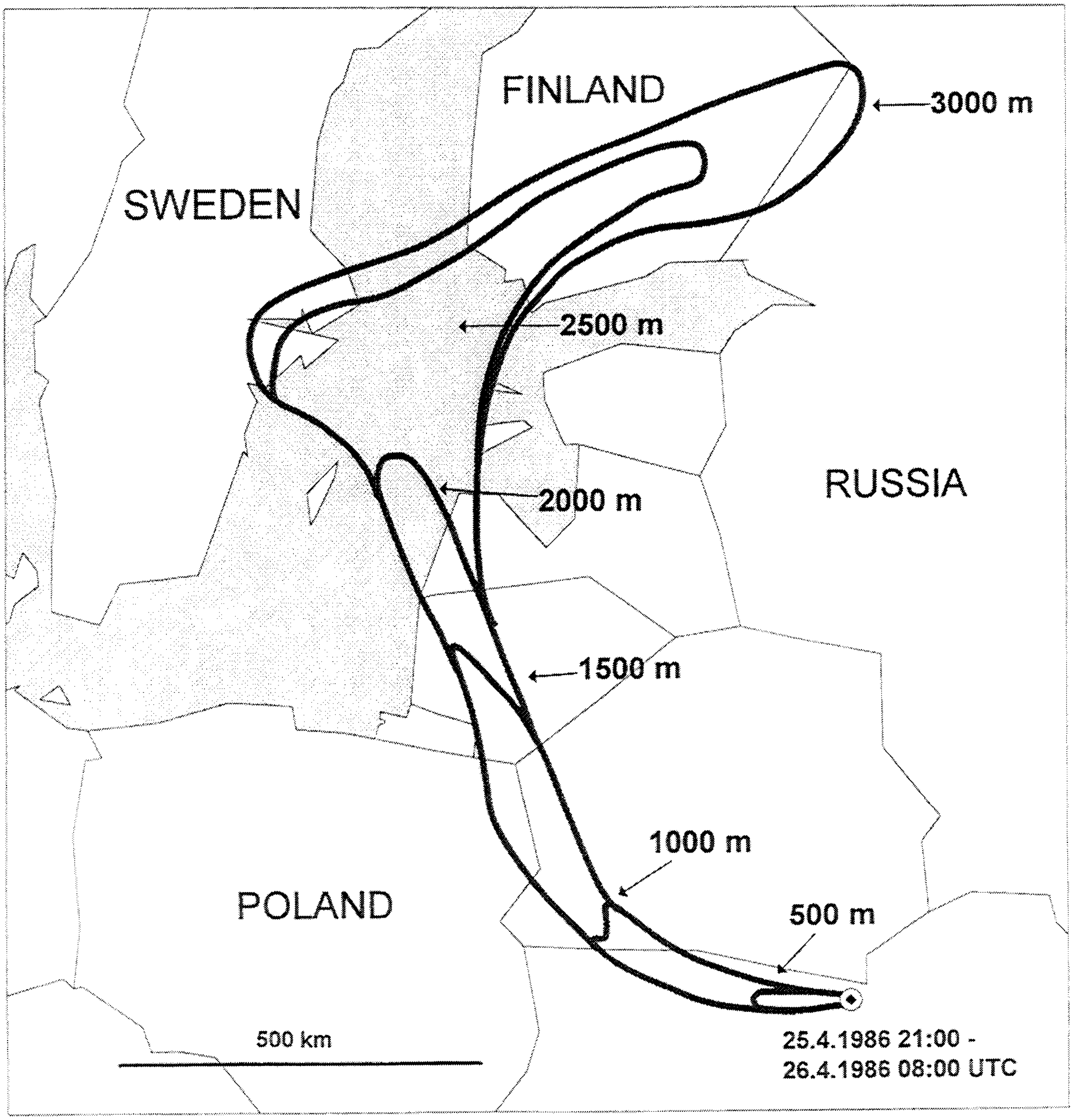

Figure 10.5 Points of impact and calculated deposition areas for 20 μm particles released from altitudes of 400m and 700 m during the Chernobyl accident, 1986.

Pöllänen et al., 1995

Black points mark the places where fuel fragments > 20 μm have been found

Model = TRADOS
Meteorological data = DMI_HIRLAM

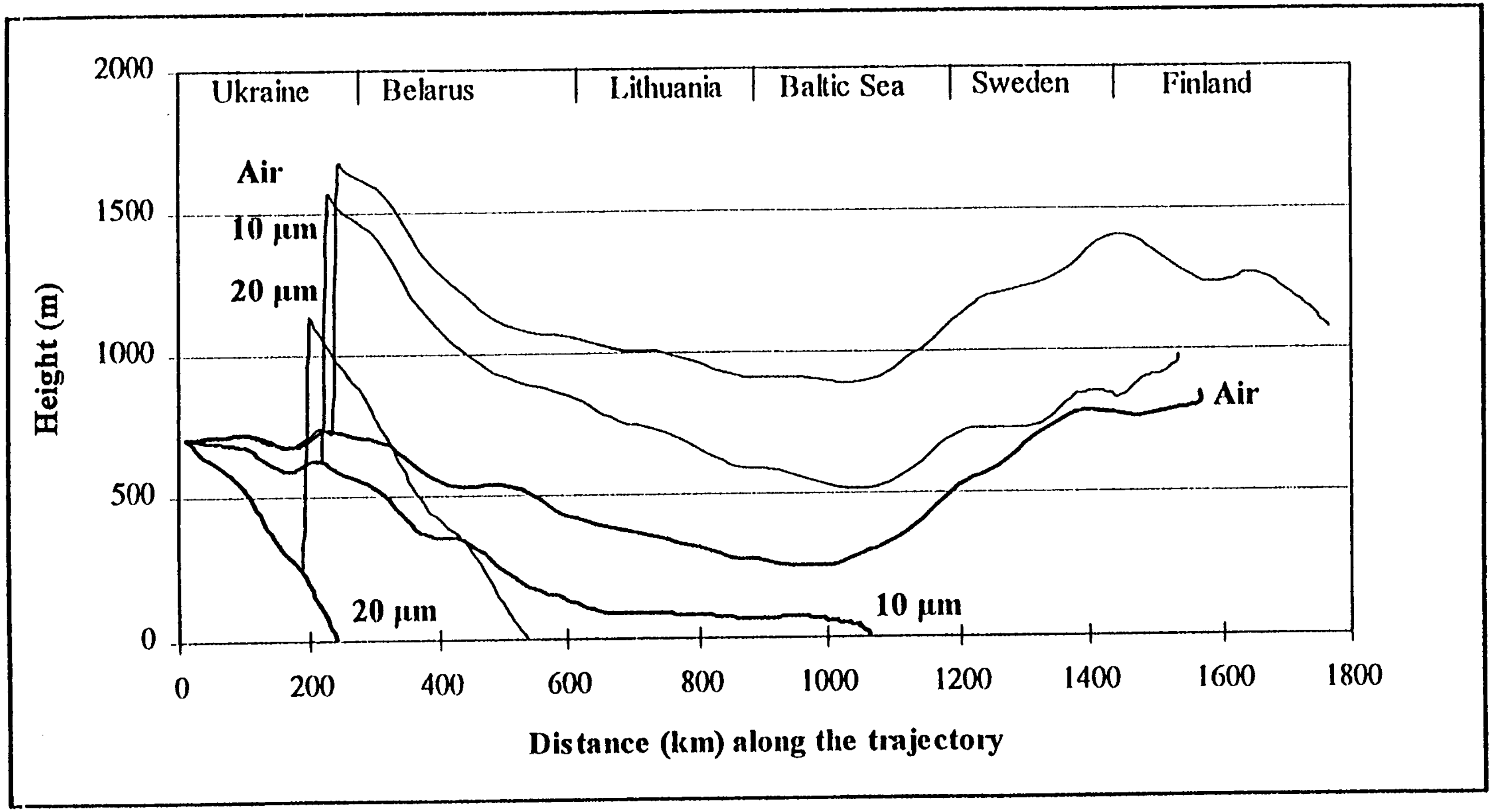

Figure 10.6 Vertical cross-sections of trajectories described by massless (air), 10 µm and 20 µm particles computed without (thick lines) and with convective uplift (thin lines) over Ukraine during the Chernobyl accident, 1986.

Figure 10.7.a The 137Cs deposition over Sweden after the Chernobyl accident, 1986, as computed with TRADOS.

FINNISH METEOROLOGICAL INSTITUTE

RADIOACTIVE DEPOSITION
Runtime: 21-NOV-1996 13:09 UTC
Chernobyl 1986
Model: Trados   Weather data: TRADOS_HIRLAM
Sweden

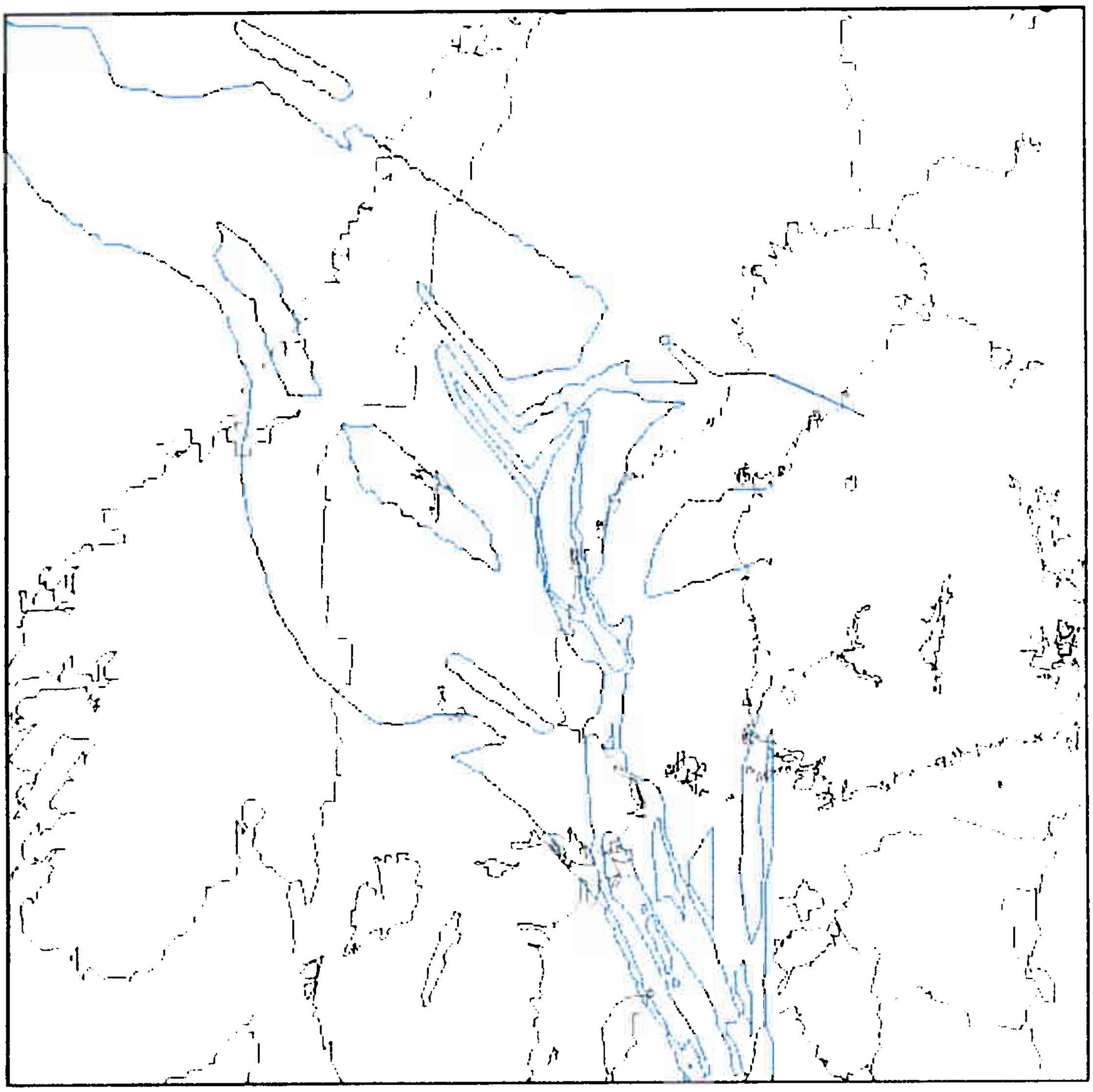

Radioactive deposition [Bq/m2]
Time of the field: 2.05.1986 21:00 UTC, +168 h
Release time: 25.04.1986 21:00 UTC Duration: 36 h
1 = 5.00e+04 Bq/m2
2 = 2.50e+04 Bq/m2
3 = 1.00e+04 Bq/m2
4 = 1.00e+03 Bq/m2

Figure 10.7.b The 137Cs deposition over Finland after the Chernobyl accident, 1986, as computed with TRADOS.

FINNISH METEOROLOGICAL INSTITUTE

RADIOACTIVE DEPOSITION
Runtime: 22-NOV-1996 09:44 UTC
Chernobyl 1986
Model: Trados   Weather data: TRADOS_HIRLAM
Finland, first 24 hours, Cs-137 release

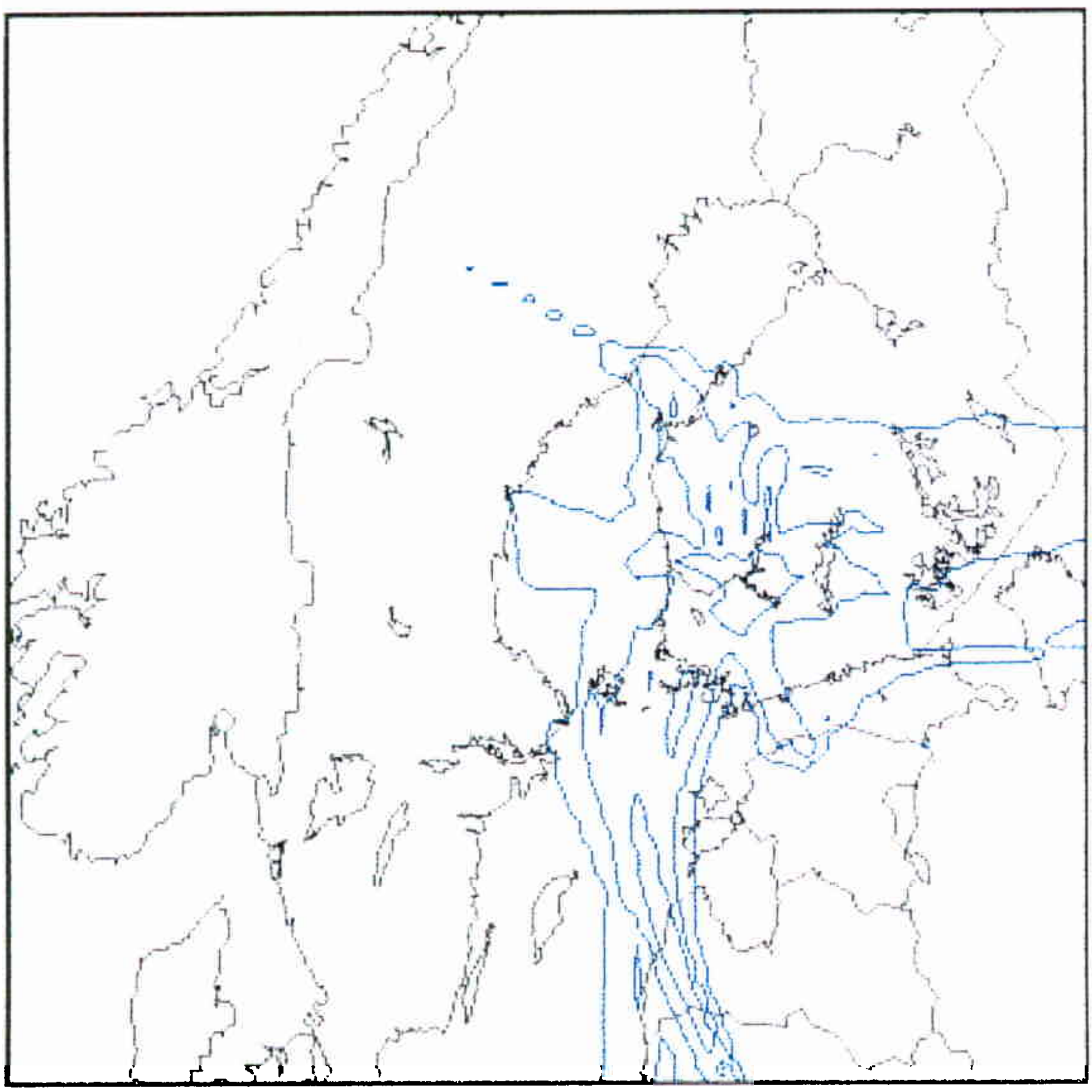

Radioactive deposition [Bq/m2]
Time of the field: 2.05.1986 23:00 UTC, +168 h
Release time: 26.04.1986 00:00 UTC Duration: 24 h
1, 10, 30

Figure 10.7.c The 137Cs deposition over the Nordic Countries as measured after the Chernobyl accident, 1986.

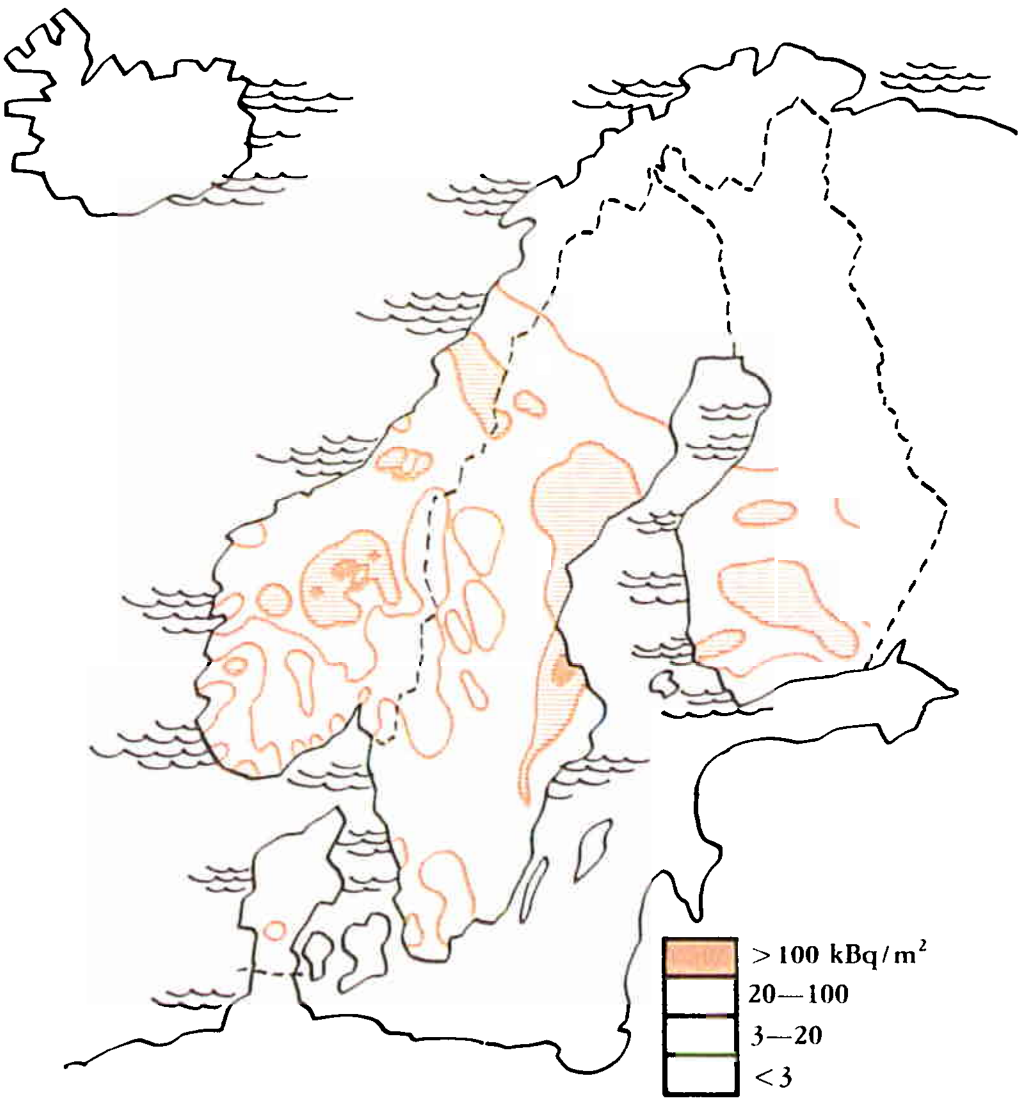

Source: SSI & STUK

11 The atmospheric transport module in RODOS for now- and forecasting of radioactive airborne spread on local, regional and European scales

Torben Mikkelsen
Risø National Laboratory
Denmark

The objective of the atmospheric dispersion module in **RODOS** (Kelly *et al.,* 1996) is to provide the decision support system with an integrated set of models for now- and forecasting of radioactive airborne spread on all (local, national, and European) scales. The module inputs real-time measured or estimated source terms and runs on actual or predicted weather conditions facilitated via on-line local network connection to local meteorological towers or by via remote network connections (Internet or ISDN) to cooperating operational national or international Numerical Weather Predicting (NWP) centers. It is designed for providing actual (real-time) and forecast (+ 36 Hour) ground-level gamma dose rates, ground-level air concentrations including ground-level wet and dry deposition estimates on all scales. It is furthermore designed to accommodate "on the fly" on-line incoming radiological monitoring data and assists source term determination via various data assimilation and back-fitting procedures.

11.1 Introduction

A set of atmospheric flow and dispersion models, suitable for real-time dose assessment on a UNIX-based workstation, have earlier been identified (Mikkelsen, 1993), cf. Table 11.1. With the aim of becoming operational in **RODOS** by year 1999, these models and modules are now becoming system integrated into a single comprehensive **MET-RODOS** module. This work, involving many partners, is coordinated as a joint R&D project within the fourth frame work of the EU (1996-1999) Radiation Protection program. The present paper summarizes the "state of art" regarding its implementation and integration.

11.2 The MET-RODOS system

With the objective to provide the **RODOS** system with system integrated atmospheric transport module for now- and forecasting of radioactive airborne spread on all ranges, the **MET-RODOS** module is composed by following three sub-systems:

1) the Local Scale Preprocessor <**LSP**>,
2) the Local Scale Model Chain <**LSMC**>, and
3) the Long Range Model Chain <**LRMC**>

The **LSP** maintains the systems real-time data base with actual and forecast local scale wind fields and corresponding micro-meteorological scaling parameters by use of preprocessor and local scale wind models. **LSMC** contains a suite of local scale mean wind and dispersion models, from which case-specific models is selected depending on the actual topography and atmospheric stability features in question. It provides local scale deposition rates, air concentrations and gamma dose rates for the **RODOS** system, and for plumes reaching the outer bounds for the local scale (20 km), it passes on the diffusion specific parameters such as cloud size and cloud position to the **LRMC**. The **LRMC** manages the long range trajectory and dose rate capability in **MET-RODOS**. It provides local-scale consistent trajectory and dose rate assessments on national and European scales by accessing the Numerical Weather Prediction (NWP) data stored in the **LSP** data base, and by integration of the **LSMC** outputs for its initialization.

Table 11.1 Models associated with the MET-RODOS system

Near-range flow and dispersion models including pre-processors:
- Meteorological preprocessor (PAD)
- Mass Consistent Flow model (MCF)
- Linearized flow model (LINCOM)
- Near-range puff model with gamma dose (RIMPUFF)
- Near range segmented plume model (ATSTEP)

Complex terrain models (stand alone system):
- Prognostic flow model (ADREA) and Lagrangian dispersion model (DIPCOT)

Mesoscale and Long-range Models:
- Eulerian K-model (MATCH) nested with puff radiation dose models (RIMPUFF)

On-line Weather Forecast data:
- Numerical Weather Prediction models (HIRLAM-DK and SPA -TYPHOON)

11.3 On-line now and forecast met-data

Real-time application of atmospheric dispersion based nuclear emergency system requires on-line access to actual (real-time) estimates of the local dispersion meteorology. Such data are usually available from a network-connected met-tower located in the vicinity of the release point (on-site) and instrumented with wind (cup and wind vanes) and temperature sensors. For off-site assessment - in particular as a given release transports to distances beyond the local (10-20 km) scale, similar on-line estimates from the regional (100 km scale) wind and temperature conditions are also requested by **MET-RODOS** to work in real time. Such on-line regional scale meteorology is in some European countries (Hungary) already available from on-line direct measurements based on a distributed network of met-towers.

Alternatively to measurements, however, quantitative medium-range estimates of actual regional wind and temperature conditions are nowadays available in most parts of Europe, obtainable as Numerical Weather Prediction forecasts, and distributed on-line from national or international operational meteorological organizations in Europe.

For **MET-RODOS** to provide both actual and forecast dose assessments, its model chain has been designed to incorporate both on-line met-towers and high-resolution (20 km grid) NWP data. With the recent (1995) EU approved ECOMET organization of the European national meteorological services (NMS), customers in the EU area are now enabled to purchase NWP data on-line from collaborating NMS's, e.g. from the joint European Centre for Medium-Range Weather Forecasts, cf. the ECMWF centers Internet Home Page, address:

www.ecmwf.int/.

During the **MET-RODOS** development and implementation phase, the active collaborating NWP centers include the Danish Meteorological Institute (DMI), and the SPA-TYPHOON center in Obninsk, Russia.

*Figure 11.1 The **MET-RODOS** nested local scale and long range atmospheric dispersion system*

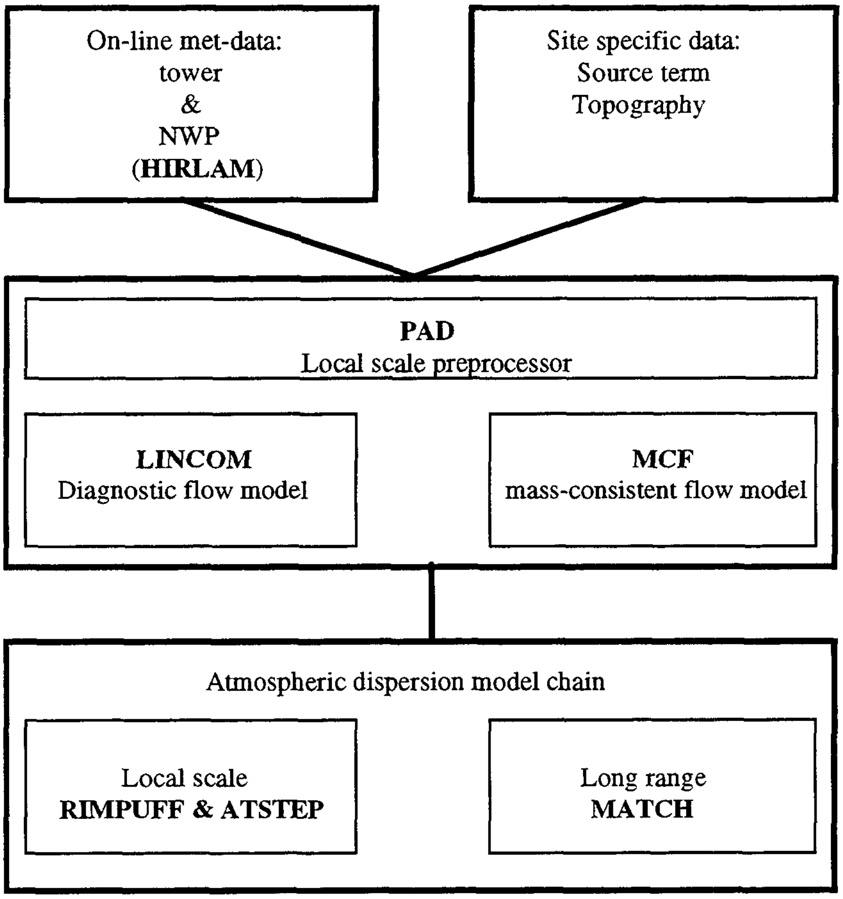

11.4 Display of NWP data and trajectories

LSP gives its user local access to a real-time display and animation feature based on the actual downloaded weather forecasts. The **VIS5D** visualization software is used on **MET-RODOS** to interactively animate the large gridded data sets. It provides instant images of wind vectors, precipitation patterns, concentration and dose contours in a 3-D grid, then rotate and animate the images in real time. It also features real-time display and animation of trajectories associated with any point inside the long-range <NWP-grid>, cf. the **VIS5D** Home Page at:

www.ssec.wisc.edu/~billh/vis5d.html.

11.5 Local scale wind models

The **LINCOM** system (Astrup *et al.*, 1996) supplies **MET-RODOS** with a fast diagnostic, non-hydrostatic dynamic flow model system based on the solution of linearized versions of the three momentum equations. It models wind flows in hilly terrain, and recently also thermal stratification effects such as valley breezes and nocturnal drainage flows, and wind and turbulence fields over areas with mixed land use (aerodynamical roughness). Initialized by met-data from a single met-tower (or from a single NWP grid point), **LINCOM** calculates momentum and continuity conserved wind and turbulence grid for the local scale domain, and these fields are subsequently used by the **RIMPUFF** dispersion model to advect, diffuse and deposit the puffs.

MCF (Massmeyer, 1991) is a mass consistent model based on interpolation of measured wind data under the constraint of minimizing the flux divergence. It is included in the **LCMC** as a complementary model to **LINCOM**. **MCF** generates mass-consistent interpolated wind fields over the local scale topography from on-line met-data from a multitude of met-towers or NWP grid points.

11.6 Local scale dispersion models

RIMPUFF (Mikkelsen, 1984) is a fast and operational local scale puff diffusion code for real-time simulation of radioactive cloud dispersion during time and space changing meteorology. It is provided with a puff splitting feature to deal with plume bifurcation and layer de-coupling over non-uniform terrain. This feature is also used with Bayesian-based real-time data-assimilation. A real puff-based gamma dose rate algorithm has been introduced (Thykier-Nielsen, 1995). Its diffusion parameterization is entirely formula-based and modular. **RIMPUFF** can with few limitations be setup to accommodate any user-requested diffusion parameterization scheme. **RIMPUFF** has standard plume rise formulas, inversion, and ground level reflection options. Its gamma dose rate capability plays an important role in **RODOS** for real-time data assimilation and back fitting procedures based on gamma radiation monitoring data.

ATSTEP (COSYMA, 1990) is a segmented Gaussian plume model which was central in earlier probabilistic risk assessment calculations. **ATSTEP** was first to be system-integrated in **RODOS**, where it now remains for training and demonstration purposes.

11.7 Long range dispersion models

MATCH is a 3-dimensional Eulerian atmospheric dispersion model, which has been developed at the Swedish Meteorological and Hydrological Institute (SMHI). MATCH is intended to be the only **MET-RODOS** resident European scale dispersion model. It will be running locally in **RODOS** by accessing the NWP data stored in the **MET-RODOS** <local scale real-time data base>. Seamless interfacing of an Eulerian long range model with the output of the Lagrangian puff model **RIMPUFF** has been achieved (Brandt, 1996).

11.8 Modes of operation

This section describes the envisioned strategy for daily operation of the **MET-RODOS** system. Technically, transfer times for downloading a new +36 Hr prognoses (done every +6 or +12 hours) is operationally feasible in less than ~1 Hr with a single (2x64 Kbit/s) point-to-point ISDN digital telephone line.

MET-RODOS is envisioned to run the local scale atmospheric model chain "around the clock" at the emergency center and automatically update during "Alert State: Normal" mode. Display windows of dispersion from any potential local sources can in this way be visualized instantly (calculated on the basis of an "unit release"). Continuous operation also exercising of the data transfer and makes long range trajectory calculations (both backward and forward) instantly at hand (via **VIS5D**) from any local or long range position. During "Alerts", or during training, specially educated personnel will have to be "called" into the emergency room for manually operating the **MET-RODOS** system. Their tasks will be to start up the runs for the long range model chain and to assist with data assimilation and back fitting procedures on the local scale, and to provide realistic source terms, and to critically evaluate and update the **MET-RODOS** prognoses etc.

11.10 Model evaluation program

Codes and modules for the atmospheric model chain have previously been evaluated experimentally during full scale tests, subsequently they are now being quality assured and documented according to the specifications set out by the overall **RODOS** concept.

11.10.1 Local Scale Model Chain evaluation

An international field study "MADONA" (after "Meteorology And Diffusion Over Non-uniform Areas") were conducted over rolling hills near Porton Down in England in 1992, cf. *Figure 11.2.* Several accidental release scenarios were here recorded in high temporal and spatial detail for subsequent comparison with modeled diffusion patterns. The resulting near-range atmospheric dispersion model training module for is available on CD-ROM (Mikkelsen *et al.,* 1995).

11.10.2 Long Range Model Chain evaluation:

The long-range "Europe-scale Tracer EXperiments" by name ETEX was conducted in 1994 in continuation of the Chernobyl-triggered Atmospheric Transport Model Evaluation Study (ATMES). ETEX was conducted to evaluate existing operational meteorological long-range models to forecast and predict - in real time - both wind fields over Europe and air concentrations from a ground based point source. During ETEX a tracer gas cloud was monitored as it dispersed over Europe during time scales of up to several days. The NWP model **HIRLAM** and the long range model match are participating in the ETEX evaluation procedures (Tveten, 1995).

References

Astrup P., N.O. Jensen and T. Mikkelsen (1996) Surface Roughness Model For Lincom. Riso report Riso-R-900(EN), ISBN 87-550-2187-5, ISSN 0106-2840; 30 pp. Available on request from: Information Service Department, Riso National Laboratory.

Brandt, J., T. Mikkelsen, S. Thykier-Nielsen and Z. Zlatev (1996): Using a combination of two models in tracer simulation. Mathl. Comput. Modelling Vol. 23, No. 10, pp. 99-115.

COSYMA - A new Programme Package for Accident Consequence Assessment. Report EUR 13028 EN. (Brussels - EU) (1990).

Kelly, G. N., J. Ehrhardt and V.M. Shershakov (1996): Decision support for off-site emergency preparedness in Europe. Radiation Protection Dosimetry, Vol. 64, No.1/2, pp. 129-141.

Massmeyer, K. and Martens, R. (1991): Regional Flow Fields in Northrhine Westfalia - A Case Study Comparing Flow Models of Different Complexity -.in: Air Pollution Modelling and its Application VIII, ed. by H. van Dop and D.G. Steyn, Plenum Press, New York, pp. 301 - 309, 1991

Mikkelsen, T., S.E. Larsen and S. Thykier-Nielsen (1984). Description of the Riso Puff Diffusion Model. Nuclear Technology, Vol. 67, pp. 56-65.

Mikkelsen, T. and F. Desiato (1993). Atmospheric dispersion models and pre-processing of meteorological data for real-time application. Radiation Protection Dosimetry Vol. 50, Nos. 2-4, pp. 205-218.

Mikkelsen, T. , H.E. Jorgensen, K. Nyren and J. Streicher (1995). MADONA: Diffusion measurements of smoke plumes and of smoke puffs. In: Proceedings of the 11th Symposium on Boundary Layers and Turbulence, Charlotte, N.C., USA, March 1995, pp. 319-322.

Thykier-Nielsen, S., S. Deme, and E. Lang (1995). Calculation method for gamma-dose rates from Gaussian puffs. Riso-R-775(EN). Available on request via e-mail: risoe@risoe.dk.

Tveten, U. and T. Mikkelsen, Eds. (1995) Report of the Nordic dispersion-/trajectory model comparison with the ETEX-1 full-scale experiment. NKS/EKO-4 intercomparison/validation exercise held at Riso, Denmark, 6-7 June 1995. Riso-Report-847(EN)/NKS Report EKO-4(95)1.

Figure 11.2 Local scale evaluation studies MADONA

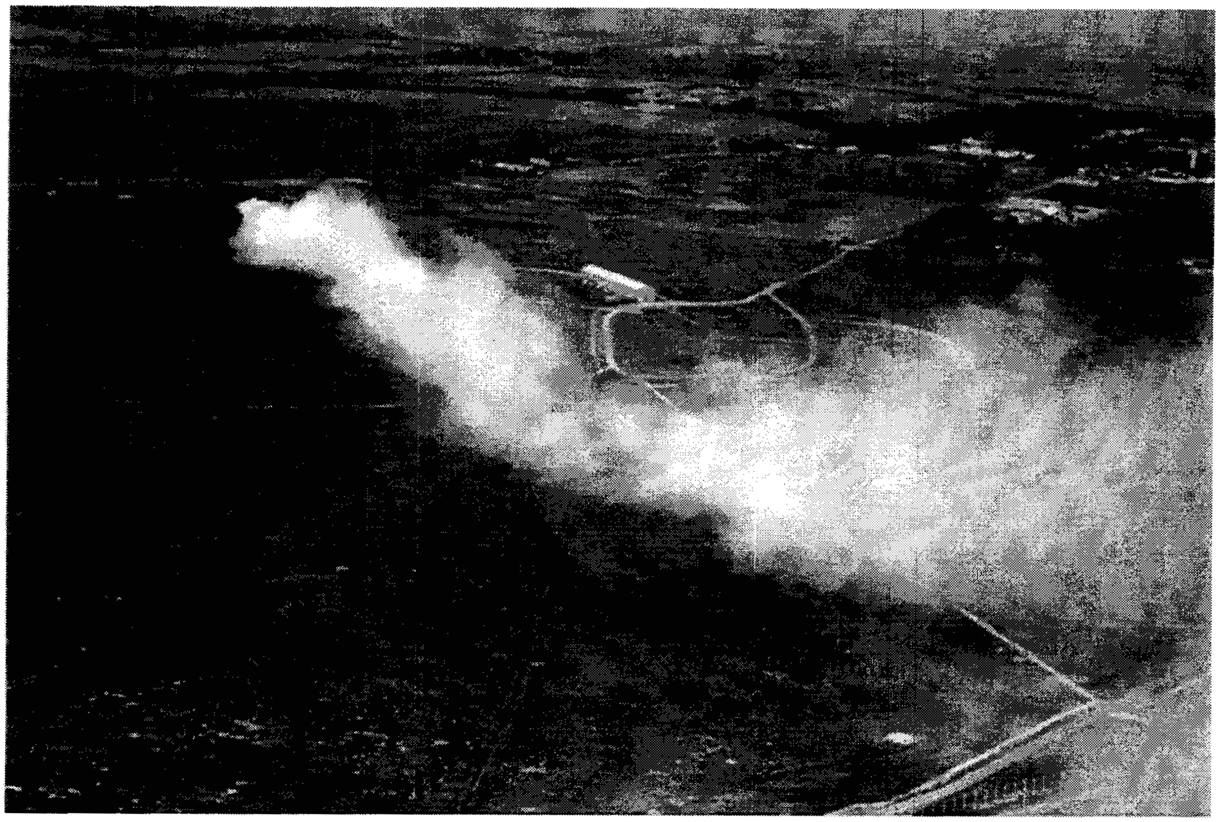

12 Experiences in development of a random-walk particle dispersion model at the Finnish Meteorological Institute (FMI)

Mika Salonoja
Finnish Meteorological Institute
Helsinki, Finland

12.1 Background

The uniting idea of SILJA research project is to create fully modular, object-based dispersion model framework system, which is as general as possible and can be used to create different kinds of dispersion models. Secondly, the goal of this research is to create new physical parametrizations and computational methods of different dispersion phenomena. These are tested using the verification material available. From the computer science point of view the project is very challenging, and the emphasis on soft-ware design is quite strong.

At present (January 1997) SILJA random-walk particle model is in operational use in case of for example an accidental nuclear release. Because of the lack of easy-to-use graphical interface and visualization the system cannot yet be used by the duty forecasters.

Later this year SILJA will be implemented as part of the new meteorological workstation software, which brings SILJA in general use, and makes it possible to visualize dispersion model results together with weather data on same map background.

In the future the SILJA-model framework will hopefully be used to numerous purposes, some of which unknown at the moment. The basic idea, a multi-purpose model frame-work easily adapted to new tasks, allows this. A lot of potential users will be found in the air-quality department of FMI. The idea is, that any scientists can take the existing framework, and create his/hers own model by adding a necessary module to the system. An example of this is a module to handle the air-chemistry of a new chemical compound/compounds yet unknown to the system. Scientists joining this common framework would have a benefit, since they could concentrate on their own specialized field, and test for example chemical properties of their submodels in high-quality and fully tested dispersion model system.

In this paper I'll present our dispersion model and software design ideas and progress made so far. SILJA-system is far from finished, and many of our ideas are still untested, but so far the project has progressed very well.

12.2 Software design

12.2.1 Background and significance

Most of the existing dispersion models are short scale models, that calculate the transport of materials within tens of kilometers from the source. These models are used for example to study the effects of one power plant in its surroundings or to make air-quality studies for regulatory purposes. There is quite a lot of verification material available for this kind of models due to many local scale release experiments. Global-and mesoscale operate within scales of hundreds to thousands of kilometers, and are used to predict the movements and possible fallout areas of an accidental nuclear release, or to examine on a continental scale the spreading of pollutants caused by energy production, industry of traffic. Global- and mesoscale models lack good quality verification material, and therefore an European long-range tracer experiment was organized.

The importance and number of applications of dispersion models are growing steadily. Also the number of transported materials has increased: sulfur and nitrogen compounds, radioactive gases or particles, tropospheric ozone, migrating insects etc. In recent years a lot of effort has been put in the field of air chemistry of dispersion modeling.

Traditionally dispersion models have been more or less designed for one specified purpose (here at FMI and elsewhere, too). Often these models are later applied to other fields on dispersion modeling, and sometimes it happens easily, sometimes with substantial amoun of pain. A typical example is a model designed for dispersion calculations of radioactive material in case of a nuclear accident. As a result of several years of development the model works well in this, but just this purpose. Model ages physically, meteorologically and the computer software grows old. The new possibilities provided by the development in numerical weather forecasting cannot be easily utilized. If the model should be developed or used for a purpose other than originally designed for, it is either difficult or even impossible. This is more often due to problems with the original software design than problems with the actual physical modeling itself.

The existing models can be classified in several ways:

- by their basic physical concept (Gaussian puff and plume models, Eulerian gridded models and Lagrangian particle- and trajectory models)
- by the transported materials (sulfur, ozone, radioactive materials etc.)
- by the horizontal scale (local, meso- and global scale)
- by the nature of the use of the model (fast, simple models for accidental use by the authorities versus large models capable of handling long time-series and often used only by the model developers themselves)
- by the computer platform used

Since for every new application a new model has been developed, has the number of dispersion models become very high. Most of the work in creating all these different kinds of models is very similar: fetching and handling large amounts of meteorological data, handling the input and output of models and storing and visualizing the model results. A big effort is used to preprocess the meteorological data and to calculate additional parameters from it (fluxes of turbulent energy etc.).

Further development of an old dispersion model program (or any other computerized model calculating physical phenomena) often becomes necessary as it is initiated by better physical knowledge of the phenomena, availability of better numerical algorithms or increased computation capability. However, introducing changes to an old program is most often extremely time-consuming and easily leads to erroneous behavior of the program. This is especially true if the program contains old-style coding that has no support for easy maintenance and reusability. Typically, there are multiple and strong dependencies between parts of the program, and to make possible a minor change, one has to introduce several other changes in the code.

According to the majority of today's software engineers, the key to better code maintainability is object-oriented programming (OOP). In OOP, the most central ideas are encapsulation of data and inheritance of properties. Encapsulation means that a certain data type (i.e. a certain object class) may only be accessed by an accompanying set of subroutines (methods) especially tailored for the type, which guarantees data integrity better than direct use of the data fields in the type by reducing the possibility of inadvertently changing their contents. Using inheritance, an object class may be used as a starting point when writing a new one, adding only those properties that are not readily contained in the base class. These principles make it easier to produce maintainable and reusable code, although the initial amount of work required may be higher than without OOP.

At present, the most widely used object-oriented language is C++. For this study, FORTRAN-90 was chosen, mainly because FORTRAN has been and in the near future continues to be the most popular language for scientific and technical computing. FORTRAN-90 makes it possible to implement the central principles of object-oriented programming.

The possibilities of developing dispersion models have improved substantially in the last few years. The new software design methods and new computer languages, the possibilities provided by computer networks, the increased power of massively parallel supercomputers and the rapid development in numerical weather models enable the development of a new kind of dispersion models. It is possible to create unified, multipurpose models instead of models designed for one specified task.

12.2.2 Background work: the object-based dispersion framework

The background work for this research is the design and realization of a fully modular, multi-purpose dispersion framework. This is done using object-oriented programming (OOP). This model framework is not a single model for all purposes (which would be unrealistic) but instead class-library or "toolkit" containing tools for creating dispersion models. Using this library it is possible to rather easily create models with totally different physics, parametrizations or scale. The target is a system, in which several scientists can reliably use the work already done by other people, and concentrate on their own field. Later, when the system is being used, it is easy to update and further develop, since the existing tools can be modified in a very reliable way or replaced altogether. By using OOP, we can be absolutely sure, that the new or modified tools fit the existing framework. This kind of program also easily adapts to the changes in the computer environment.

All the data types used in models (grid geometry, fields of numerical weather data, physical quantities, chemical compounds etc.) and the processes for creating and handling them are placed in their own, closed modules. Single modules can be developed and tested alone, outside the actual dispersion model system, and then inserted when ready. By using existing modules, higher-level modules can be created by inheriting their properties. The dispersion models are on the highest hierarchy level of this class l models become rather short and simple-looking. Object-oriented programming increases the amount of work in the first phase, but makes the program far more flexible and increases its life span. It also makes it possible to apply the model to new areas, which are not yet known.

Object-oriented programming is today the standard method of designing large, complex computer programs. It is now perhaps the first time applied to atmospheric dispersion modeling. There is already a ground work for this (see chapter "The present state of project" later in this paper). It must be stressed that object-oriented programming not scientific research, although the approach in this project is new. The object-based dispersion model framework is however a vital precondition of reaching the research goals of this project. It enables us to combine the work and results of the subgroups of this project.

12.2.3 Parallel computation concepts

The rising trend in hardware is parallel computation. Parallelization can be done on many different levels, ranging from chip-level parallelism (e.g. vector processors) through intra-computer parallelism (multiple processors) to inter-computer parallelism (a cluster, or totally distributed computers in network). Ever more experts think that the speed of a single microprocessor is approaching the physical limits. Then it will eventually become much cheaper to use a large number of existing processors working on a single task than to develop a faster one. There are difficulties in achieving an even distribution of load and in interprocessor communication, but methods for these are evolving rapidly.

Multiprocessor architectures can be categorized by memory access. The main categories (in some cases overlapping) are shared memory (at the Finnish Centre for Scientific Computing, or CSC, there are Cray C94 and SGI's Power Challenge "cypress") and distributed memory (IBM SP2 "cactus" and the future Cray T3E at the CSC). Another distinction can be made between SIMD (Single Instruction, Multiple Data, e.g. vector processor) and MIMD hardware (Multiple Instruction, Multiple Data). MIMD systems can be further divided into symmetric multiprocessors (SMPs) and massively parallel processors (MPPs).

Good performance in a parallel machine cannot be expected when using traditional programming languages as such. To widely accepted means for achieving parallelism are data-parallel languages and message passing. In a data-parallel language, the compiler distributes array operations among processors automatically, and other operations according to given directives. For example, High Performance FORTRAN, based upon FORTRAN-90, is a data-parallel language. However, it is not efficient and general enough to be the only means of parallelization. Message passing requires MIMD hardware. It can be used with both distributed and shared memory. At present, the most promising tool for making a program parallel appears to be a machine-independent library called Message Passing Interface (MPI). However, it is by no means an automatic tool, but leaves much in the programmer's responsibility.

This year, Finland's national supercomputation capability is spreading from fast vector processors (Cray C94), as the new Cray T3E will be installed at the CSC. The T3E will have 192 of DEC's Alpha EV5 processors, each with 64 MB memory of its own.

The theoretical maximum speed of the whole system will be 115.2 Gflops. The dispersion model framework system used in this study has been developed on Cray C94, and the development will continue on Cray T3E.

The main objective in the field of computer science in SILJA-project is to perform research on the applicability of different parallel computation paradigms to a large mathematical model of physical phenomena. Possible communication bottlenecks must be located and the best axes (those of minimal communication), along which to divide calculations, must be found. Communication is usually very time consuming when compared to computation. Existing procedures will be tested and the best combinations of them will be developed further. Parallelization applies to every part of the dispersion model framework system. Examples include the movements of a large number of particles, advection and dispersion in a large 3D grid, sink and source processes distributable into independent parts (e.g. decay chains), and various high-order integrals.

Secondary objectives are also related to parallel computation. Parallel operations must be scaleable so that any number of available processors can be utilized. The decisions on the number of processors should be made at run time. Furthermore, processors should never have to wait for the slowest one to get ready. If a parallel machine is to be used efficiently, each processor must be kept busy working until reduction (return from parallel section), which might not always be straightforward. For example, when calculating values of a function f(x) with a given accuracy using a series expansion, the number of terms needed may vary with x. One cure is to use much more subtasks than there are processors, so that each processor can do a suitable number of subtasks.

Any attempts to parallelize the dispersion model framework system have not yet been done. However, requirements of a future parallelization have been taken into account when writing code. Work on this subject can start after the new massively parallel multiprocessor Cray T3E is installed at the CSC in 1996.

12.3 Meteorological research

So far the meteorological processes and parametrizations used have been rather simple, since we have strongly concentrated on software design and basic tools. Also we have wanted to have an operational system for nuclear preparedness use as quick as possible. Later we'll concentrate more on actual meteorological research and here's some of our plans and ideas in that field.

12.3.1 Mixing phenomena of transported pollutants

The first meteorological goal in this SILJA-research deals with the mixing processes of the lower atmosphere, which generally have a substantial effect on the dispersion of pollutants. The atmosphere is usually vertically layered. Pollutants that are mixed to different heights also get into slightly different atmospheric flows, and are therefore finally transported to different areas. At the same time mixing processes dilute the pollutants affecting their concentrations in breathing air and the deposition on ground.

In this project it is our goal to develop and test new computational methods for mixing of pollutants used in dispersion models, and to realize the necessary computational tools as a set of modules of the dispersion model framework (described elsewhere in this paper). The computational cost of different parametrizations is also studied.

Most of the mixing processes occur in the so called atmospheric boundary layer (ABL). This layer can be defined as the part of the troposphere that is directly influenced by the presence of the earth's surface, and responds to surface forcings with a timescale of about an hour or less. In ABL turbulent eddies are caused either by mechanical friction of ground on wind or by thermal instability.

There are many field and laboratory studies and theoretical papers on the different mixing processes. In principle the phenomena are well known. However, the parametrization methods used in most of the usable "real-world" dispersion models are very rough. The reason for this is often the large computational cost of the more realistic parametrizations when compared to the actual benefit gained.

Turbulent mixing in the atmospheric boundary layer is parametrized using the fluxes of mechanical and thermal energy, which are available as internal quantities of the HIRLAM weather model. In HIRLAM the vertical diffusion (caused by turbulence) is a parametrization of the vertical fluxes of momentum, sensible heat and moisture. The actual formulation for dispersion model use is unclear at the moment, especially for random-walk type particle models.

A parametrization of convective mixing of pollutants is also to be developed, and the effect of introducing convective mixing on the dispersion model results is studied. Convective mixing of radioactive materials was found to be the explanation of some properties of dispersion during the Chernobyl accident in 1986, for example the large nuclear fuel particles found in the Northern Poland.

The parametrization of convective mixing in dispersion models will be parametrized using the internal quantities available from HIRLAM. At the moment in the HIRLAM model the parametrization of penetrative convection (a convection that travels through the top of the boundary layer) is based on the scheme proposed by Kuo (1965, 1974). In this scheme any conditionally unstable layer is a potential convective cloud layer, but convection only takes place, if there is net moisture convergence in the layer. The boundary layer parametrization of HIRLAM also includes shallow convection inside the boundary layer. Shallow convection is occurred for example when low cumulus clouds are formed on a summer day. The roles of shallow convection and thermal turbulence require studying, since they may appear to be different definitions of one phenomenon from the dispersion model point of view. It is possible that for dispersion purposes only penetrative convection must be parameterized. The parametrization of both convection and conditions of boundary layer are to be developed in the HIRLAM-model itself in near future. The boundary layer parametrization is to be replaced by the so called Holtzlag-scheme.

In dispersion models the methods for using the convective vertical movement have be developed both for Eulerian gridded models and Lagrangian particle models. In particle models the amount of convection could have an effect on the probability of single particles to enter vertical displacement, but it has to be studied. This is the subject of the doctoral thesis of the meteorological part of this research.

12.3.2 Integration of weather and dispersion models

Normally dispersion models use numerical fields of weather data stored in files or database. These fields are provided by numerical weather models and are typically available at intervals varying between one and six hours. Between these so called observation times the dispersion model produces the meteorological data by interpolation. A lot of information originally created by the weather model is lost in these interpolations. Also many quantities that are used for parametrizations inside the weather model are not written out of it, since they are of no importance in making weather forecasts. In dispersion modeling point of view the most important of these to are the quantities of turbulent energy and instability in the lower atmosphere. Therefore the vertical mixing is usually calculated using approximative methods (Monin-Obukhov length etc.). Many of these methods have originally been designed to be used with weather observation data.

In this project it is studied, how the maximal usage of meteorological data affects the dispersion model results. To study this the dispersion model environment is integrated directly to a numerical weather model. This provides theoretically the best time resolution of data, plus the possibility to use all the internal quantities of the weather model. The effects of small weather systems, convective mixing and also the coastal effects, which are important to Finland, should be seen. It is interesting to study the difference of results when compared to a traditional approach of using existing fields stored during weather model run. In many weather situations this difference will probably be negligible, but in some case the new method will show some new details in dispersion. The new model environment enables us to make all kinds of experiments, which should reveal the amount of benefit of this new approach.

A weather-model-integrated dispersion model is very heavy to run, since every dispersion calculation requires a full numerical weather forecast run. This kind of model has therefore two applications: 1) it is a tool for meteorological research and 2) a model for situations, where maximum accuracy is needed, and the computational cost is not the issue. An example of the latter would be a nuclear accident with radioactive release.

Essentially the maximum accuracy of a dispersion forecast depends on the numerical weather model used. In this case it would be HIRLAM (high resolution limited area model). It is a very high quality weather prediction model created through several years of international cooperation. It has been operational at FMI since 1990 and has been continuously developed.

12.4 Schedule of meteorological research

The development of the dispersion model system is divided into levels described in the following. An estimation of the amount of work needed for each level is mentioned. Each level introduces some new methods or parametrizations of physical processes, and at the same time a new version of the computer code.

Level 0. (done in 1995-1996)

This is the basic level of the system, and its main purpose is to study the ways of applying object-oriented coding to dispersion modeling. At the moment this level already exists, since there has been a ground-work (see chapter "Present state of project"). The only working "model" on this level is a simple trajectory model. This level contains the following parts:

- the basic modules and internal data structures of the model framework
- the standardization of the interfaces of modules
- high-level tools for fetching meteorological data from the HIRLAM-archive
- basic input and output
- the definition of common source term, that can be easily during the model transferred into the source terms required by different kinds of dispersion models
- Lagrange-type advection of particles

Level 1. (done in 1996)

This level introduces a non-depositing random walk particle model to the framework. In this kind of model the cloud of pollutants is described as a large number (10.000 - 100.000) independent particles. This model is suitable for example to operational dispersion calculations in case of radioactive release. The new parts are:

- modules for parametrization of turbulent diffusion of particles using flux-quantities from the HIRLAM weather model
- radioactive decay of materials carried by the particles
- storing of model results to the FMI operational NEONS database (based on Oracle) and visualization of model results using the tools of the meteorological C++ -class library created at FMI. The actual software is still open at the moment.

Level 2. (years 1996 - 1997)

This level introduces the convective mixing of particles. The use of the so called K-index and convergence of moisture to characterize probability of convection of particles is studied. The new schemes of cloud formation and rain in the HIRLAM-model are studied. The convective mixing is realized as an encapsulated model of the model framework, and a lot of tests is carried out to study the effect of introduction of convective mixing on dispersion model results. The Chernobyl accident is used as one case study, if possible.

Level 3. (years 1997 - 1998)

This level introduces a weather-model-integrated model framework. Once this work is done, all the dispersion models created later can also be run in this integrated, maximum accuracy mode.

- integration of the dispersion model to the weather model
- study of the usage of internal quantities of HIRLAM
- comparisons and testing

Level 4.

This level introduces the general principles of sink-and source-mechanisms of the model framework. Since these processes operate on the material-type of framework, and not actual particles, all the sink- and source-modules can be used both to particle models and gridded models. The new parts of the framework are:

- dry deposition of different gases and particles on ground and sea
- the interactions of pollutants with atmospheric water and ice
- parametrization of in-cloud scavenging (rain-out) and sub-cloud washing (wash-out)
- possibly the implementation of an existing air-chemistry model as one, closed module of the model framework, and its interface to the rest of system

Level 5.

This level introduces an Eulerian, gridded dispersion model. In this work we benefit from experiences of colleges in other European countries.

- study of the best possible advection scheme for a dispersion model to avoid numerical diffusion as much as possible
- realization of Eulerian advection and diffusion in a way not yet determined

Level 6.

This level introduces the model framework better to modern computer network environment. The model system is developed into a system, which can receive messages and requests and send results to any authorized client in the Internet. The model would then always be running to be available. The model results will be sent as a set or an animation of pictures on a map background to the www-pages of FMI, from where they would be available to all the interested parts. Also a system is developed to make automatically model calculations for a set of interesting cases, for example the nuclear power plants. The reliability of safety-problems have to be taken into account.

Level 7. (years 1999 - 2000)

This levels introduces new sources of meteorological data to the framework. Also global wind-data in a lower resolution is introduced for simple dispersion calculations for a release point anywhere in the world.

- satellite data and possibly in the future also satellite soundings
- wind- and rain data from Doppler radars
- model data from some other European weather prediction models
- automatic fetching of wind-data from ECMWF (European Centre for medium range weather forecasts) global model. The data is fetched from England over Internet from the MARS-database of ECMWF.

Levels 8....n.

These levels are not yet clear and go beyond this research project. The new levels consist basically of introductions of chemical submodels, each placed in one encapsulated module. These modules enable the model system used by the scientists to make dispersion calculations of different pollutants.

Our e-mail addresses (Mika Salonoja, Mikko Ilvonen and Ilkka Valkama) are listed in Appendix 1 (List of Meeting Participants).

SILJA's www-pages are at:
http://www.fmi.fi/TUT/MET/silja/ (unfortunately only in Finnish at the moment)
http://www.vtt.fi/ene/eneydi/NW/research/oeptp.html (in English)

13 Dose assessment in the new Finnish SILJA system

Mikko Ilvonen
VTT Energy/Nuclear Energy
Espoo, Finland

13.1 Background

-all ETEX results in Finland were calculated with TRADOS

-the main problems in TRADOS were

- time step in other calculations than transport was fixed to 3 hours
- only a few trajectories could be utilized in the calculation of concentrations
- spread in the direction of transport was obviously too small
- calculation of dispersion and doses were strongly intermingled in the code
- a finite number of vertical concentration profiles, from which the best suitable was chosen

-especially the last point directly affects the magnitude of doses, because doses depend on deposition or concentration in air near ground surface

-because of program structure, there was NO easy way to overcome these limitations in TRADOS

-in the SILJA system, the above-mentioned problems do not exist any more

13.2 The main features of SILJA dose assessment:

- relatively detailed modeling (500 nuclides, 80 dose pathways, freely adjustable accuracy of dose integrals)
- external doses from cloud and fallout, internal via inhalation and ingestion
- includes all nuclides and all human target organs (23) present in
    - D.C. Kocher's tables of the dose rate conversion factors for external exposure to photons and electrons
    - NRPB tables of dose conversion factors for intakes of radionuclides
- a totally new method for calculation of cloud gamma dose: fast and accurate, for arbitrary vertical profiles (full 3D integration is optional)
- at present, the model runs on Cray (same as HIRLAM and SILJA dispersion assessment)
- the model is implemented by object-oriented programming (FORTRAN-90) conforming to strict rules on source code style; this leads to easy maintenance and further development, as the structure of the program should not force to any limitations

13.3 Radioactive chain decay in SILJA

- at present, chains are modeled by the same three-nuclide scheme as in TRADOS:

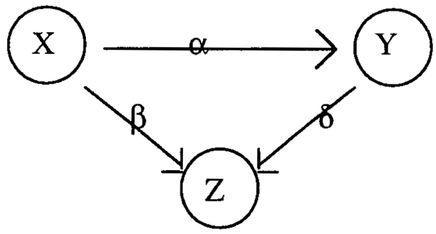

- with x, y and z equal to the amounts of nuclides X, Y and Z in Becquerel, they can be solved from the following equations:

$$\frac{dx}{dt} = -\lambda_x x$$

$$\frac{dy}{dt} = -\lambda_y y + \alpha\lambda_y x$$

$$\frac{dz}{dt} = -\lambda_z z + \beta\lambda_z x + \delta\lambda_z y$$

- SILJA uses analytical solution

more complex chains are to be solved by the matrix exponential method

13.4 A special method for solving deposition and near-surface concentration for dose assessment purposes

- when using a particle-type dispersion model, a huge number of particles is needed to make the near-surface concentration estimates (by counting numbers of particles in grid cells) as reliable as is needed for dose assessment

- for this reason, a method based on numerical solution of vertical concentration profiles is being tested (a rather similar method was already used in TRADOS)

-starting from the 'atmospheric diffusion equation'

$$\frac{\partial c_k}{\partial t} + v_k \cdot \nabla c_k = \nabla \cdot K_c \nabla c_k + \underbrace{D\nabla^2 c_k}_{1} + \underbrace{R(c_{1k},\ldots,c_{nk},T)}_{2} + \underbrace{S(x,y,z,t)}_{3}$$

and simplifying with

D = 0 (no molecular diffusion)
R = 0 (no reactions)
S = 0 (no source)
1D case (z direction only)
v = 0 (no wind, because moving along with the particle)
one gets

$$\frac{\partial c}{\partial t}=\frac{\partial}{\partial z}(K_z\frac{\partial c}{\partial z})$$

- the vertical profile simply develops as a function of time
- at each time step, the previous vertical profile is the initial condition
- fluxes to ground surface (dry deposition) and out from the boundary layer are the boundary conditions (flux = concentration * dry deposition velocity)
- one has to calculate the K_z from meteorological data at each time step
- dry deposition means that the concentrations of affected nuclides approach zero when approaching ground surface
- realistic modeling of deposition processes is extremely important for dose assessment purposes

- **How to get the next vertical profile from the previous one ?**

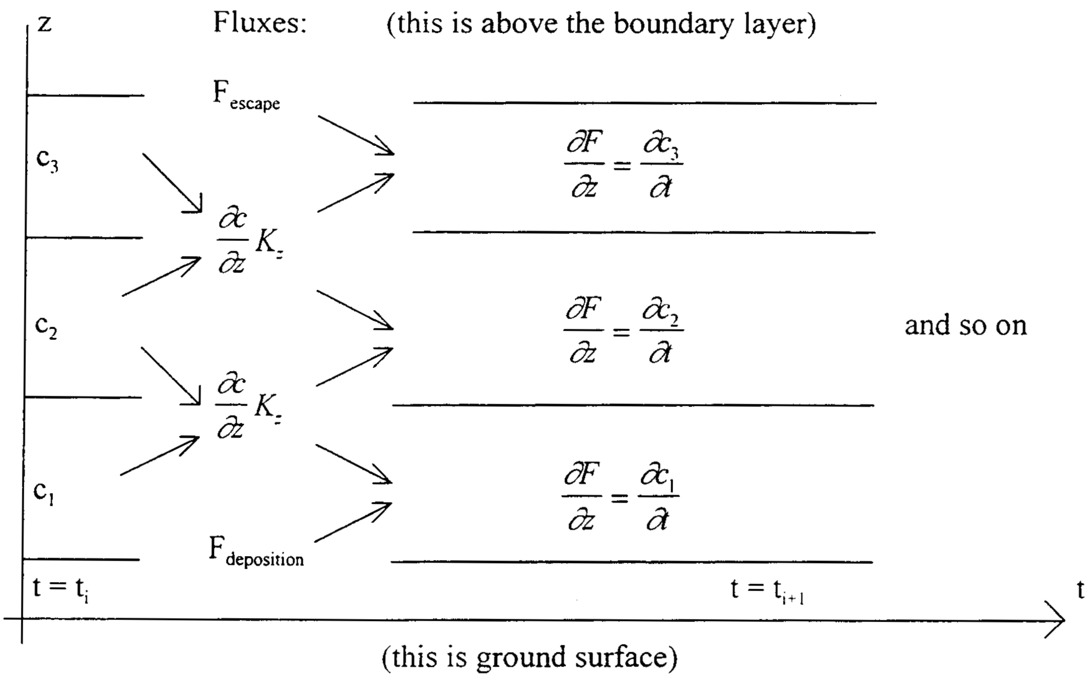

In the picture, the boundary layer is divided into only three layers for clarity. The quantities in the layers are:

-concentration
-gradient of flux
-time derivative of concentration

The quantities at layer boundaries are:

-gradient of concentration
-turbulent diffusion coefficient
-flux

- the above method is explicit (each new value based on old values only)
- what's bad: use of this method means that a vertical column of air (represented by the vertical profile) remains attached to a single particle trajectory
- what's good: one gets reasonable (?) values of deposition and concentration near ground surface even for deposible nuclides
- for wet deposition, one may add for each layer $\Lambda \cdot c \cdot h$ downwards to the flux, were Λ = washout coefficient, c = concentration and h = layer height
- **this method is not yet operational in SILJA environment !**

13.5 New method for calculation of external cloud gamma dose - fast and accurate

- the dispersion and dose calculation model starts by creating a file that contains dose rates for each combination of nuclide used and atmospheric layer
- the layers are optimal when they are the same as the ones used for the vertical concentration profile
- the method is applicable sufficiently far away from the source, where concentration does not change significantly in the horizontal plane in practical photon range

-doses are calculated starting from the energy flux density or energy fluence rate, Ψ, the amount of energy per unit time [J/m^{2}s] that has entered an infinitesimally small sphere-shaped volume around a point divided by the area of a circle with the same radius as the sphere

$$\Psi(t)= \int_{x=-\infty}^{\infty} \int_{y=-\infty}^{\infty} \int_{z=h_1}^{h_2} c(x, y, z, t)\, E_\gamma \frac{1}{(4\pi r^2)} B\, e^{-\mu r}\, dz\, dy\, dx ,$$

where

Ψ (t)	= energy flux density [W/m^2],
c(x, y, z, t)	= activity concentration of nuclide [Bq/m^3],
E_γ	= gamma energy [J],
B	= build-up factor [ ],
$\mu=\mu(E_\gamma)$	= linear attenuation coefficient [1/m],
h_1	= height of lower bound of the layer,
h_2	= height of upper bound of the layer,
r^2	= $x^2 + y^2 + z^2$ [m^2]

$$B(\mu r)=\begin{cases} 1+\mu r+(\mu r)^2\, 1/(7E^{2.4}) & 0.5\ \text{MeV} < E < 2\ \text{MeV} \\ 1+1.1\mu r+(\mu r)^2 & E < 0.5\ \text{MeV} \end{cases}$$

-then the dose rate caused by photon γ is

$$\dot{D}(t) = \eta * \sigma_{en} * G * \Psi(t)$$

where

η = an approximate coefficient without a unit (0.5 ... 1.0), which results from, among other things, the semi-infinite cloud approximation

σ_{en} = mass energy absorption coefficient in the organ observed [m^2/kg]

G = ratio of the dose rate in the target organ to the dose rate at body surface

- all photons from the NEA Joint Evaluated data Files (JEF) are used for each nuclide
- no need to divide photons into energy classes, because the dose rate file is calculated before dispersion and dose calculation model
- no assumptions on the vertical concentration profile - practically any profile can be treated accurately
- by rotational symmetry, one layer can be calculated with 1D integration (see figure):

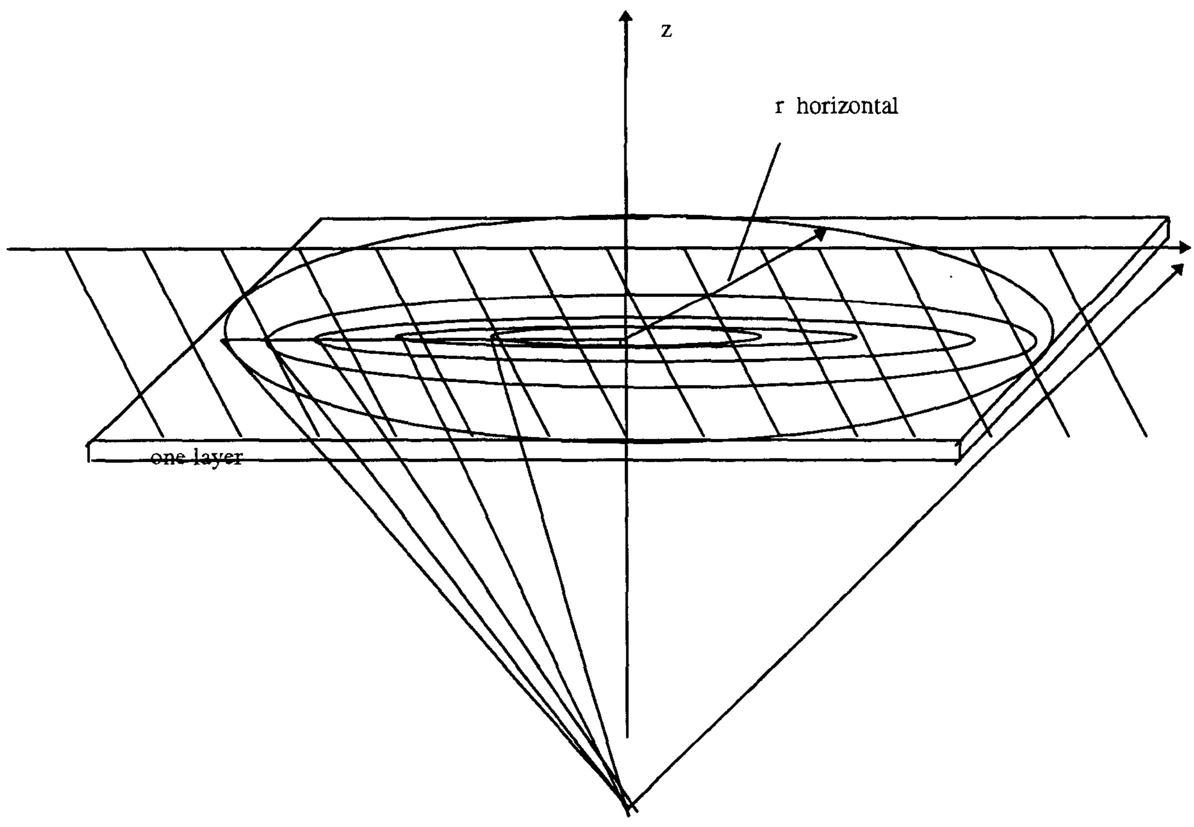

Figure 13.1 The geometry of the cloud gamma dose problem

13.6 To be done in near future:

13.6.1 Modeling aspects

- arbitrary decay chains instead of the present at-most-three-nuclide ones; solution by the matrix exponential method
- solving of deposition processes and radioactive chain decay in a coupled manner, because nuclides have different dry deposition velocities and wash-out coefficients; at present these processes are separated
- Completion and updating of dose exposure pathway calculation methodology and database - especially concerning food chain pathways
- Practical verification and validation of the SILJA dose assessment methods against older methods

13.6.2 Usability aspects

- built-in intelligence in parameter choice:
    - find the optimal set of parameter values (e.g. grid sizes, time steps, alternative methods) to get as much accuracy as possible in a limited execution time
    - when necessary, the program should run almost arbitrarily fast (e.g. during the first few minutes of an emergency)
- speed without loss of accuracy through parallelization using MPI (Message Passing Interface); the massively parallel Cray T3E with 64 processors has been installed in Finland
- dose assessment should run both as
    - an integral part of the system, receiving dispersion results through subroutine calls (to be done)
    - a separate program, using pre-calculated dispersion data files, allowing fast experimentation with source term (present situation)
- user interfaces for different purposes (at the moment, visualization is done by using TRADOS user interface as a tool)
- development of options to analyze independently (i.e. in a non-dispersion integrated fashion) the effects of the following input data on the calculated radiation doses in the environment:
    - temporal and height distribution of release
    - source magnitude and composition
    - countermeasures

Some further information may be found at http://www.vtt.fi/ene/eneydi/NW/research/

14 Nordic dose assessment exercise, NKS/EKO-4.1e. Presentation of the results from trajectory calculations

Åsa Wiklund
Swedish Radiation Protection Institute - SSI
Stockholm, Sweden

A Nordic dose assessment exercise was carried out in the Spring of 1996. The exercise was performed as a sort of "home-work", so each country decided its own exercise data within a range of three weeks in March 1996. The purpose of the exercise was to exercise and evaluate the dose assessment tools available at present in the Nordic countries.

Calculations were performed for a postulated release in Värmland, Sweden; a position from which the pollutant could potentially reach all the countries (except Iceland). The duration of the release was 10 hours. One had chosen "kind" weather conditions, actually the weather on the 8 May 1995. It was, accordingly, not a real-time exercise. The source term, place of release and weather conditions were defined by the Project group. Calculations were performed up to 36 hours after end of release. Norway did not take part in the calculations, because it was the intention to use MEMBRAIN, and that system is still not operational. Finland used TRADOS to calculate trajectories, but no concentrations. MATCH was used in the Swedish calculations, and the Danish results were calculated with DERMA.

The project group consisted of the following members:
Steen Cordt Hoe, Emergency Management Agency, Denmark
Juhani Lahtinen, STUK, Finland
Eldrii Naadland, Norwegian Radiation Protection Authority, Norway
Sigurdur Emil Pàlson, Geislavarnir Rikisins, Iceland
Åsa Wiklund Swedish Radiation Protection Institute, Sweden

After the exercise, on the 20 - 21 May 1996, there was a follow-up seminar in Stockholm. The report from the exercise is under preparation when this is written, and expected publication is in March 1997. In addition to the results of the calculations, the report will contain the conclusions from the Stockholm seminar and descriptions of the different dose assessment models used in the exercise.

Some of the results are presented in *Figures 14.1 to 14.8*. The visual appearance of the results from the different institutions is still not at all well harmonized. The results from the different institutions, although reasonably well in agreement, appear very different to the eye and are difficult to compare, particularly in a situation of high tension, as can be expected post-accident. This is a problem on which it was focused repeatedly in the previous NKS-project BER-1 (Tveten, U., ed., 1995), evidently without much practical impact. These problems should once more be brought into focus, possibly in the next NKS project-period.

Reference

Tveten, U. (ed.) Dispersion prognoses and consequences in the environment. Final report from the NKS, Project BER-1. TemaNord 1995:544. Kjeller, Norway, December 1994.

Figure 14.1 DK-Hirlam results for the exercise

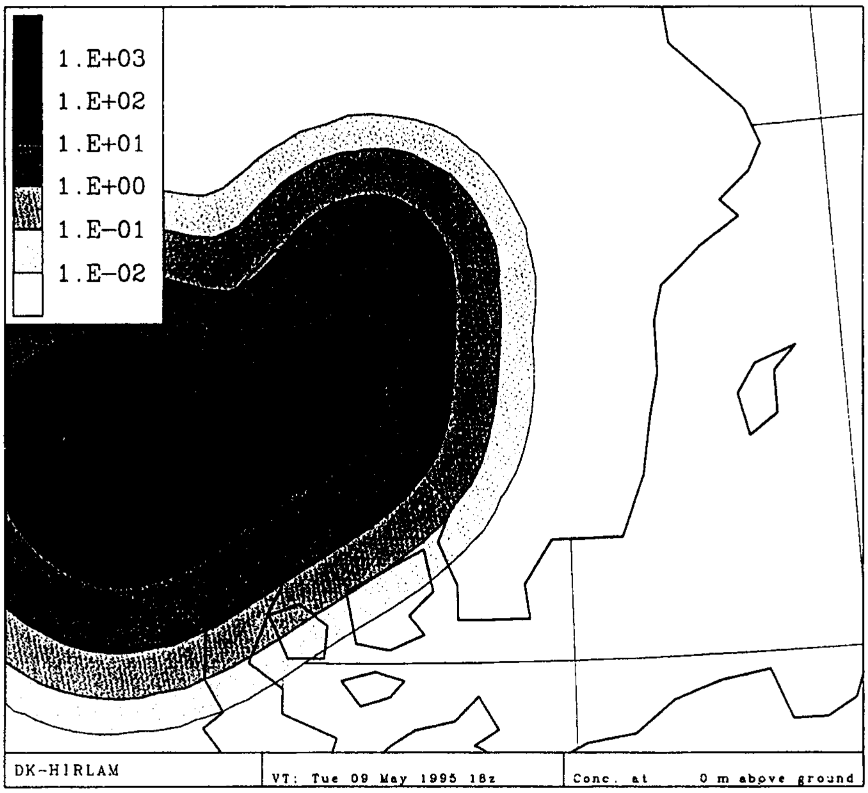

+ 12 h

Figure 14.2 DK-HIRLAM results for the exercise

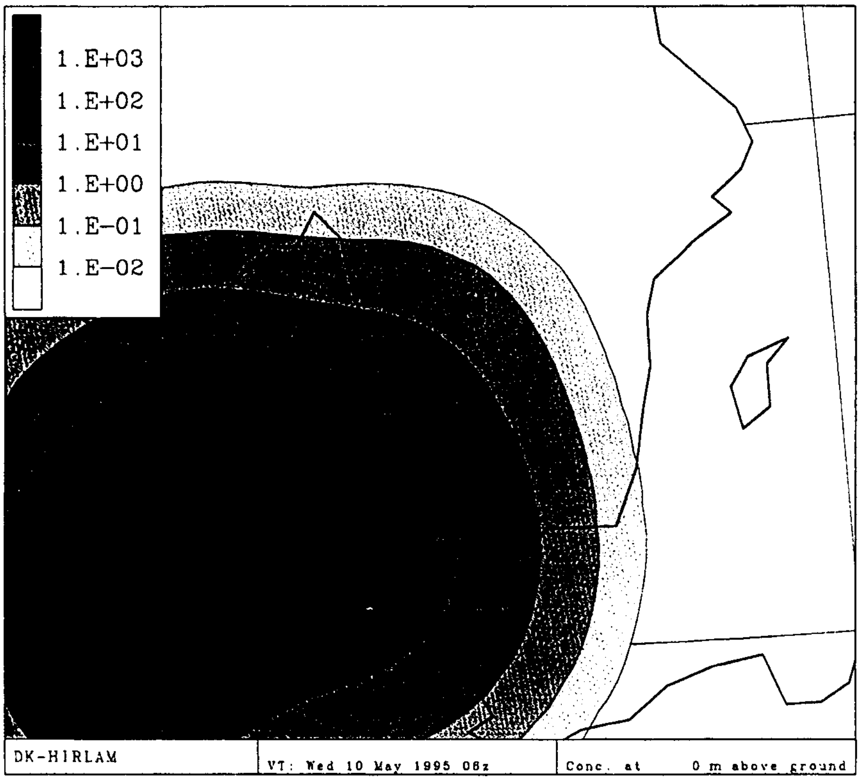

24 h

Figure 14.3   DK-HIRLAM results for the exercise

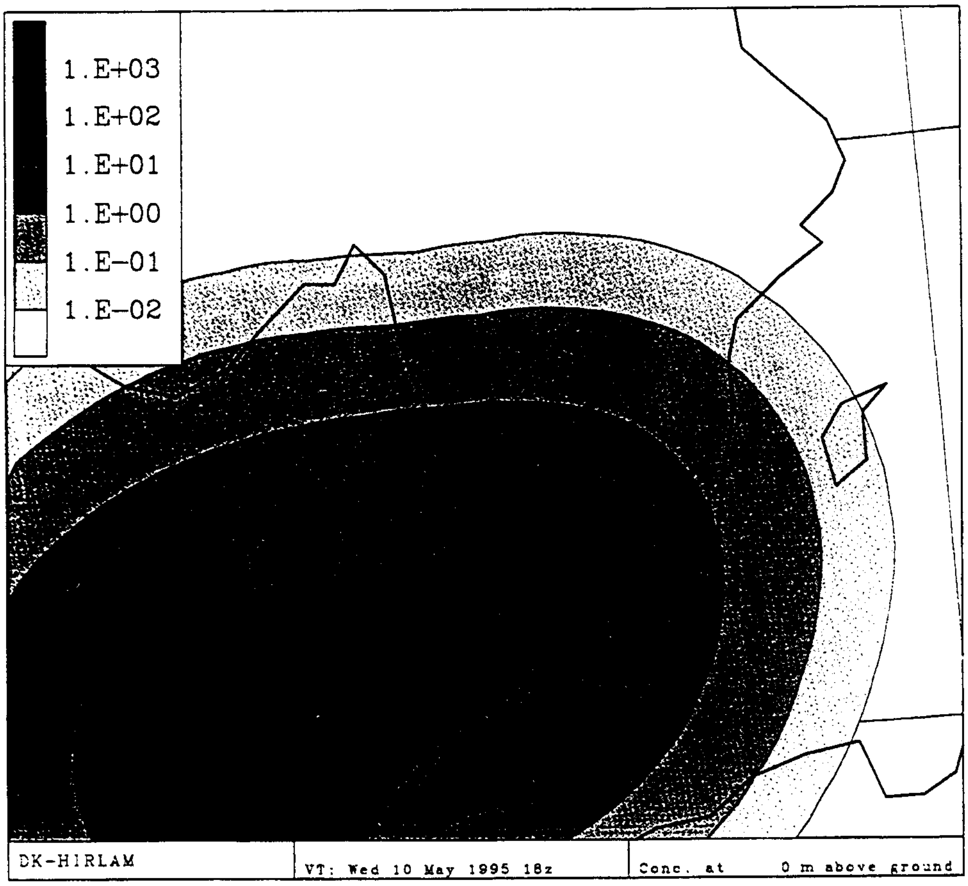

36 h

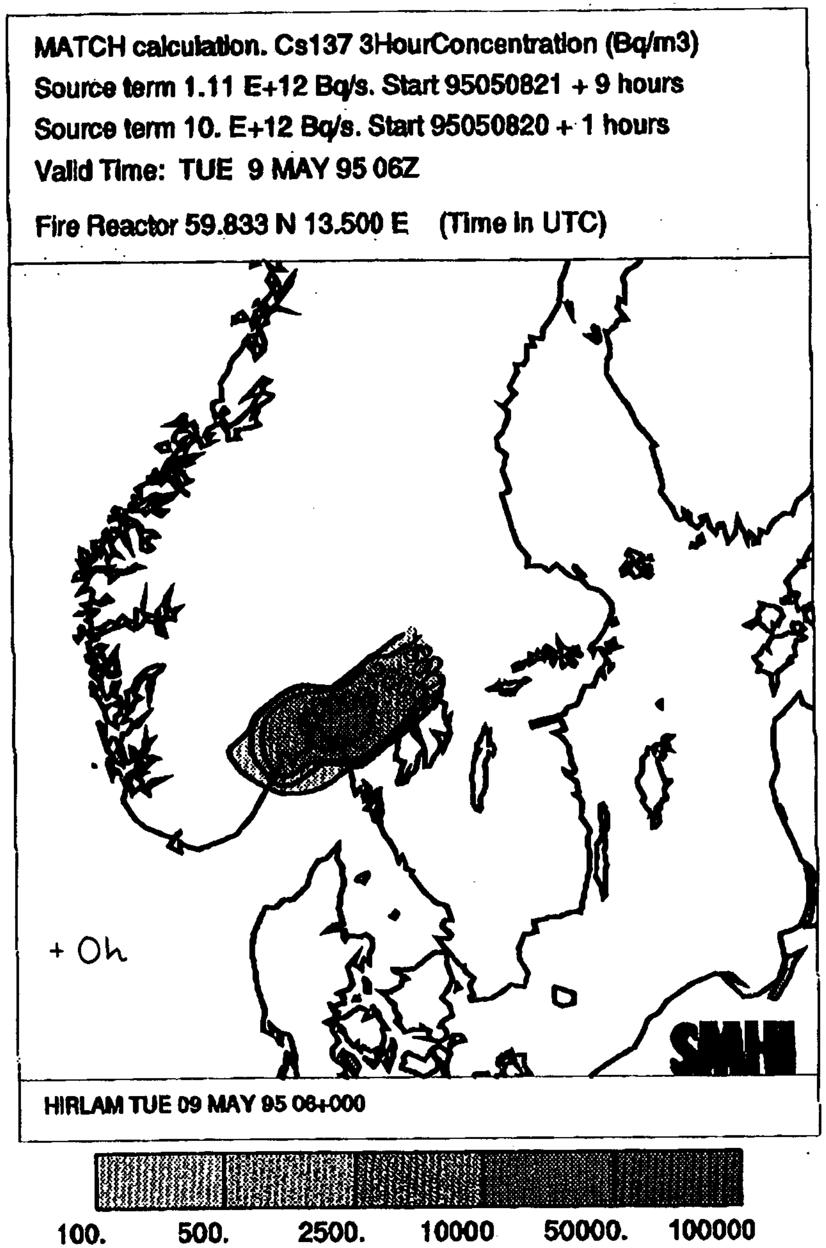

Figure 14.4 MATCH results for the exercise

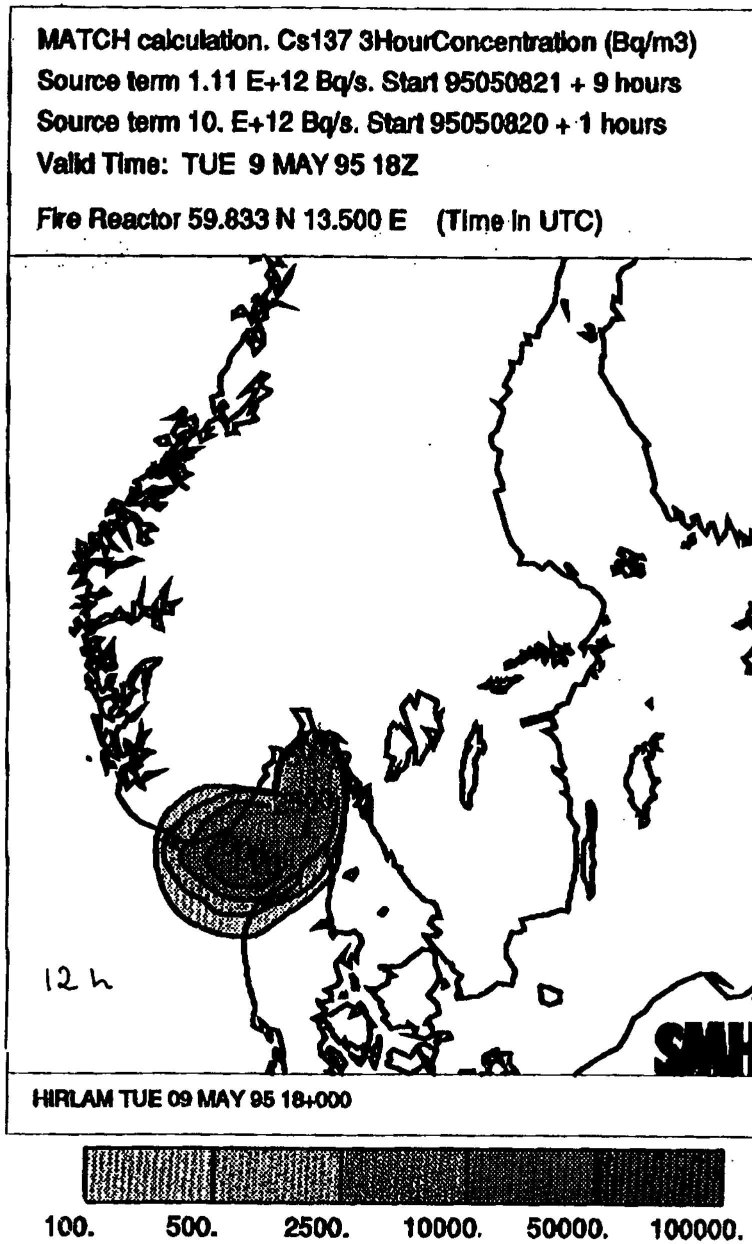

Figure 14.5 MATCH results for the exercise

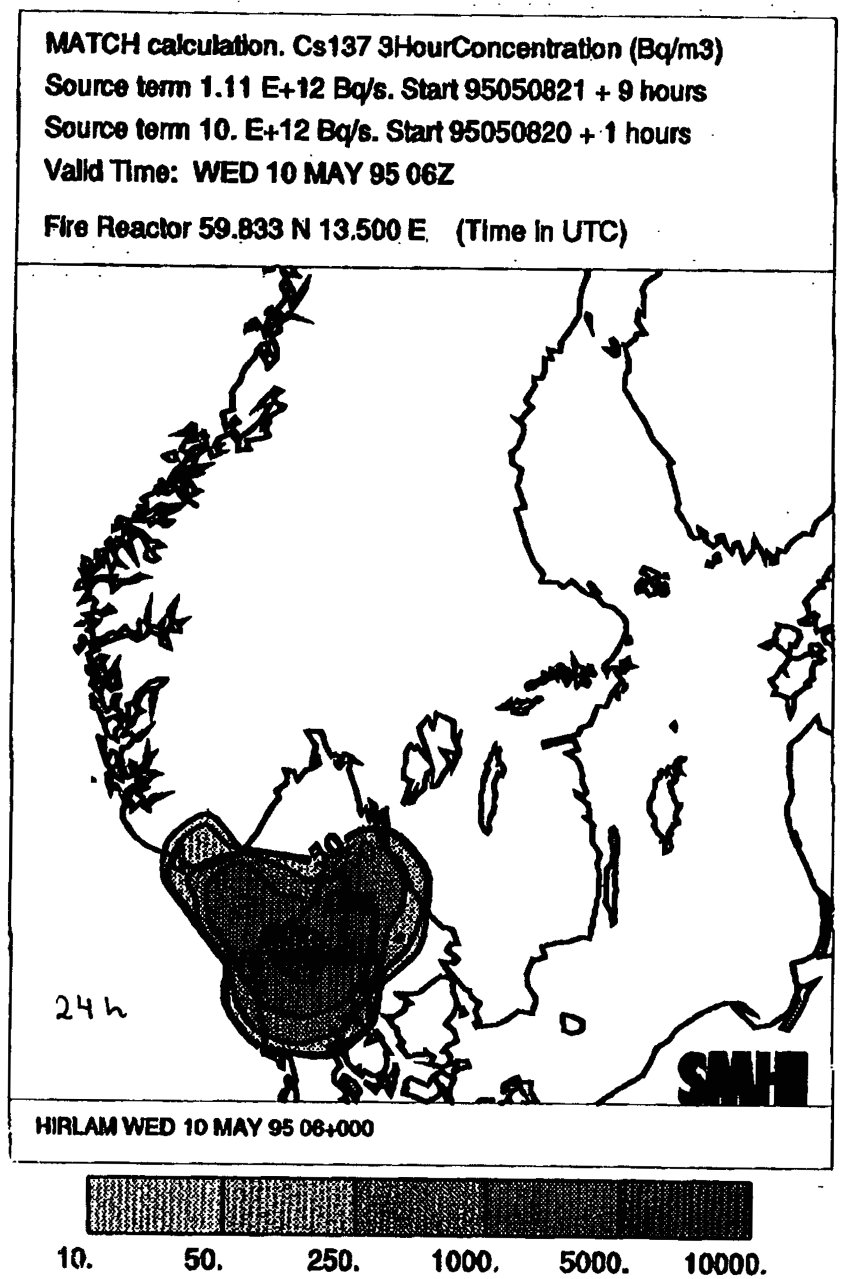

Figure 14.6 MATCH results for the exercise

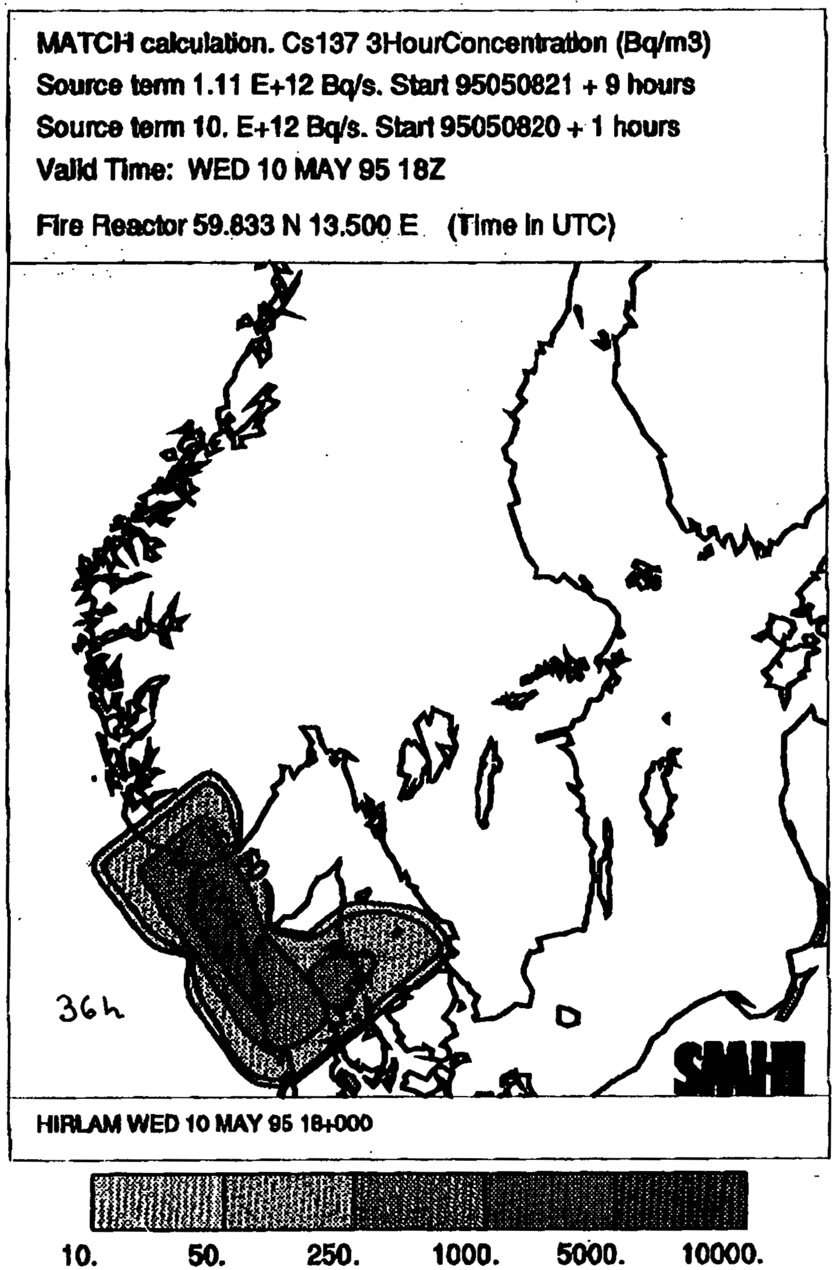

Figure 14.7 MATCH results for the exercise

Figure 14.8 TRADOS results for the exercise

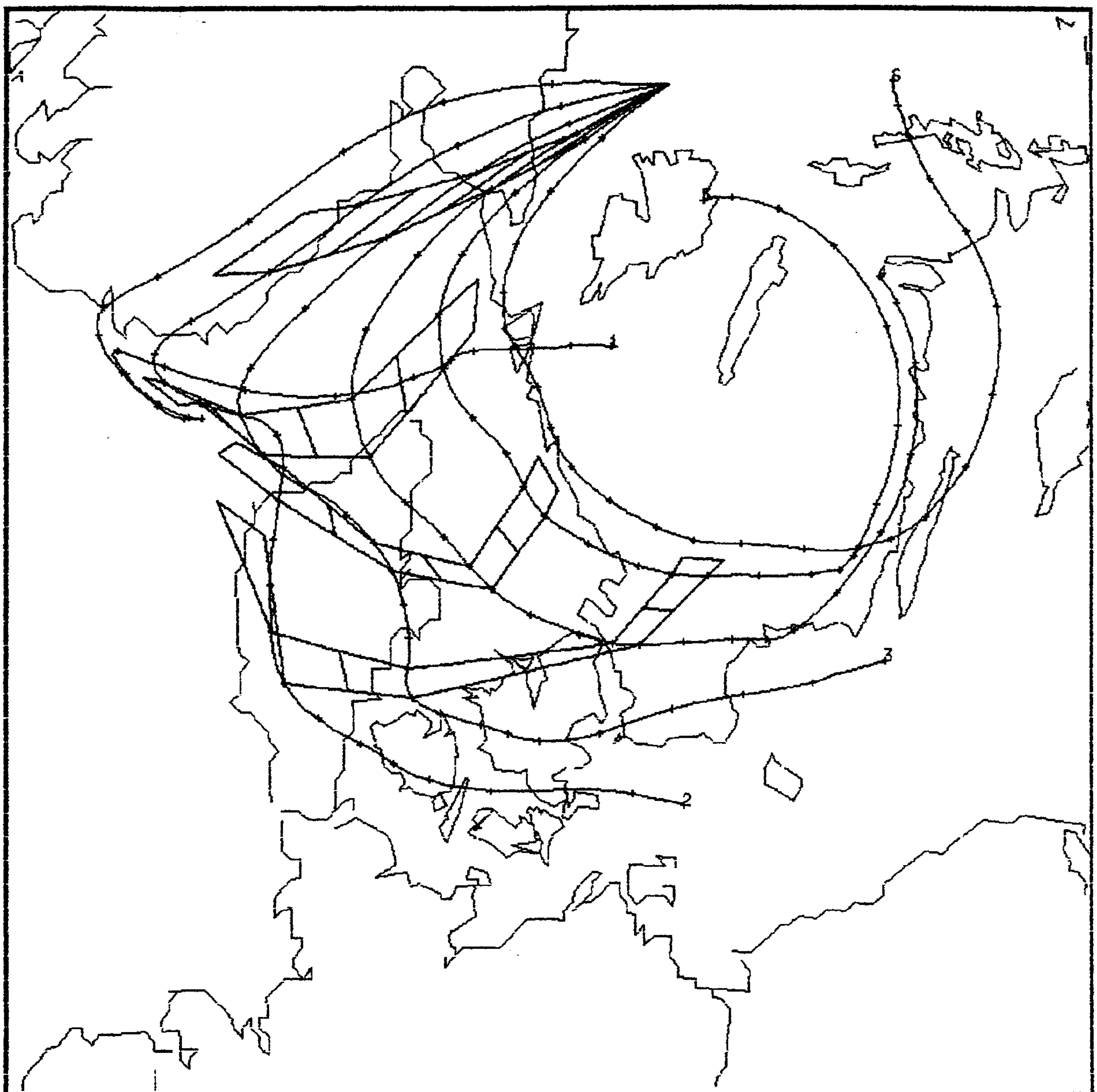

NKS / EKO-4.1e Nordic dose assessment exercise 21.03.1996
Release location: near Munkfors in Vaermland County, Sweden
Duration of release: 20.00 - 06.00 UTC
Release fractions: Kr, Xe 1.0; I 0.03; Cs, Rb 0.025; Te, Sb 0.01; Sr, Ba 4e-4; ...
Calculated by: Mika Salonoja (FMI) and Mikko Ilvonen (VTT)
Localisation of the plume 0, 12, 24, 36 h after end of release

15 Informal presentation of results from the RSMC nuclear accident response exercise of 7th November 1996

Roy Maryon
Meteorological Office
Bracknell, United Kingdom

The RSMC (Regional Specialized Meteorological Centers) are part of the WMO arrangements for nuclear accident response (in addition to national and European structures!). Regional Specialized Meteorological Centres with activity specialization in environmental emergency response were set up under protocols agreed at the Montreal Conference of September 1993. They were to be National Met Services with facilities for forecasting long range dispersion, and full operational manning. Two were to be recommended for each WMO region, those for Region VI being Toulouse and Bracknell. Authorized bodies (usually the NMS) in any country could request dispersion model products from their RSMC. In the event of a full emergency, as declared by IAEA, model products were to be sent to every country in the region, by both RSMC's.

Default emission scenarios and standardized model outputs were agreed at Montreal and subsequent meetings. The RSMC's liaise during an incident (and during exercises), comparing the model outputs and agreeing a statement to accompany the charts of forecast plume spread, etc.

Some regions are still without RSMC's, and are covered temporarily by RSMC's for other regions; more countries are becoming interested in this purely voluntary service, however. Even countries as well off for dispersion facilities as the Scandinavian might usefully compare the Bracknell and Toulouse outputs with their own, as they are based on independent NWP products.

<u>Results of the nuclear release exercise of 7th November 1996 at Bracknell</u>

Exercises are invaluable for highlighting unexpected problems which can arise in an emergency. The release postulated for this exercise took place at Liebstadt, Switzerland, over the 6 hours from 0600 UTC on 7th November 1996, although some early responses used 0500 UTC as the release time for the model simulations. Results of the calculations from the operational version of the UKMO NAME dispersion model, and the RSMC Toulouse model, are presented in *Figures 15.1 to 15.8* These figures are largely presented in the manner in which they were submitted during the exercise. It can be seen that they leave much to be desired as to clarity, although further reproduction for this publication has reduced the quality further. The research version of NAME, used for some of the figures (where the operational output was no longer available), uses gray tones which are particularly difficult to reproduce, but this format would not be used for emergency response. Apologies are made for the stretched grid of the research output.

The default release rate used for the operational models was 1/6 Bq/h, (1 unit over six hours) and the contours plotted as logarithms to the base 10. The NAME research model released 1 gram/h and plotted contours in ngrams.

The following points concerning the exercise performance are extracted from a note by R.G. Owens of the National Met Centre (NMC, formerly Central Forecast Office) Bracknell.

* The first run of the NAME nuclear accident model took an hour to complete. The meteorological files are spooled onto cassette so that if an operational NWP model run is pending (and there is a risk of the on-line files being updated during the NAME run, causing it to crash) NAME can be run from restored, non-interruptible data. This duly occurred, the data restoration causing delay.

* The job priority for the NAME model remained as normal, and in contention with other jobs in the computer mainframe. There was no information available to the forecasters on the progress of the NAME integration.

* The instructions to forecasting staff for running the model were easy to follow, but there were difficulties interpreting the general procedures where irregularities had arisen (e.g. no confirmation from IAEA). Instructions not clear on priorities where international and domestic requirements might conflict.

* The location of Liebstadt, the release point, was incorrect in the file of Nuclear installations.

* No problem with the automatic data dissemination, although not many countries were involved.

* Communications and liaison with Toulouse went well, despite language difficulties. Discussions `to the point and constructive'. A useful statement was agreed and written for issue with model products.

* Very poor communications with IAEA Vienna. No start of emergency message received at Bracknell. Toulouse had no success either. Notification of incident was received from Romania, starting the emergency response! Unable to contact RSMC Washington at that hour.

* Only about 6 countries requested output, and only two (Austria and Ireland) got the procedures quite right.

* Bracknell needs to install a dedicated, properly equipped office for such contingencies, not just use the forecast office.

* Two people are required to carry out all the duties and liaison. Bob Owen, who bore sole responsibility for organizing the response and liaison during the exercise, spent 14hr on shift without proper mealbreaks, or indeed meals.

Figure 15.1 Operational trajectories for 500, 1500 and 3000 m. Bracknell

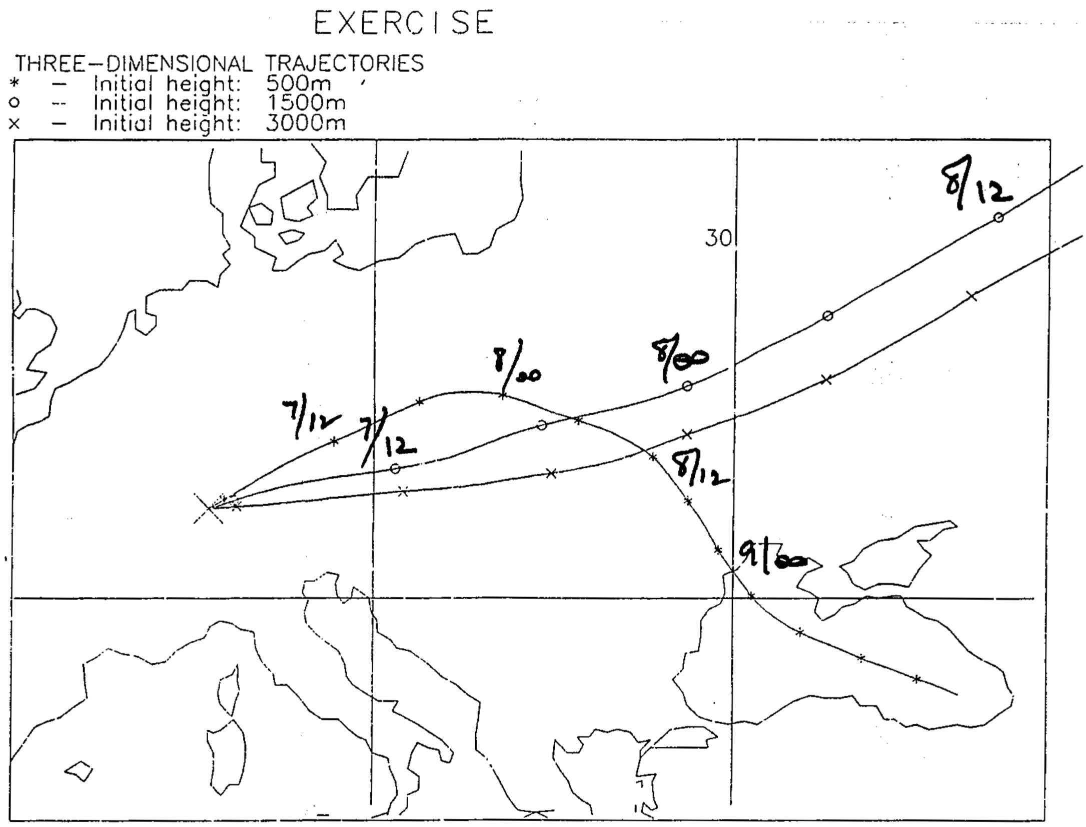

Simulation description:

(Standard default values used)
Pollutant released: CAESIUM-137
Start of the emission: 05 UTC 07/11/1996
Duration of the emission: 6.0 Hours
Release point: 47.58N 8.17E marked X
Place: no name
Amount of pollutant released per hour: 0.16667E+00 Bq

UK Meteorological Office – RSMC Bracknell.

Figure 15.2 Operational NAME time-integrated surface concentrations for the 24 hours to 00 UTC 9th November

EXERCISE

TIME INTEGRATED SURFACE TO 500 m CONCENTRATIONS (Bq.s/m3) for OUTC 09/11/1996

Contours at: 1E−12./1E−14./1E−16./1E−18. Maximum is: 0.32396E−11
(contour values may change from chart to chart.)

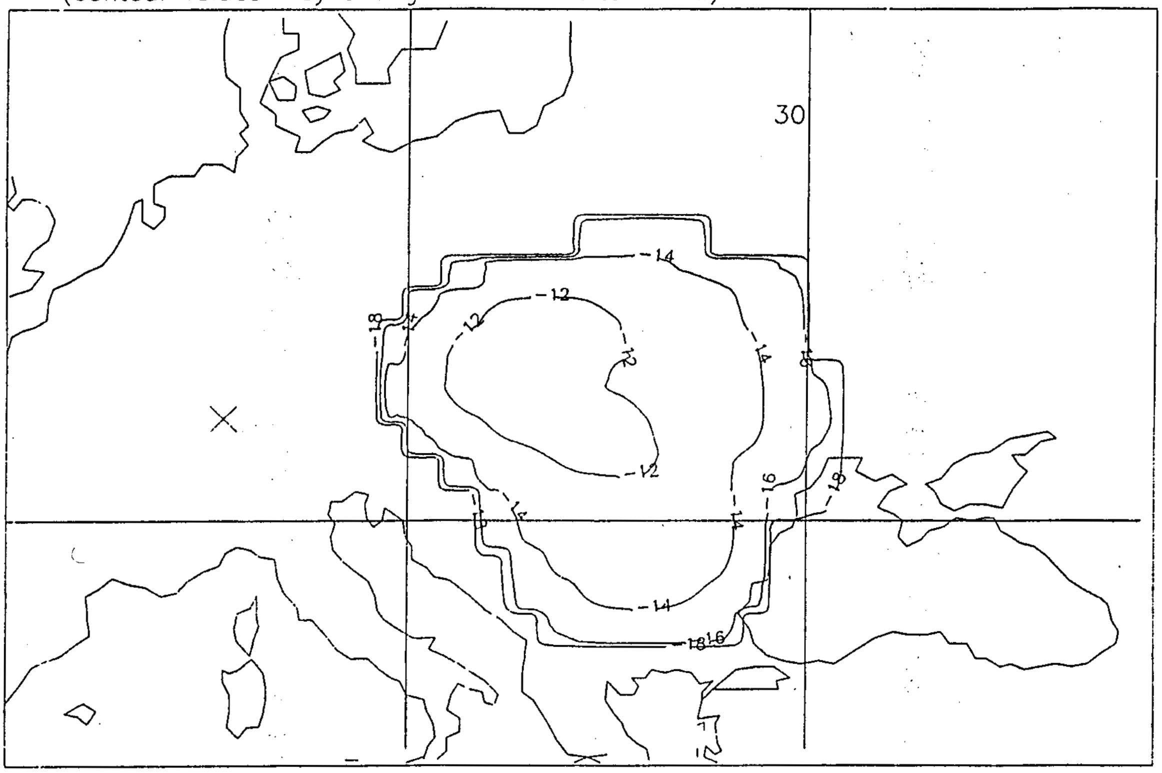

Simulation description:

(Standard default values used)
Pollutant released: CAESIUM-137
Start of the emission: 05 UTC 07/11/1996
Duration of the emission: 6.0 Hours
Release point: 47.58N 8.17E marked X
Place: no name
Amount of pollutant released per hour: 0.16667E+00 Bq

UK Meteorological Office − RSMC Bracknell.

Figure 15.3 *RSMC Toulouse time-integrated surface concentrations for the 24 hours to 00 UTC 9th November*

TIME INTEGRATED SURFACE TO 500 m
LAYER CONCENTRATION OVER 24 HOURS
961109 at 0 UTC

existence or strength of the event is unknown

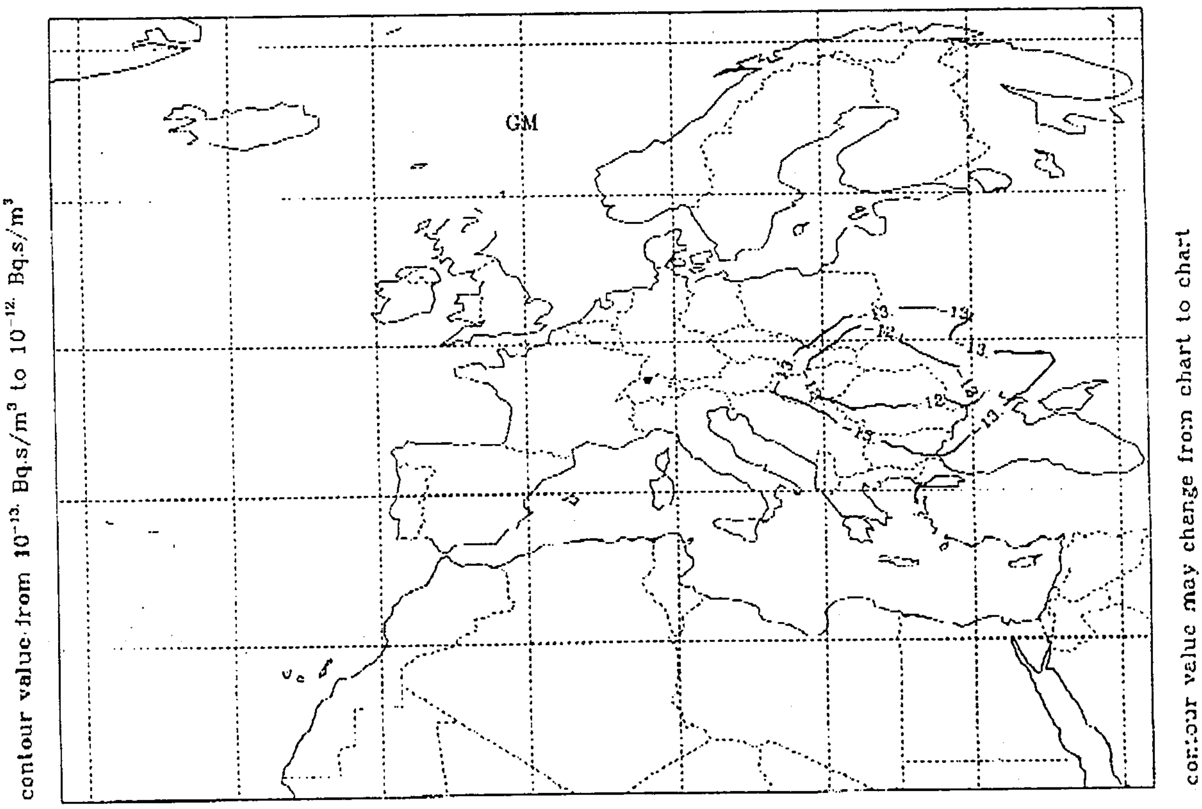

Simulation description

Pollutant released : CESIUM
Start of the emission : 961107 at 0h15m 0s UTC
End of the emission : 961107 at 12h15m 0s UTC
Standard default value
Latitude : 47.58N Base : 0. m
Longitude : 8.15E Top : 500. m Maximum 0.23E 11 Bq.s/m²

METEO FRANCE
RSMC TOULOUSE

Chart 2 / 4

Figure 15.4 NAME total deposition for the 42 hours to 00 UTC 9th November (results from the research version used as the operational were not readily available)

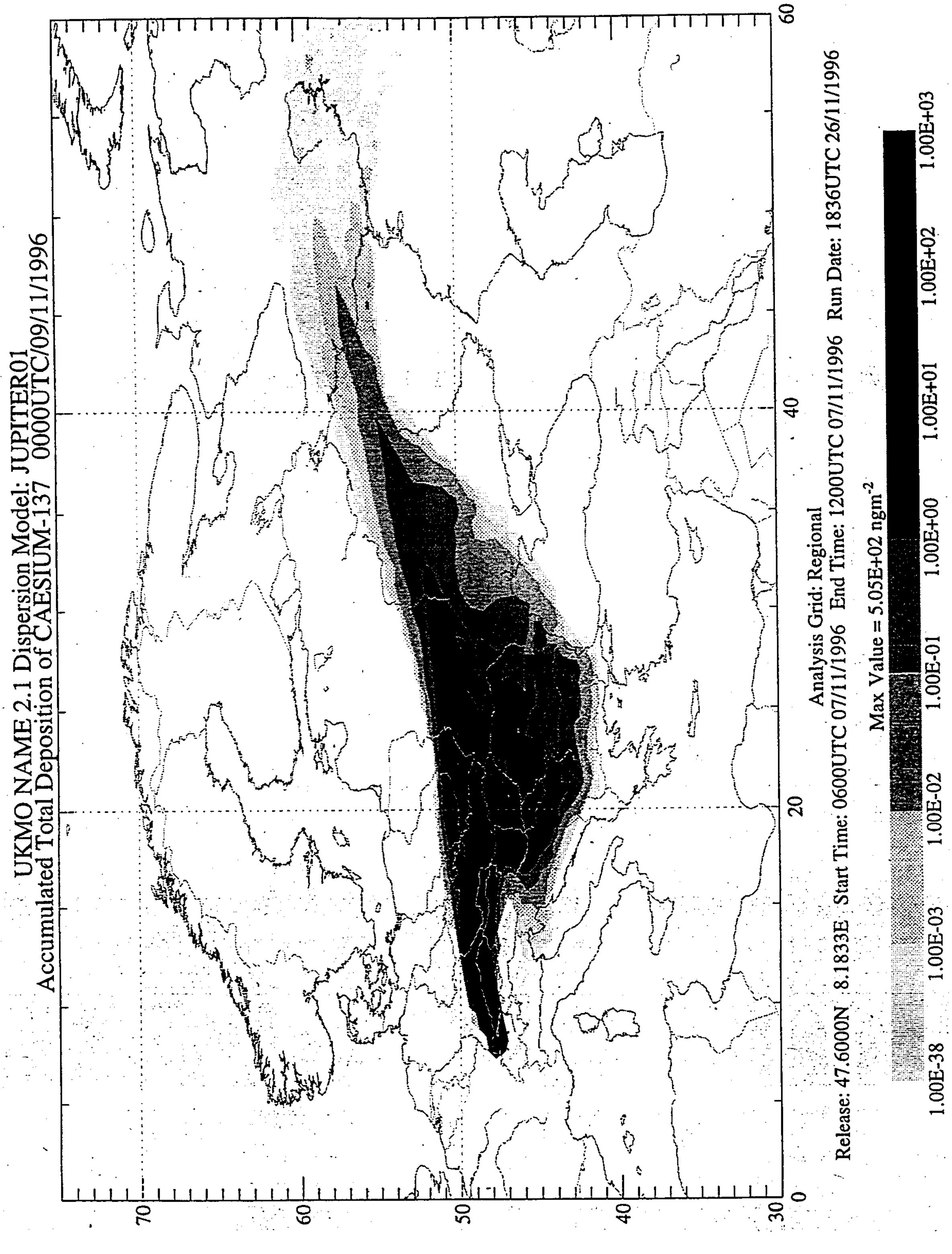

Figure 15.5 Toulouse total deposition for the 42 hours to 00 UTC 9th November

TOTAL DEPOSITION (WET + DRY) IN Unit / m² FROM THE RELEASE TIME TO THE END OF THE THIRD PERIOD

961110 at 0 UTC

existence or strength of the event is unknown

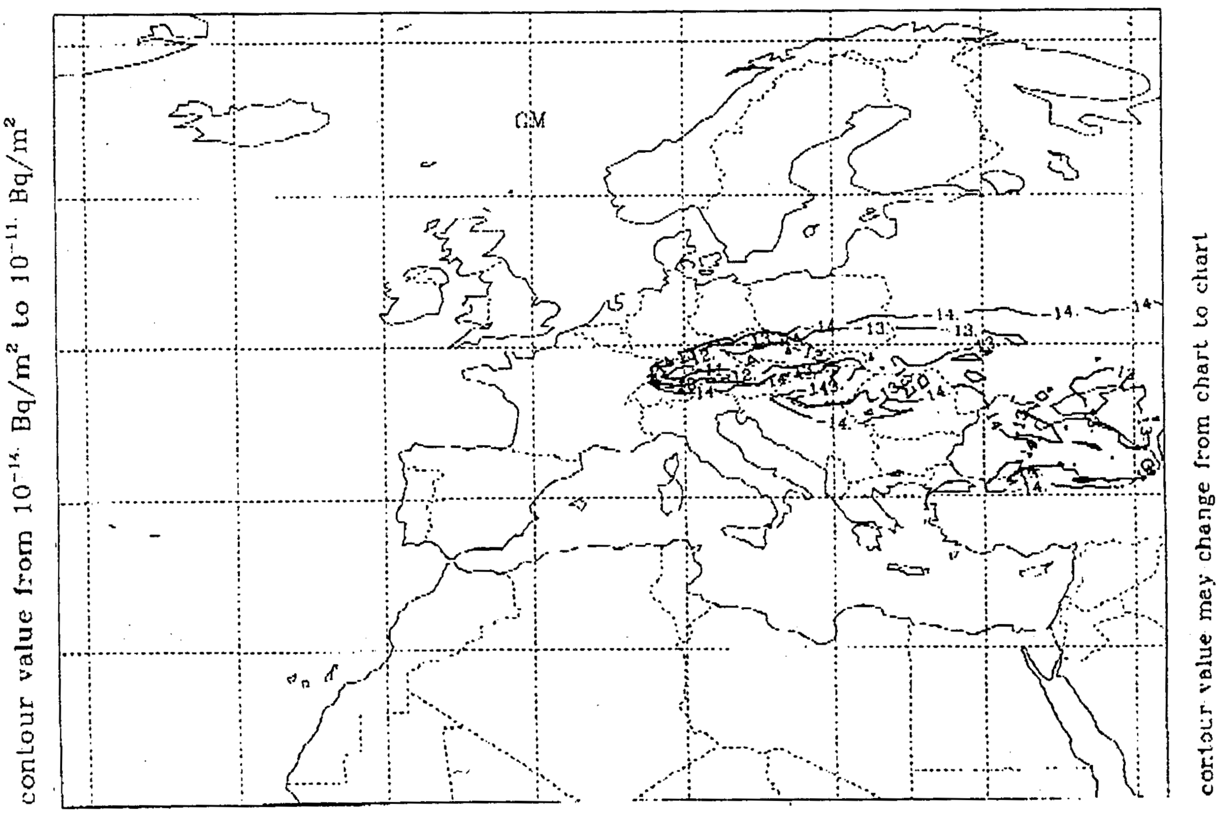

Simulation description

Pollutant released : CESIUM
Start of the emission : 961107 at 6h15m 0s UTC
End of the emission : 961107 at 12h15m 0s UTC
Standard default value
Latitude : 47.58N Base : 0. m
Longitude : 8.15E Top : 500. m   Maximum 0.32E−10 Bq/m²

METEO FRANCE
RSMC TOULOUSE

Chart 4 / 4

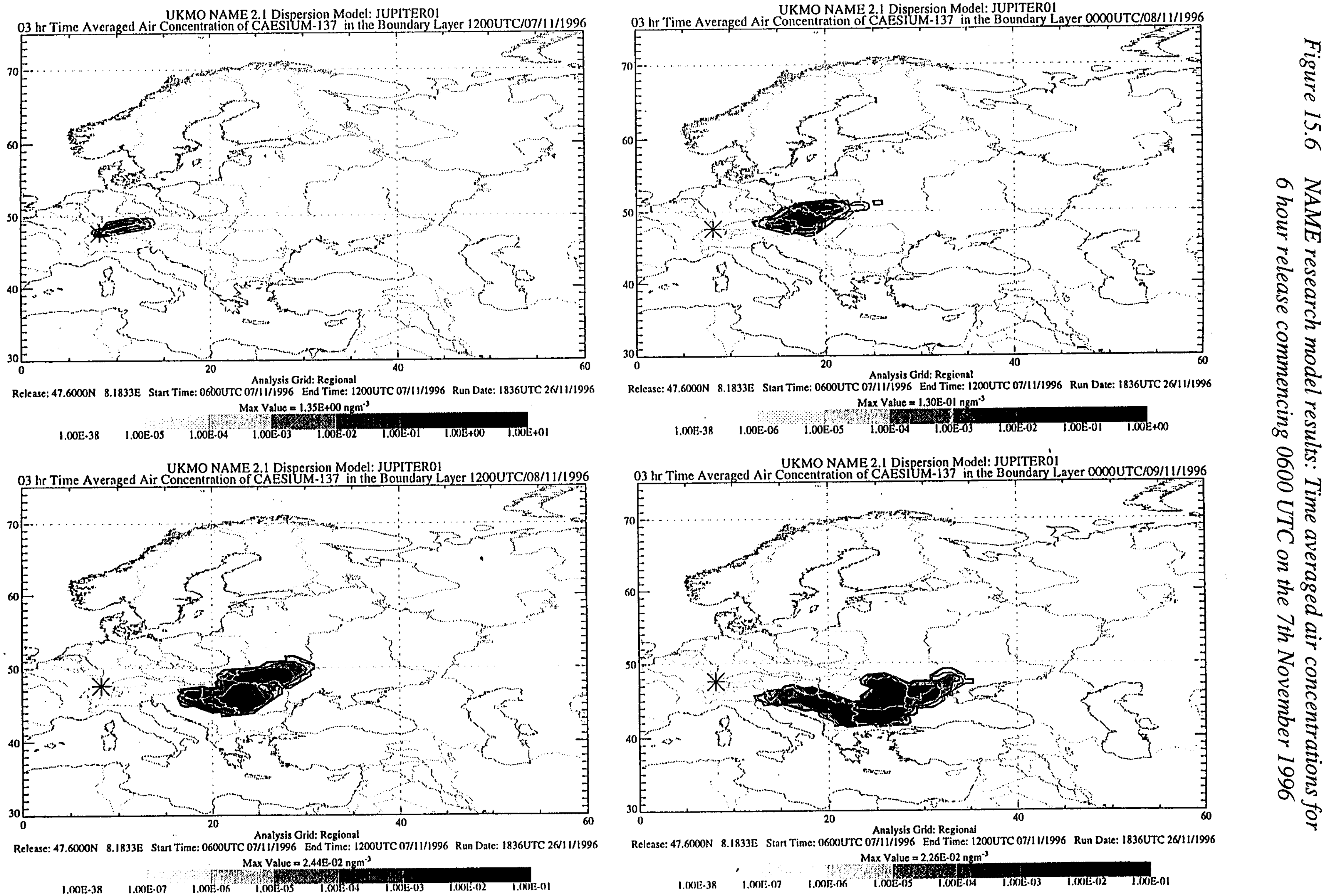

Figure 15.6 NAME research model results: Time averaged air concentrations for 6 hour release commencing 0600 UTC on the 7th November 1996

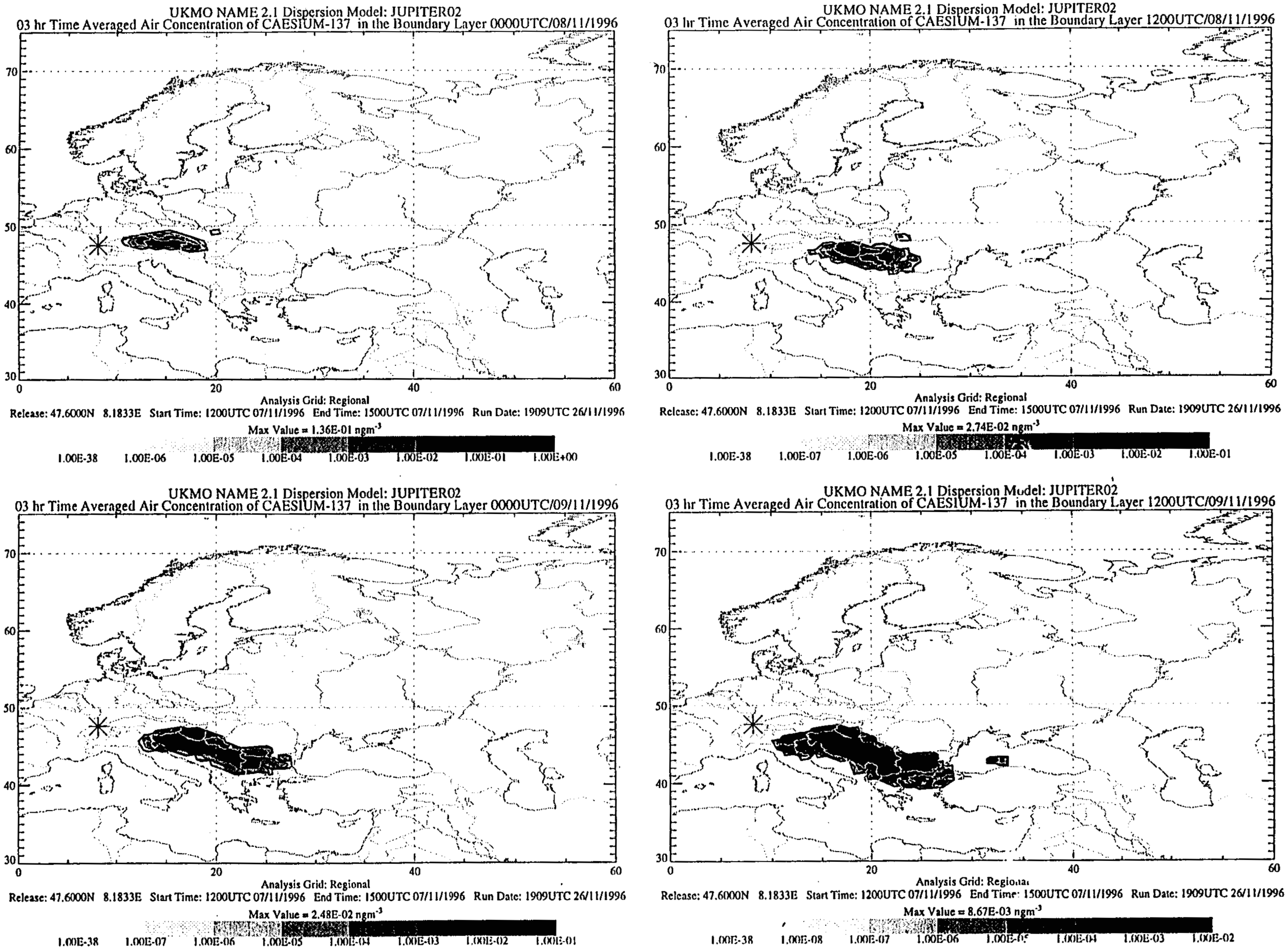

Figure 15.7 NAME research model results: time averaged air concentrations for 3 hour release commencing 1200 UTC on the 7th November 1996

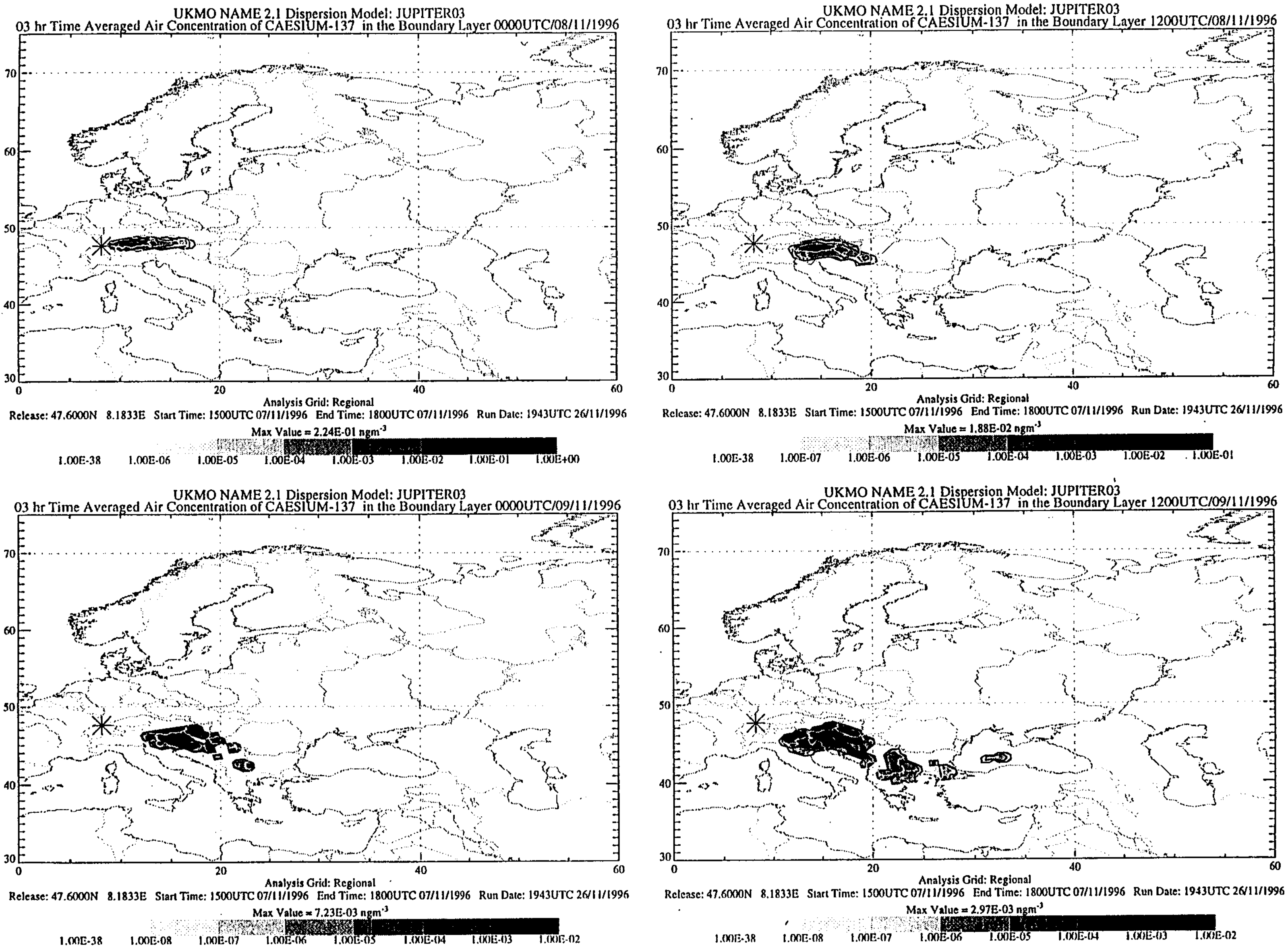

Figure 15.8 NAME research model results: time averaged air concentrations for 3 hour release commencing 1500 UTC on the 7th November 1996

16 Consequences of potential releases from the Kola Nuclear Power Plant - Climatological study

Jerzy Bartnicki
Meteorological Institute of Norway, DNMI
Oslo, Norway

16.1 Climatological Trajectory Analysis

Introduction

The Kola region has probably the greatest density of nuclear installations and potential sources for accidental releases of radioactive substances in the world and possible consequences of hypothetical nuclear accidents in the region are of great interest for the Scandinavian countries. Up to now, the studies of the consequences of a potential accident with releases of radioactive substances to the atmosphere from the Kola NPP has mainly focused on the local scale, how-ever, a potential accident at Kola NPP can have severe consequences for a much wider region. To analyze and assess long-distance consequences of hypothetical nuclear accidents, a joint project has been established between NRPA (project leader), DNMI and IFE. The main objective for the project was the analysis and assessment of `worst' possible consequences of a nuclear accident in the Kola NPP. In the analysis, different aspects were taken into account; like for example, security conditions and physical barriers at the source, atmospheric transport and deposition of released radioactive material and calculation of effective doses due to radioactive contamination of air and soil. DNMI's contributions to the joint project is limited to analyze long-range atmospheric transport and deposition of radioactive material emitted from a potential accident at the Kola NPP.

Trajectory analyses can be a useful tool for analyzing the consequences of reactor accidents. It is important, however, to keep in mind that this tool can be used in two basically different types of situations: When an accident has actually taken place - and when the existence of a nuclear installation poses a "threat". It is the latter case which is addressed in this paper. Such analyses should be probabilistic; the *probability* of a certain magnitude of the consequences should always be presented together with the consequences. The concept of "risk" is useful in this connection, and is defined as the probability multiplied with the consequence, summed over the whole spectrum of consequence magnitudes.

The *operational* decision makers "handling" a nuclear accident (which has actually taken place) in another country, ask: "Will the radioactive cloud come to (or pass over) a location of interest - or not?". If the answer is yes, the follow-up questions will be: "When will the "cloud" arrive?". Then: "What will be the air concentration and deposition in the area of interest?". The answers to these questions must be based on dispersion model calculations or trajectory calculations in "forecast mode". This will be the "operational" situation for the decision maker when the accident has happened.

In the "preparedness of planning phase" - when no accident has yet happened, but we feel a threat from a given nuclear installation, similar questions are asked, but now formulated as: "What is the *probability* for a radioactive cloud from a given "source" to come (or pass over) a specified location of interest? To answer such a question for a relatively large areas of interest, we have used what we have denoted a *"climatological trajectory analysis"* approach. This approach enabled us to produce "probability and travel time maps" for the region of interest.

The number of trajectory crossings for grid squares in the model domain was computed and taken as a measure for the probability of pollution transport to a specific location from the "source". Since our approach is source oriented, we have used "forward trajectories" in our present analysis.

Problem formulation

To be able to assess the environmental risk from a specified threat for a given location, we must know both the consequences of this threat and the probability for this threat to occur. The consequences must be connected to the probability in a functional manner. Usually, risk is defined as a product of probability and consequences:

Risk = Probability x Consequences

In our case we deal with the threat represented by a potential nuclear accident at the Kola NPP and the connected environmental risk for specific locations as a result of this threat. The main objective for the joint project is the estimation of this risk. The analysis of interacting events which could add up to accidental releases of nuclear substances were analyzed by the other partners in the project (NRPA and IFE).

DNMI has limited its approach to the following setup: - *Assume that the accident (with releases) could happen at any time with a given probability. What would the be the probability for a specific location to be harmfully effected by these accidental releases?*

For this aim, we have developed our version of a *"climatological trajectory analysis"*.

16.1.1 Choice of methodology

The *climatological trajectory analysis* was performed in the following way:

First step:

> We compiled 11 years of meteorological data (1985 - 1995) with assured homogeneous characteristics in time frequency for the meteorological fields was 6 hours. This data set has previously been used at DNMI for calculations of transboundary transport of air pollutants in Europe (European Monitoring and Evaluation Programme). The methods and procedures for setting up this data set, are described in details in the DNMI Research Report no. 40. This data set includes *precipitation fields* for the ground level (accumulated 6-hourly values) and *wind fields* for the model level $\sigma = 0.925$ in the LAM50E model (instantaneous values). This level roughly corresponds to 600 m height and represents reasonably well the level for the bulk transport in the atmospheric boundary layer (ABL).

Second step:

> The compiled wind fields were used to compute *forward trajectories* (10 days long), starting from the location of the Kola NPP. One such forward trajectory was released *every* hour during the 11 years. The time step between the points along each trajectory was set to 15 minutes, to be sure that the distance between sequential points during one time step will be shorter than the grid square size (~ 50 km). All together 96.162 trajectories were released during the 11-years period.

The area under consideration is covered by two numerical grid systems. The first, in which meteorological data were available, has a mesh size of 150 x 150 km at 60°N in the Polar Stereographic Projection. It consists of 39 by 37 nodes in x- and y-direction respectively and is shown in *Figure 16.1*. The second grid system, in which all maps were computed, consists of grid squares 50 x 50 km in size, covering the same area as the 150 km grid system. The 50 km grid system consists of 117 x 111 nodes in x- and y-direction respectively and is shown in *Figure 16.2*. The only difference between these two grid systems is the mesh size. We have used 50 km mesh size for computing numerical results from our climatological trajectory analysis in order to achieve good spatial resolution for the maps. As an example of the trajectory computations, four "air parcels" released from Kola NPP within 24 hours interval are shown in *Figure 16.3*.

16.1.2 Results from the Climatological Trajectory Analysis

1. The main body of results from the climatological trajectory analysis described in the previous subchapter are:

2. Probability of arrival map - more precisely - *the probability for a grid square (i,j) to be hit (or crossed) by the trajectories starting from the Kola NPP.*

3. Maps of *(a) average and (b) relative standard deviation of the travel time, as well as (c) minimum travel time.*

4. Distributions for the travel time for selected sites in Norway.

5. Calendar for selection of episodes for closer study (SNAP runs)

Some examples of preliminary results:

A map of the probability of arrival in the grid system with 50 km resolution is shown in *Figure 16.4*. The probability distribution presented in *Figure 16.4*, for different probability values is rather smooth and surprisingly isotropic (note the logarithmic scale). The isoline pattern for different probability values, and especially for the larger values, seems close to flattened circles extending slightly in the north-east direction. A clear blocking effect of Greenland, as well as a less pronounced blocking effect of the Scandinavian mountains, are visible in *Figure 16.4*.

A map of the average travel time from the Kola NPP to each 50 km grid square (i,j) is shown in *Figure 16.5*. As in the case for the probability of arrival, computations were based on the same 11 years of meteorological data. The maximum of average travel time in *Figure 16.5* is 239.75 hours, which is almost the same as 10 days.

The pattern on *Figure 16.5* is quite regular. However, it can be seen that the transport in north-east direction is slightly faster then in other directions, which can be seen from the slightly elongated isolines in this direction. Among the Nordic countries, Finland can be reached relatively fast. Typical values for the average travel time are 1-2 days. However, we must bear in mind that the radioactive cloud in case of an accident, seldom travels according to average meteorological conditions.

Average travel time to Norway is between 2 and 6 days depending on the location. The influence of mountains in the south-western part of the country is visible. For example, average travel time to Oslo is shorter than to Bergen.

Of special interest is perhaps a map for the minimum travel time from Kola NPP to any grid square (i,j) as shown in *Figure 16.6.* It is somewhat surprising to see how isotropic this map look like. No direction show up with markedly stronger winds then any other direction. We do not claim that this map shows the absolute extreme values for the minimum travel time, but it shows the minimum found from a quite large data set - covering a period of 11 years from 1985 to 1996. We can see from *Figure 16.6* that a "radioactive cloud" from Kola NPP can reach the Norwegian boarder in Eastern Finnmark in less then 3 hours, Bodø in less then 12 hours and Trondheim within 24 hours.

A statistical analysis of the travel time have therefore been performed for some selected receptors: Kirkenes, Tromsø, Bodø, Trondheim, Oslo, Bergen and Kristiansand. In addition, we have included one grid square (52,90), located in Russia next to the grid square containing the Kola NPP. The location of the selected grid squares are shown in *Figure 16.7.* For each receptor grid square, we have calculated - average travel time, standard deviation, median and the three statistical moments for the distribution of the travel time: variance, skewness and kortosis. The results are shown in *Table 16.1.*

Table 16.1 Statistical analysis of the travel time (in hours) from Kola NPP to selected receptors

Receptor	Mean (h)	Median (h)	St.dev. (h)	Variance (h^2)	Skewness	Kortosis
Kirkenes	51.3	30.00	52.65	2771.92	0.0190	-2.971
Tromsø	77.72	62.25	54.95	3019.16	0.0182	-2.982
Bodø	99.18	89.62	58.73	3448.71	0.0170	-2.988
Trondheim	109.39	97.50	59.05	3486.78	0.0169	-2.992
Oslo	118.48	102.25	58.01	3365.16	0.0172	-2.992
Bergen	131.61	124.75	48.84	3176.21	0.0177	-2.996
Kristiansand	132.03	128.50	55.23	3050.63	0.0181	-2.996
Near Kola NPP	9.04	1.50	26.55	704.77	0.0376	-2.808

Since the average and the median for the travel time are quite different for all receptors, the distribution of the travel time must be rather irregular. This irregularity is confirmed in *Figure 16.8*, where distributions of the travel time for each of the selected receptors are shown.

We can make the following statement for Kirkenes: If the "cloud" hits this location (probability of arrival range ~ (3 - 10)% from *Figure 16.6*), there is ~ 45% probability (see *Figure 16.8*) that the "cloud" will arrive within 24 hours after the release. For Bergen - and further away - we observe from the distribution of travel time, no clear decrease in the frequency distribution representing the longer travel times, class (5-10). This means that - if the cloud hits Bergen (~0.5% probability from *Figure 16.6*), - there is almost the same probability that it will arrive at day no. 10 (~10% probability) as any of the days from 3 to 10, (maximum probability ~15% for day 5).

In *Table 16.2*, we have listed the number of arriving air parcels from the Kola NPP and their trajectories, probability of arrival and minimum travel time - for the selected receptors. Of the - 96 162 - hourly releases of air parcels from the Kola NPP through the 11 years period (1985 - 1995), - 4 212 had trajectories which passed over the 50 km grid square where Kirkenes is located. This gives a probability of arrival of 4.38%. Among all these released air parcels, the one with the shortest travel time, will make its presence felt within 3 hours after its release from Kola NPP. As far away as Oslo, we still have 921 `crossings', representing about 1% probability of arrival and the shortest travel time is 26.5 hours. For Bodø the numbers are - 1560 crossings, 1.6% probability of arrival and 9 hours as the shortest travel time.

Table 16.2 Number of arriving trajectories, probability of arrival and minimum travel time from the Kola NPP to selected receptors

Receptor	Number of arriving trajectories	Probability of arrival (in %)	Minimum travel time (hours)
Kirkenes	4212	4.38	3.00
Tromsø	2030	2.11	7.50
Bodø	1560	1.62	9.00
Trondheim	867	0.90	22.75
Oslo	921	0.96	26.50
Bergen	777	0.81	35.75
Kristiansand	935	0.97	35.50
Near Kola NPP	21343	22.19	0.50

Figure 16.1 *Numerical grid system in which input meteorological data: wind, precipitation and mixing height are available for the trajectory analysis. The grid squares are 150 x 150 km in size at 60° N*

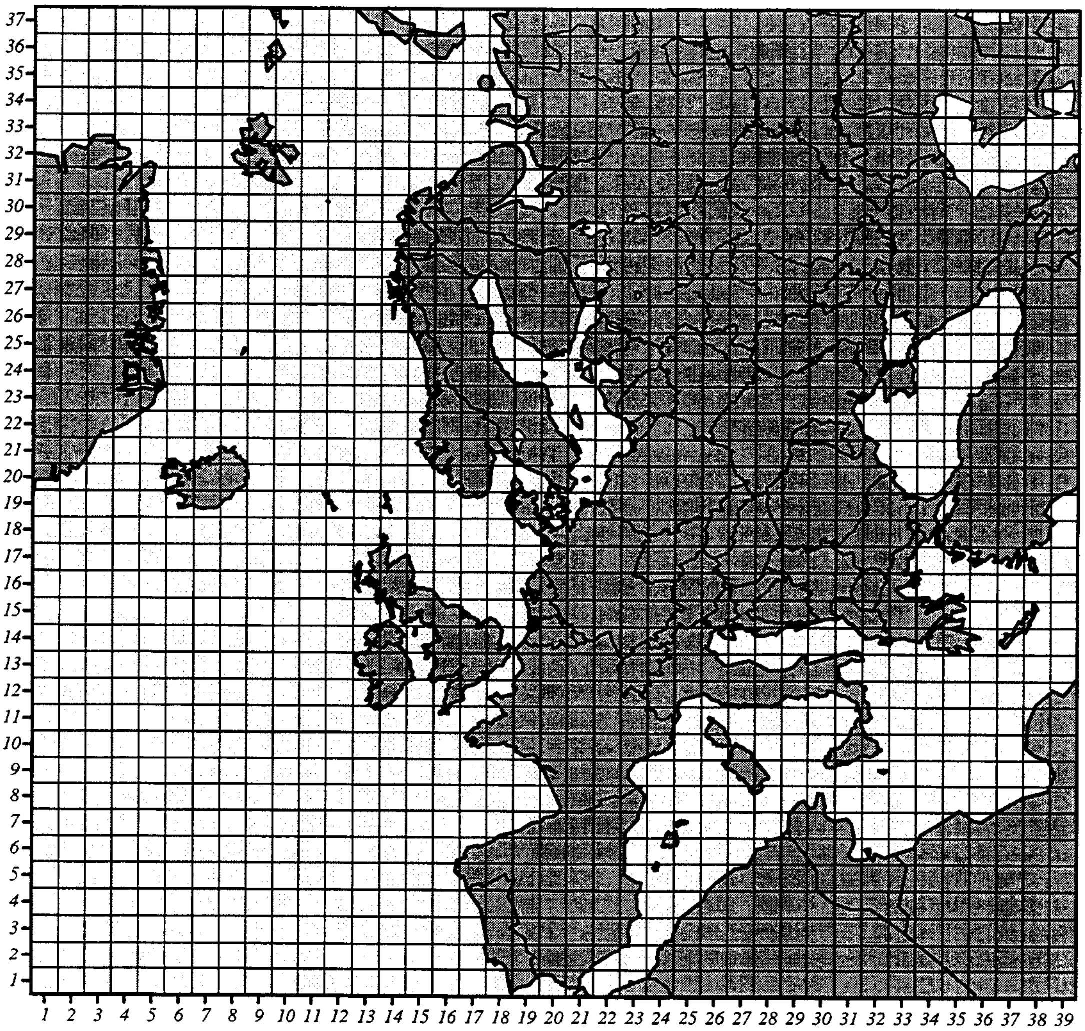

Figure 16.2 Numerical grid system in which 10-days trajectories are computed. It consists of 117 x 111 nodes with the mesh size 50 x 50 km

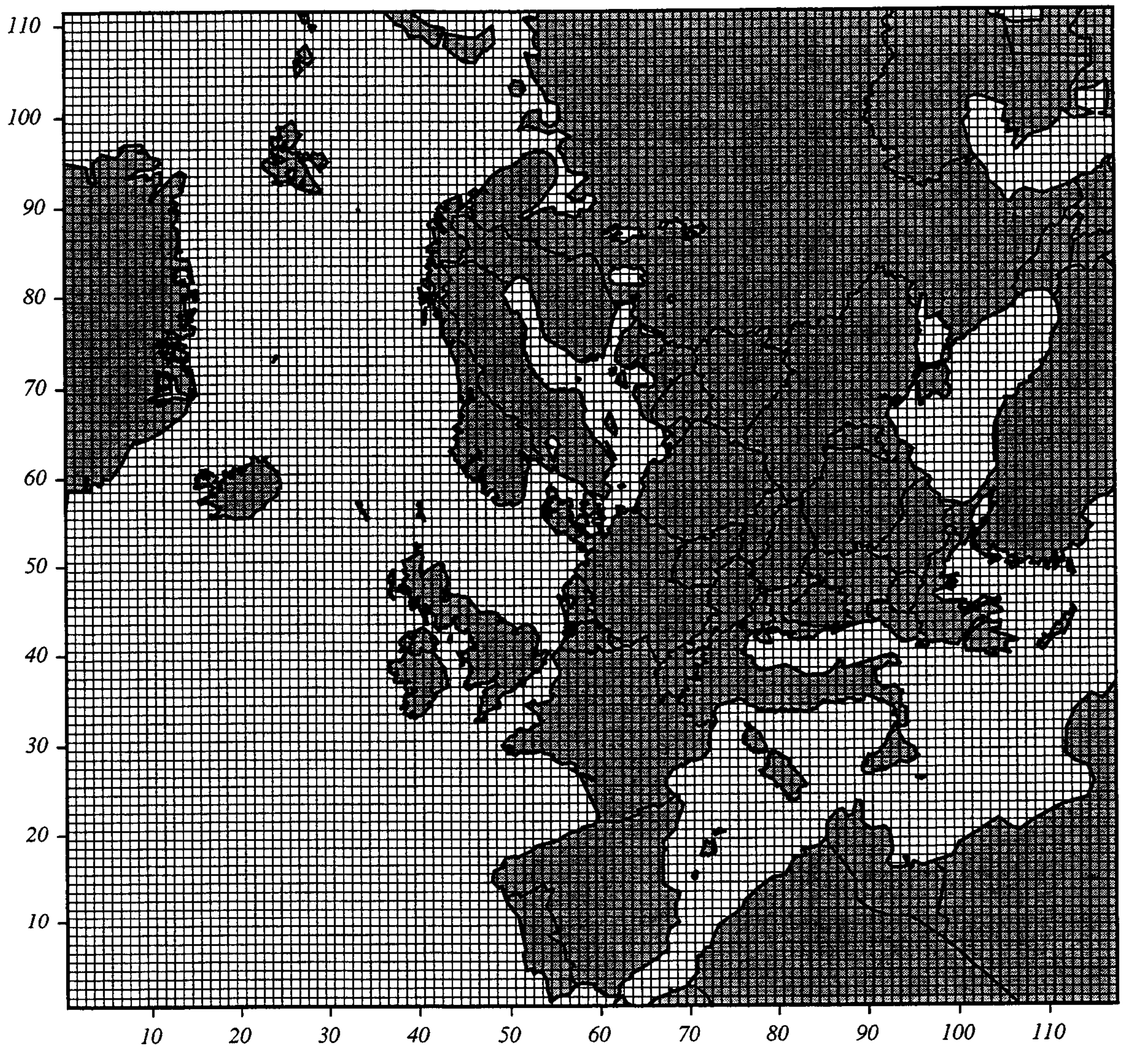

Figure 16.3 *10-days trajectories for air parcels released from Kola NPP at 12 UTC for four consecutive days in 1985: 1/2, 2/2, 3/2 and 4/2. All four trajectories reach the boundary of the meteorological data domain*

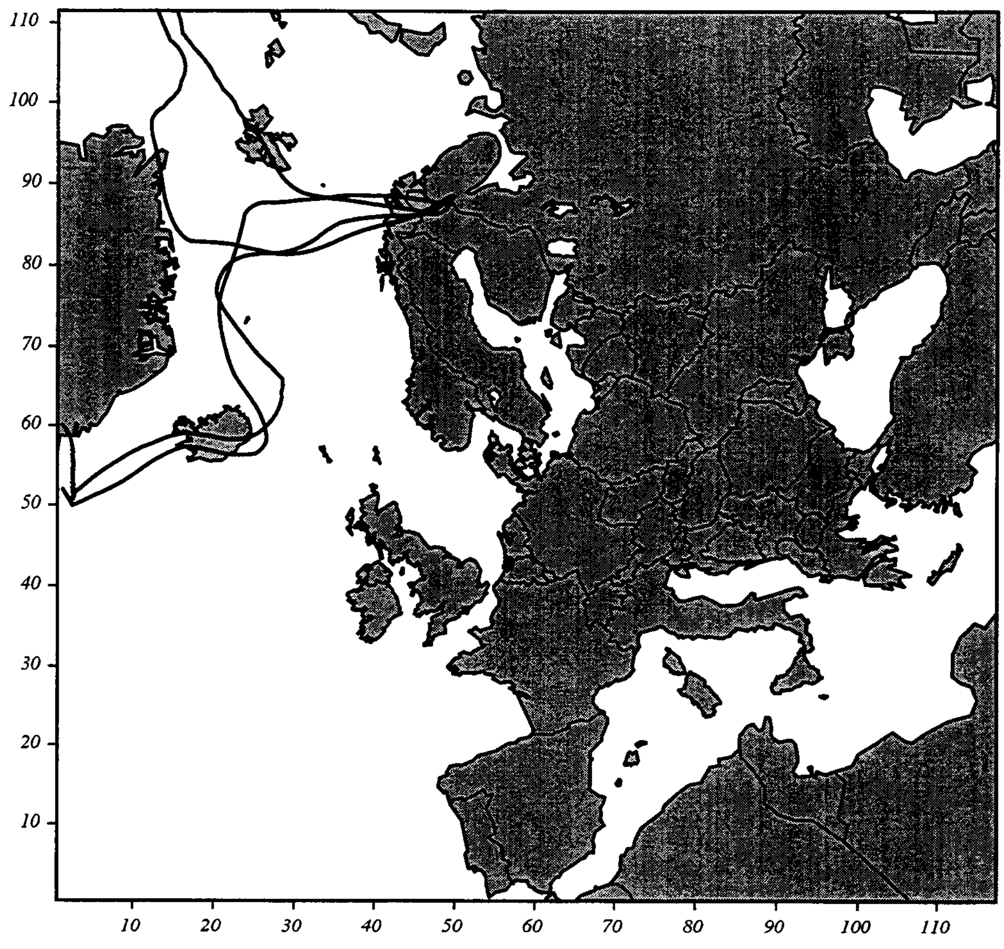

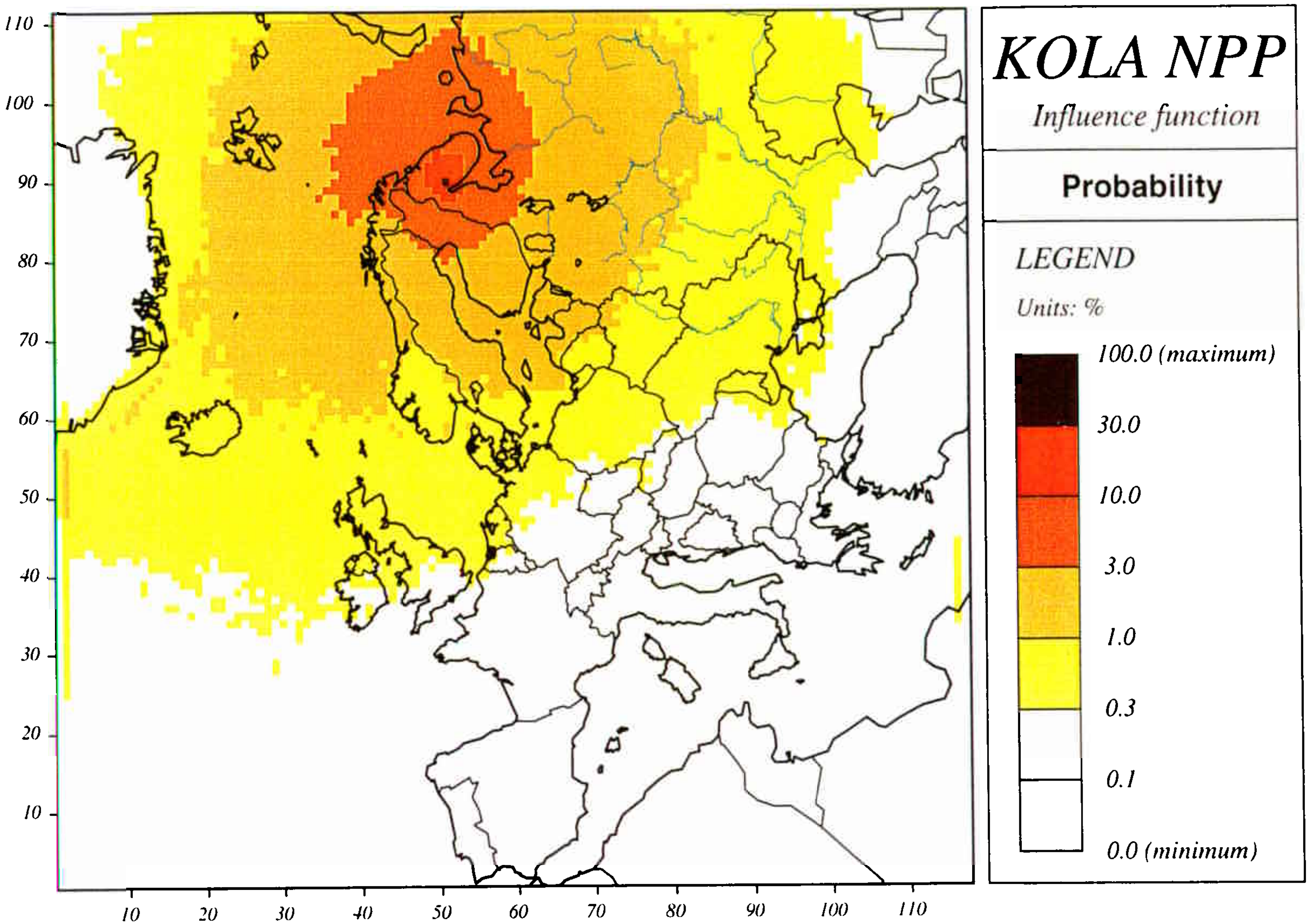

Figure 16.4 *Map for the probability of arrival calculated for the trajectories of air parcels released from the Kola NPP every hour for a period of 11 years: 1985 - 1995*

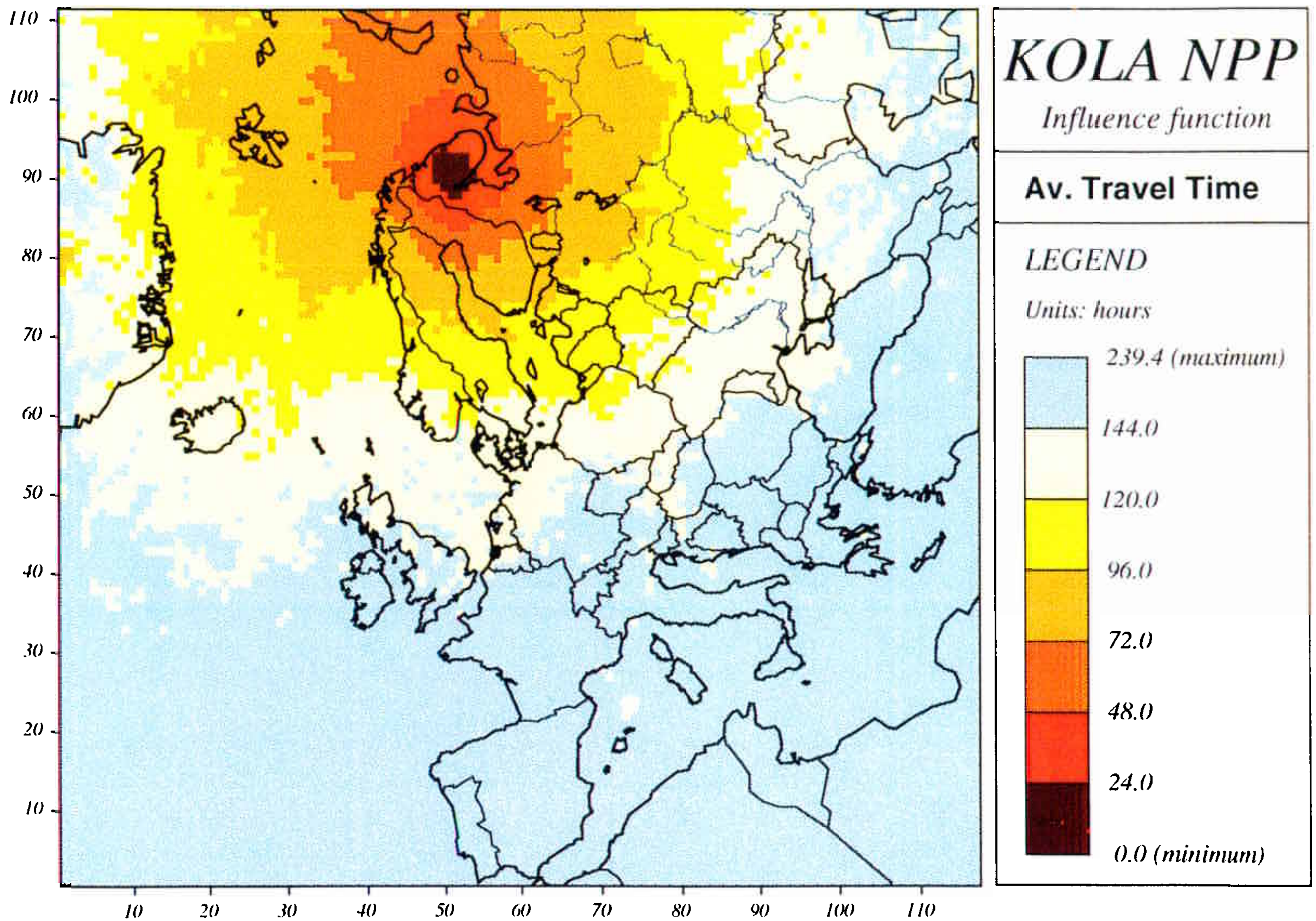

Figure 16.5 Map of the average travel time from the Kola NPP to any given grid square (i,j) based on 11 years of meteorological data: 1985 - 1995

Figure 16.6 Map of the minimum (shortest) travel time from the Kola NPP to any given grid square (i,j) based on 11 years of meteorological data: 1985 - 1995

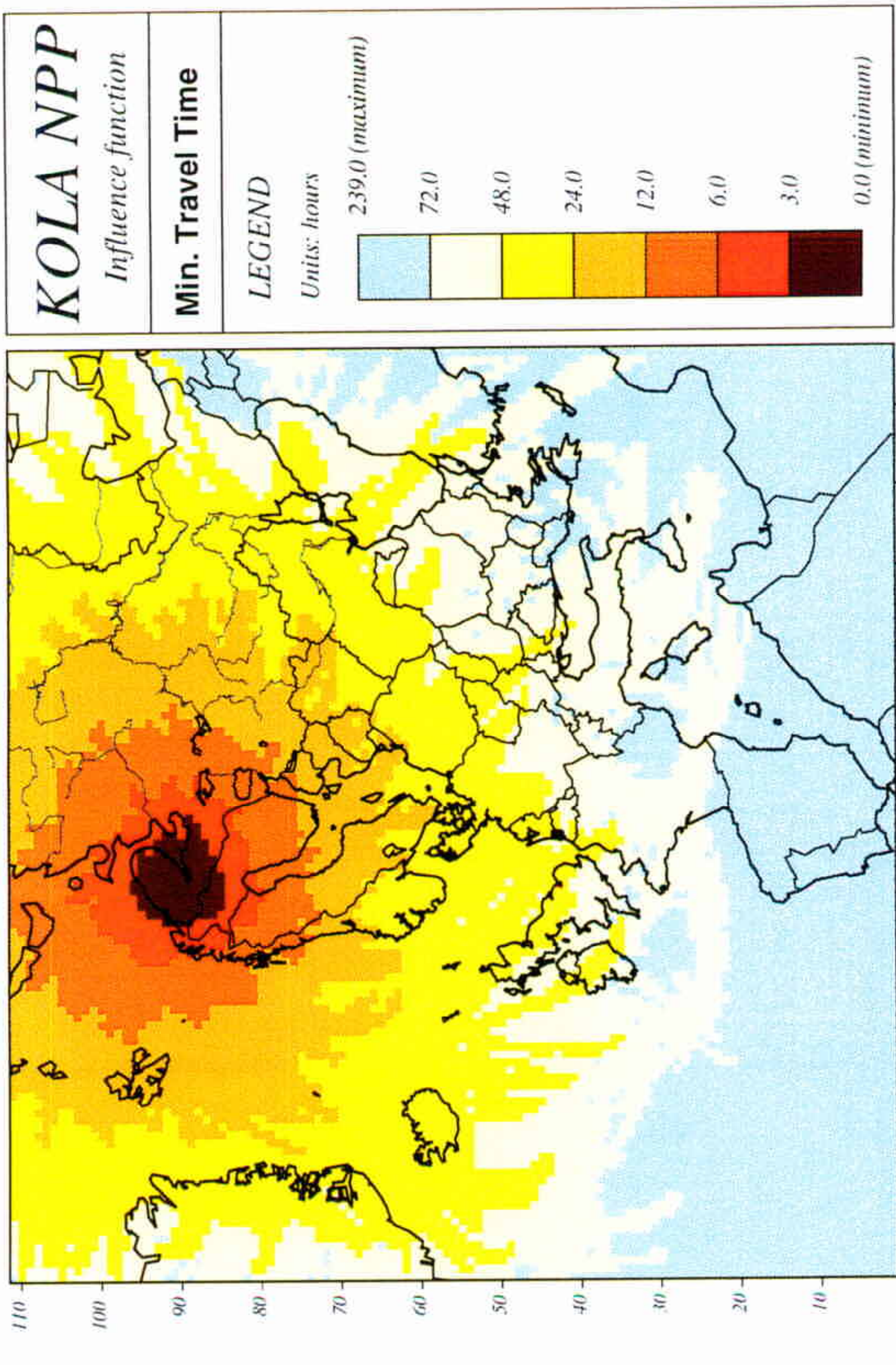

Figure 16.7 Geographical location of the selected receptors for the statistical analysis of the distribution of travel time from Kola NPP

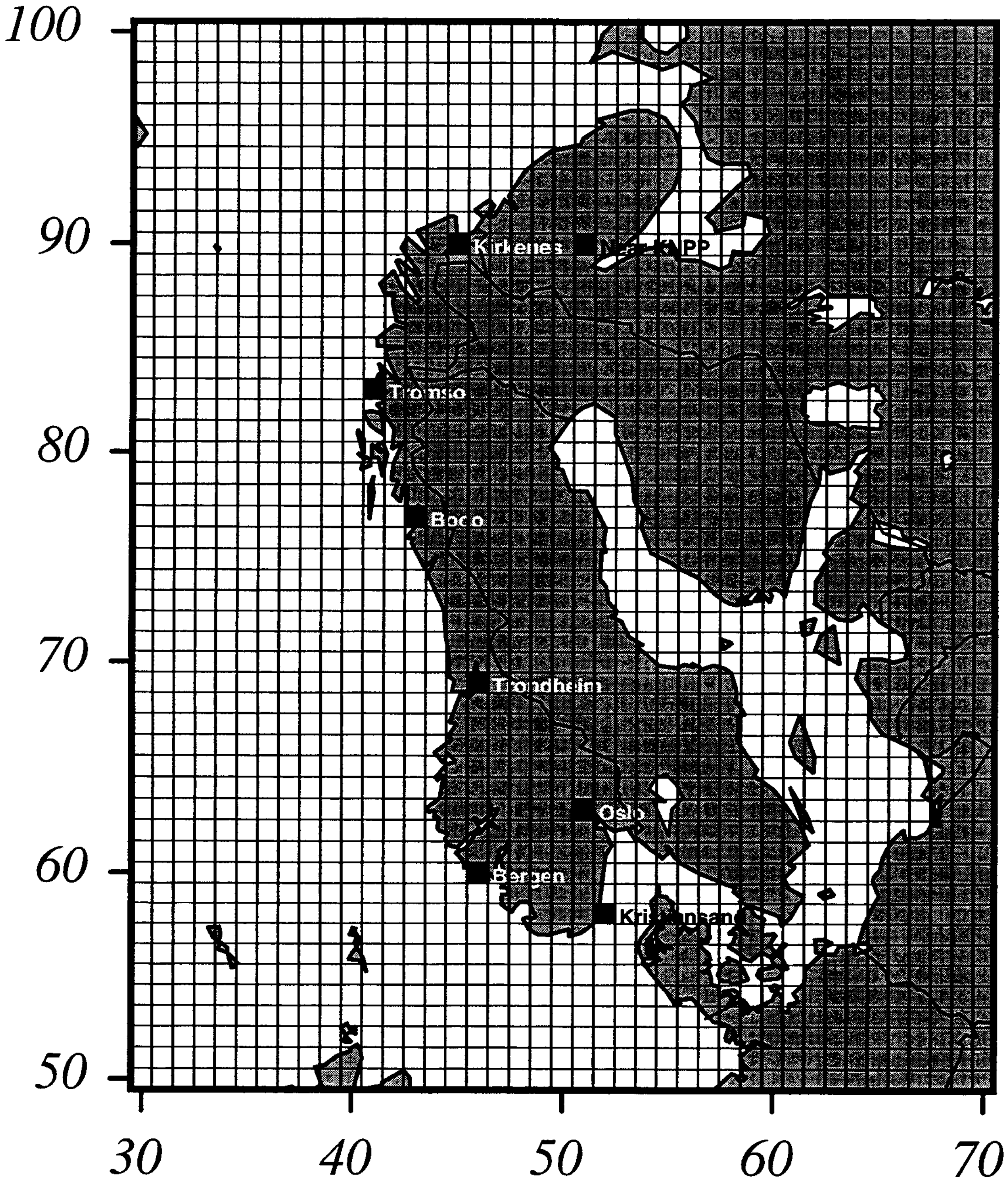

Figure 16.8 *Distribution (in %) of the travel time from the Kola NPP to the selected receptors in ten classes. Class 1, 2, ... , 10 correspond to 1, 2, ... , 10 days of transport, respectively*

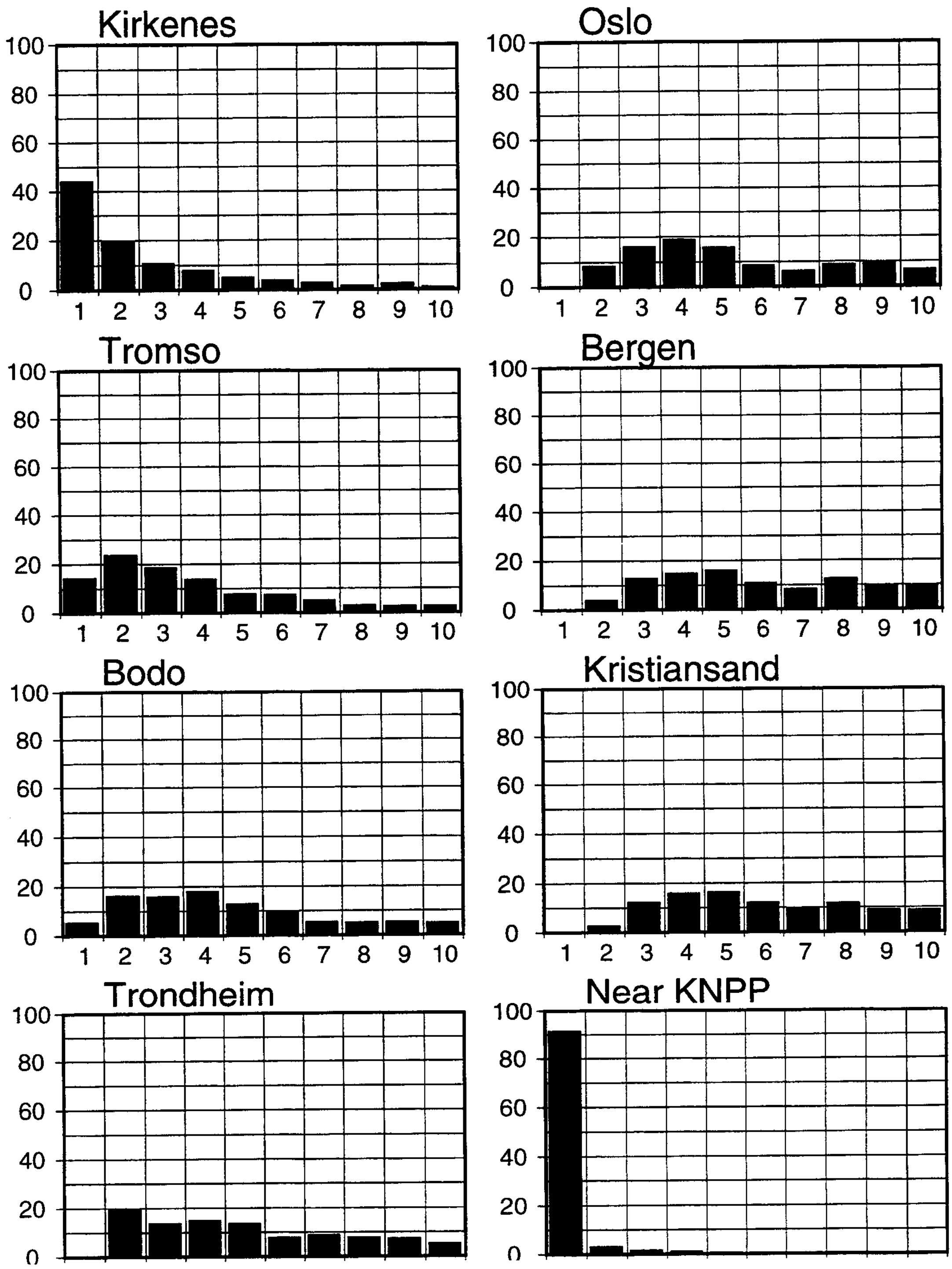

17 Conclusions of the meeting

The participants stressed repeatedly the great benefit of meetings like the present one, where one can meet for truly relaxed and informal discussions. The British participant also expressed that he was impressed by the very open character of the discussions and the productive cooperation between the Nordic countries.

Participation of representatives of the authorities was very much larger than in the previous ETEX meeting, both concerning the number of participants and active participation.

The Icelandic Meteorological Office participated for the first time and expressed strongly the wish to participate in future similar meetings.

There were extensive discussions after, and during, most of the presentations. These have not been referenced in this report, but many of the points raised were taken up again during the concluding discussions.

The participants of the meeting agreed that the following list reflect the current status, major concerns, and desires and needs for future activities:

a) The progress in this area on code development and modes of application of the methods has been substantial over the last few years.

b) The progress in modeling has greatly outstripped that in application and operational structures. Results from calculations for the same accident situation performed by different institutions may look confusingly dissimilar; even though the results actually turn out to be in excellent agreement upon closer inspection. However; in an emergency situation one can often not afford to spend the extra time needed. It ought to be possible "at a glance" to immediately understand results and to see whether different predictions are in agreement or not.

A concern of obvious importance is to satisfy the needs of the "end user"; often (a) member(s) of an emergency organization. For this reason it is **strongly recommended that the efforts on harmonization of result presentation initiated in the NKS-project BER-1 are revitalized within the next NKS program**. It is imperative that this work is coordinated with other harmonization efforts; e.g. the format for presenting the results which has been laid down for the Regional Specialiced Meteorological Centres (RSMC's). However, RSMC requirements do not coincide with national requirements; an additional complication.

c) The mode of communication is another matter of grave concern during the concluding discussions of the meeting. It is generally agreed that faxmachines, at least in this context, are outmoded. However, there does not seem to be any obvious available alternative.

Communicating via e-mail is efficient for short messages, but often impossible for transfer of more complicated information. This has been amply demonstrated during preparation of this report.

Internet is an alternative, provided restricted access and an acceptable response time can be assured.

Relevant efforts have been undertaken in another part of the EKO-4 project to find a standard way of exchanging this kind of information. The meteorological Institutes have, however, not been involved till now, but should look more closely to this in the future.

d) A more definite problem concerning proper understanding of potential differences in predictions, is the fact that different versions of HIRLAM, giving somewhat different results, are used in the different Nordic countries.

e) It was also suggested that expanded **contact with the Baltic States** in this area is highly desirable, and ought to be an **area of concern within the next NKS program.**

Appendix 1

List of participants

Denmark:

Jørgen Brandt
National Environmental Research Institute -DMU
Department of Atmospheric Environment
P.O.Box 358 (Fredriksborgvej 399)
DK-4000 Roskilde
Tlph.: +45 - 46 30 11 57
Fax: +45 - 46 30 12 14
e-mail: lujbr@sun4.dmu.dk

Steen Cordt Hoe
Ministry of the Interior
Emergency Management Agency
Datavej 16
DK-3460 Birkerød
Tlph.: +45 - 45 82 54 00
Fax: +45 - 45 82 65 65
e-mail: hoe@brs.dk

Torben Mikkelsen
Risø National Laboratory
Department for Meteorology and Wind Energy
P.O. Box 49
DK-4000 Roskilde
Tlph.: +45 - 46 77 50 09
Fax: +45 - 46 75 56 19
e-mail: torben.mikkelsen@risoe.dk

Alix Rasmussen
Danish Meteorological Institute - DMI
Lyngbyvej 100
DK-2100 Copenhagen Ø
Tlph.: +45 - 39 15 74 31
Fax: +45 - 39 15 74 60
e-mail: ali@dmi.min.dk

Jens Havskov Sørensen
Danish Meteorological Institute - DMI
Lyngbyvej 100
DK-2100 Copenhagen Ø
Tlph.: +45 - 39 15 74 32
Fax: +45 - 39 15 74 60
e-mail: jhs@dmi.min.dk

Finland:

Mikko Ilvonen
VTT Energy / Nuclear Energy
P.O. Box 1604
FIN-02044 VTT
Finland
Tlph: +358 9 456 5054
Fax: +358 9 456 5000
e-mail: mikko.ilvonen@vtt.fi

Juhani Lahtinen
Finnish Centre for Radiation and Nuclear Safety - STUK
P.O.Box 14
FIN-00881 Helsinki
Tlph.: +358 9 7598 8426
Fax: +358 9 7598 8433
e-mail: juhani.lahtinen@stuk.fi

Raimo Mustonen
Deputy Director, Research Department
Finnish Centre for Radiation and Nuclear Safety - STUK
P.O.Box 14, FIN-00881 Helsinki
Tlph.: +358 9 7598 8492
Fax: +358 9 7598 8498
e-mail: raimo.mustonen@stuk.fi

Göran Nordlund
Finnish Meteorological Institute - FMI
Air Quality Research
Sahaajankatu 20 E
FIN-00810 Helsinki
Tlph.: +358 9 1929 5420
Fax: +358 9 1929 5403
e-mail: goran.nordlund@fmi.fi

Roy Pöllänen
Finnish Centre for Radiation and Nuclear Safety - STUK
P.O.Box 14
FIN-00881 Helsinki
Tlph.: +358 9 7598 8425
Fax: +358 9 7598 8433
e-mail: roy.pollanen@stuk.fi

Juhani Rinne
Finnish Meteorological Institute - FMI
Meteorological Research/Atmospheric Modelling
P.O.Box 503
FIN-00101 Helsinki
Tlph.: +358 9 1929 4104
Fax: +358 9 179 581
e-mail: juhani.rinne@fmi.fi

Mika Salonoja
Finnish Meteorological Institute - FMI
Meteorological Research/Atmospheric Modelling
P.O.Box 503
FIN-00101 Helsinki
Tlph.: +358 9 1929 4135
Fax: +358 9 179 581
e-mail: mika.salonoja@fmi.fi

Anna Liisa Savolainen
Finnish Meteorological Institute - FMI
Meteorological Research/Atmospheric Modelling
P.O.Box 503
FIN-00101 Helsinki
Tlph.: +358 9 1929 3350
Fax: +358 9 179 581
e-mail: anna-liisa.savolainen@fmi.fi

Kari Sinkko
Finnish Centre for Radiation and Nuclear Safety - STUK
P.O.Box 14
FIN-00881 Helsinki
Tlph.: +358 9 7598 8493
Fax: +358 9 7598 8433
e-mail: kari.sinkko@stuk.fi

Ilkka Valkama
Finnish Meteorological Institute - FMI
Air Quality Research
Sahaajankatu 20 E
FIN-00810 Helsinki
Tlph.: +358 9 1929 5424
Fax: +358 9 1929 5403
e-mail: ilkka.valkama@fmi.fi

Iceland:

Knutur Arnason
The Icelandic Meteorological Office
Bustadavegur 9
IS-150 Reykjavik
Tlph.: +354 - 56 00 600
Fax: +354 - 55 25 411
e-mail: ka@vedur.is

Norway:

Jerzy Bartnicki
Meteorological Institute of Norway - DNMI
P.O. Box 43 Blindern
N-0313 Oslo
Tlph: +47 - 22 96 33 15
Fax: +47 - 22 69 30 50
e-mail: jerzy.bartnicki@dnmi.no

Inger Margrethe Eikelmann
Norwegian Radiation Protection Authority - NRPA
Svanhovd
N-9925 Svanvik
Tlph.: +47 - 78 99 51 70
Fax: +47 - 78 99 51 80
e-mail: inger.eikelmann@nrpa.no

Jørgen Saltbones
Meteorological Institute of Norway - DNMI
P.O. Box 43 Blindern
N-0313 Oslo
Tlph: +47 - 22 96 33 13
Fax: +47 - 22 69 30 50
e-mail: jorgen.saltbones@dnmi.no

Ulf Tveten
Consultant - NKS
Institute for Energy Technology - IFE
P.O. Box 40
N-2007 Kjeller
Tlph.: +47 - 63 80 60 00
Fax: +47 - 63 81 29 05
e-mail: ulft@ife.no

Finn Ugletveit
Norwegian Radiation Protection Authority - NRPA
P.O. Box 55 Østerås
N-1345 Østerås
Tlph.: +47 - 67 16 25 74
Fax: +47 - 67 14 74 07
e-mail: finn.ugletveit@nrpa.no

Sweden:

Christer Persson
Swedish Meteorological and Hydrological Institute - SMHI
Climatic Section
Folkvorgsvägen 1
S-601 76 Norrköping
Tlph.: +46 11 - 15 80 00
Fax: +46 11 - 17 02 07, 17 02 08
e-mail: cpersson@smhi.se

Lennart Thaning
National Defence Research Establishment - FOA 4
S-901 82 Umeå
Tlph.: +46 - 90 10 66 50
Fax: +46 - 90 10 68 00
e-mail: thaning@ume.foa.se

Åsa Wiklund
Swedish Radiation Protection Institute - SSI
S- 171 16 Stockholm
Tlph.: +46 - 8 729 7100
Fax: +46 - 8 729 7108
e-mail: asa.wiklund@ssi.se

United Kingdom:

Roy Maryon
Manager, Atmospheric Dispersion
Meteorological Office
London Road, Bracknell
Berkshire RG12 2SZ
Tlph.: +44 - 1344 856 242
Fax: +44 - 1344 854 493
e-mail: rhmaryon@meto.gov.uk

Nordic Nuclear Safety Programme - NKS:

Torkel Bennerstedt
PL 2336
S-760 10 Bergshamra, Sweden
Tlph: +46 - 176 624 28
Fax: +46 - 176 625 95
e-mail: torkel.bennerstedt@ssi.se

Appendix 2

SECOND MEETING ON NORDIC DISPERSION/TRAJECTORY MODEL INTERCOMPARISON WITH THE ETEX-1 EXPERIMENT

Finnish Meteorological Institute, Vuorikatu 24, Helsinki
4th and 5th December 1996

Meeting Agenda

Wedensday, 4th December
The ETEX experiment and some Chernobyl-calculations

Jens Havskov Sørensen: A short summary about the ETEX-1 experiment.

Alix Rasmussen: Quality validation of analyzed and forecast wind and temperature from the DMI-HIRLAM model.

Jens Havskov Sørensen: Evidence for mesoscale influence on long-range transport obtained from DERMA, DMI-HIRLAM and ETEX observations by NERI.

Jørgen Brandt: The Danish RIMPUFF and Eulerian accidental release model (the DREAM) - Results with ETEX-1.

Ilkka Valkama: The ETEX experiment - The Finnish results and conclusions.

Jørgen Saltbones: ATMES II - ETEX runs using SNAP.

Lennart Thaning: ETEX-1 - Measurements compared to calculations performed with the MATHEW/ADPC model at FOA, Sweden.

Christer Persson: MATCH - A regional transport model. The ETEX-1 validation.

Roy Maryon: The sensitivity of the ETEX simulations to different diffusion schemes.

ETEX-related discussions.

Ilkka Valkama: A summary of experiments on the dispersion of radioactive particles from the Chernobyl accident using a simple trajectory model.
Christer Persson: Chernobyl-validation of MATCH and Chernobyl-video.
Jørgen Saltbones: Chernobyl-video from SNAP.

Chernobyl-related discussions.

Thursday, 5th December
New developments, exercises, computer program demonstrations.

Torben Mikkelsen: The atmospheric transport module in RODOS for now- and forecasting of radioactive airborne spread on local, regional and European scales.

Mika Salonoja: Experiences in development of a random-walk particle dispersion model at the FMI.

Mikko Ilvonen: Dose assessment in the new Finnish SILJA system.

Computer program demonstrations:
Possibly a demonstration of SILJA, depending upon the status of the program. (Mika Salonoja).
Demonstration of the RODOS model MATCH. (Christer Persson).

Åsa Wiklund: Nordic dose assessment exercise, NKS/EKO-4.1e. Presentation of the results from trajectory calculations.

Roy Maryon: Informal presentation of results from the RSMC nuclear accident response exercise of 7th November 1996.

Jerzy Bartnicki: Consequences of potential releases from the Kola Nuclear Power Plant - Climatological study.

General discussions.
Closure of the meeting.